Potential and application of vis-NIR spectroscopy for assessment of humus properties of forest soils

Dissertation

der Mathematisch-Naturwissenschaftlichen Fakultät
der Eberhard Karls Universität Tübingen
zur Erlangung des Grades eines
Doktors der Naturwissenschaften
(Dr. rer. nat.)

vorgelegt von
Felix Emanuel Thomas
aus Friedrichshafen

Tübingen
2024

Gedruckt mit Genehmigung der Mathematisch-Naturwissenschaftlichen Fakultät der Eberhard Karls Universität Tübingen.

Tag der mündlichen Qualifikation:	21.10.2024
Dekan:	Prof. Dr. Thilo Stehle
1. Berichterstatter:	Prof. Dr. Peter Dietrich
2. Berichterstatter:	Prof. Dr. Thomas Scholten

Contents

Abstract **vii**

Zusammenfassung **viii**

1 Introduction **9**

1.1 Current situation of forests 9

1.2 Challenges for forest management 10

1.3 Soil formation factors and proximal soil sensing as basis for digital soil mapping 11

1.3.1 Pedogenesis 11

1.3.2 Digital soil mapping using proximal soil sensing 12

2 Objectives **17**

3 Material and Methods **18**

3.1 Proximal soil sensing and vis-NIR spectroscopy 18

3.2 Spatial prediction of soil properties 20

3.3 Application of vis-NIR spectroscopy for estimation of humus properties (manuscript 1) 21

3.4 Application of low-cost MEMS spectrometers for forest topsoil properties prediction (manuscript 2) 22

3.5 Integrated framework for the assessment and spatial prediction of humus properties (manuscript 3) 24

4 Results and Discussion **27**

4.1 Application of vis-NIR spectroscopy for estimation of humus properties (manuscript 1) 27

4.2 Application of low-cost MEMS spectrometers for forest topsoil properties prediction (manuscript 2) 30

4.3 Integrated framework for assessment and spatial prediction of humus properties (manuscript 3) 33

5 Conclusion **39**

References **42**

Appendix **53**

List of Figures

1 Overview of visual (left) and near infrared (right) regions of the electromagnetic spectrum and known correlations to various soil properties, example based on own data from Saxon forests, information by Rossel et al. (2011) 19

2 Absorbance and its first derivative of specra from Oh and Ah soil samples, raw and pre-processed (standard normal variate and Savitzky-Golay-Filter), remarkable differences are marked by letters A-D 27

3 Best predicted and observed values of humus properties based on vis-NIR data for Oh and Ah horizon, SVM = support vector machine, plsr = partial least squares regression, CEC = cation exchange capacity, BS = base saturation 29

4 Raw and pre-processed reflectance spectra of forest soil samples collected with MEMS (Hamamatsu, Neospectra) and conventional spectrometer (Veris) devices 31

5 Data distribution of C/N, pH values, cation exchange capacity (CEC) and base saturation (BS) of chemical measurement and vis-NIR based estimations 34

6 Final map of C/N ratio and pH values of Oh horizon and 0-5 cm depth at forest stand level in the case study area "Zellwald", including measured input values at the sampling points 36

List of Tables

1 Overview of technical specifications for the selected MEMS and conventional devices used for spectral data acquisition 24

List of publications and submitted manuscripts in this thesis

Manuscript 1	**Thomas, F**., Petzold, R., Landmark, S., Mollenhauer, H., Becker, C., Werban, U. (2022): Estimating Forest Soil Properties for Humus Assessment—Is Vis-NIR the Way to Go?. Remote Sensing, 14(6), 1368.
Manuscript 2	**Thomas, F**., Petzold, R., Becker, C., Werban, U. (2021): Application of Low-Cost MEMS Spectrometers for Forest Topsoil Properties Prediction. Sensors, 21(11), 3927.
Manuscript 3	**Thomas, F**., Becker, C., Petzold, R., Schmidt, K., Scholten, T., Werban, U., (submitted to Journal od Plant Nutrition and Soil Science): Integrated framework for the assessment and spatial prediction of humus properties of forest soils.

Abstract

Forests soils are exposed to changing environmental conditions on a global level and influenced by atmospheric element input and acidification processes. For forest management, the ongoing changes depict a major challenge in both the present and future. Thus, mitigation strategies are needed, which rely on up-to-date information about soil and humus conditions. Conventional mapping schemes are time-consuming and partly unreliable. Digital soil mapping approaches, in combination with proximal soil sensing procedures like visual and near-infrared spectroscopy (vis-NIR), have the potential to overcome the mentioned shortcomings. They could provide information at the forest stand scale, where currently no information about humus condition is available. These methods are already widely used for investigations on agricultural areas, but studies focusing on forests and organic humus layers are scarce. The objective of this thesis is therefore to investigate the potential and application of vis-NIR spectroscopy to predict and asses humus properties of forest soils, with respect to the utilisation of the results in silviculture. The included studies present the possibilities of using vis-NIR spectroscopy to predict various properties of the organic layer of forest soils in Saxony and assess different regression and machine learning methods, devices, and spatial scales. Practical application is shown by presenting an integrated framework that derives spatial information about humus conditions at forest stand scale, closing a known data gap. Our results show that vis-NIR spectroscopy is suitable to estimate various soil properties (C and N content, C/N ratio, pH value, cation exchange capacity, base saturation) for the so far not investigated humus layer of forest soils. The application offers a reduction of the required laboratory analysis. No clear preference could be determined regarding the different algorithms used for the humus property estimation. We found that micro-electro-mechanical-systems devices are suitable for humus property prediction. Their performance can compete with benchtop devices. The usage of the NIR region is crucial to achieve satisfying prediction accuracy. The presented framework is applicable and derives spatial predictions of humus properties at forest stand level. Vis-NIR spectroscopy can facilitate the data acquisition procedure. The improved data availability compensates the uncertainties of the predictions. Both vis-NIR spectroscopy and digital soil mapping approaches can be applied for humus property prediction of forest soils. The methods have the potential to play an important role for forest soil characterization in the future by enhancing data availability and support forest management regarding ongoing environmental changes and challenges.

Zusammenfassung

Waldböden sind weltweit sich verändernden Umweltbedingungen ausgesetzt und werden zudem von Stoffeinträgen und Versauerungsprozessen beeinflusst. Für die Waldbewirtschaftung stellen die Veränderungen eine große Herausforderung dar, für deren Bewältigung effektive Bewirtschaftungsstrategien erforderlich sind. Diese sind jedoch auf aktuelle Informationen angewiesen. Herkömmliche Kartierverfahren sind zeitaufwändig und teilweise unzuverlässig. Digitale Bodenkartierung und proximal soil sensing Verfahren wie visuelle und Nahinfrarotspektroskopie (vis-NIR) bieten die Möglichkeit, diese Probleme zu überwinden und Informationen über den Humuszustand auch auf Bestandesebene bereitzustellen. Die Methoden sind aus der Landwirtschaft bekannt, aber Untersuchungen von Waldböden und der Humusauflage sind rar. Das Ziel dieser Arbeit ist es daher, das Potenzial und die Anwendung der vis-NIR Spektroskopie zur Vorhersage und Bewertung von Humuseigenschaften von Waldböden zu untersuchen und die mögliche Nutzung in der Waldbewirtschaftung aufzuzeigen. In den vorgestellten Studien wird der Einsatz der vis-NIR Spektroskopie zur Vorhersage verschiedener Humuseigenschaften von Waldböden in Sachsen untersucht. Es werden verschiedene Regressionsmethoden und Ansätze des maschinellen Lernens, sowie Spektrometer und räumliche Skalen verwendet. Zudem wird ein integriertes digitales Bodenkartierungssystem für die Regionalisierung von Humuseigenschaften vorgestellt. Wir zeigen, dass vis-NIR Spektroskopie geeignet ist, um verschiedene Bodeneigenschaften (C- und N-Gehalt, C/N Verhältnis, pH-Wert, Kationenaustauschkapazität, Basensättigung) auch für die bisher nicht untersuchte Humusauflage vorherzusagen. Hinsichtlich der verwendeten Algorithmen konnte kein eindeutiges Ergebnis erzielt werden. Micro-electro-mechanical-systems Geräte sind für die Vorhersage von Humuseigenschaften geeignet und die damit erzielten Ergebnisse sind mit herkömmlichen Geräten vergleichbar. Die Benutzung des NIR-Bereichs ist dabei essenziell für eine ausreichende Vorhersagegenauigkeit. Das vorgestellte Bodenkartiersystem ermöglicht die Regionalisierung von Humuseigenschaften auf Bestandsebene. Der Einsatz von vis-NIR Spektroskopie kann dabei die Datenaufnahme erleichtern. Die verbesserte Datenverfügbarkeit gleicht dabei die Unsicherheiten der Vorhersagen aus. Vis-NIR Spektroskopie und digitale Bodenkartierung können zur Vorhersage von Humuseigenschaften eingesetzt werden. Beide Methoden haben das Potenzial, eine wichtige Rolle bei der Kartierung von Waldböden zu spielen, indem sie die Datenverfügbarkeit verbessern und die Waldbewirtschaftung im Hinblick auf die laufenden Umweltveränderungen und Herausforderungen unterstützen.

1 Introduction

1.1 Current situation of forests

Forests are amongst the largest ecosystems on earth, covering around 31% of the global land area Food and Agriculture Organization of the United Nations, 2020. They are recently exposed to changing environmental conditions caused by various processes on a global level. These changes are affecting climate in general, but as well have remarkable effect on water availability and soil nutrient supply (Jandl et al., 2019). Forests are therefore especially sensitive, as the duration of the trees life span makes rapid adaption to changes impossible (Lindner et al., 2010). In managed forests, the rotation time of the trees also exceeds the time range suitable for fast mitigation possibilities.

In addition, an interplay of different processes can take place, and extreme events are likely to occur more often. This can further increase the impact on the forest ecosystems. In the case of droughts, Anderegg et al. (2020) showed that subsequent events generally have a more deleterious impact than the initial drought. Therefore, future forests may be substantially different from today, with unprecedented species mixtures (O'Hara, 2016).

In Europe, rising temperatures and frequent droughts are causing severe problems for forest stands, and facilitate the occurrence of further disturbances like insect or fungal calamities (Schuldt et al., 2020). Excess forest mortality is consistently linked to drought across Europe (Senf et al., 2020).

Forest soils are known to be one of the main factors influencing forest growth (Binkley & Fisher, 2020). They have an impact on water balance and nutrient supply and are as well exposed to the ongoing global and regional climatic changes. In Europe, other processes have serious impact on the current state and development of forest soils.

Soil acidification is a natural process dependant on parent material, precipitation and vegetation. The process can however be accelerated by anthropogenic factors (Augusto et al., 1998). Activities with high influence can be tree species changes, management measures and element input. Amongst these, the most important factor can be seen in particular in the deposition of sulfur and nitrogen compounds (Kazda & Zvacek, 1989; Richter, 1986).

Since the industrialization, sulfur was the main acid element introduced into soils. In the 1990s, nitrogen depositions in form of nitrate and ammonium, originating from fuel combustion of cars and the usage of agricultural fertilizer, have affected the nutrient balance of European forest soils (De Vries et al., 2014; Schöpp et al.,

2003).
These processes have already altered forest soils, humus layers and forest ecosystems (De Vries et al., 2014; Meesenburg et al., 2019). Typical effects are loss of base cations, decreasing pH values, and the release of aluminium that can not be bound into organic complexes (Borůvka et al., 2007). The depositions particularly affect the humus layer as well as the mineral topsoil as the element input from the atmosphere naturally has the most impact on the uppermost soil layers.

1.2 Challenges for forest management

For forest management, the ongoing changes and their impact on forest ecosystems represent one of the major challenges in the present and near future.
The situation can be seen as particularly complex as all undergoing processes and their consequences are hard to depict, and therefore great uncertainties are inherent to the situation.
In order to adapt to the changes, an understanding of the processes and effects is needed. One important part of this involves the implementation of monitoring methods (Keenan, 2015).
The availability of up-to-date information about the current situation is crucial for assessment of the predominant conditions, as well as for the creation and implementation of meaningful management strategies. Adaption strategies will be of great importance in the future, and for the development of such strategies, high quality data at sufficiently accurate scales is needed as a basis. Soil properties in the organic horizon show high variability at the small scale (Qian & Klinka, 1995), which highlights the need of high resolution data for proper representation of the current situation.
Well founded decision-making in silviculture could allow a forest conversion towards more resilient ecosystems. For this, up-to-date information on soil and humus conditions is a crucial part, as it is needed for the assessment of nutrient availability. Further, information on humus properties allows for inferences about soil biological activity, estimation of tree species germination behavior, potential nutrient imbalance, assessment of soil fauna and subsequent effects on biodiversity.
Remote sensing techniques can be used for a wide range of monitoring applications. Its focus lies on the measurement of vegetation cover, structure and moisture, but soil characteristics can be investigated as well (Lechner et al., 2020). However, the permanent vegetation cover prevents direct measurements of the soil via remote sensing methods. It is therefore only possible to derive information about the soil using measurements of vegetation as proxy. Furthermore, the vegetation structure

of European forests are influenced by past anthropogenic activities to the point that natural factors are completely masked (Behre, 1988). This can limit the explanatory power of vegetation-based sources of information when investigating soil properties.
Traditional mapping methods rely on direct analysis of soil samples. For example, the current mapping scheme in East Germany differentiates between stem properties, that are hard to influence and steady over long time periods, and state properties that are more variable. The latter are characterised by the humus form, which is derived from chemical properties of the humus layer and uppermost mineral layer (Ah horizon) (Schulze and Kopp, 2013). However, the mapping scheme requires natural conditions in nitrogen and acid-base classes. In reality, anthropogenic changes led to deviations from the natural balance (Wellbrock et al., 2015). In this case, the conditions are disharmonic, and the existing scheme can not be applied (Becker et al., 2022). For the lowlands in the north east of Germany, there is a mapping scheme based on indicator plants that can be used for humus mapping (Schulze and Kopp, 2013). The application is limited to lowlands as there is no scheme for hilly terrain and secondary mountains. In addition, vegetation is nowadays often overprinted by forest management and element input.
In order to overcome the mentioned problems and obstacles, new methods for mapping humus properties are needed in order to provide information about the current conditions in forest stands.

1.3 Soil formation factors and proximal soil sensing as basis for digital soil mapping

Digital soil mapping techniques can avoid the shortcomings of traditional approaches, especially limitations due to the needed amount of labour and financial resources (Baruck et al., 2016). The approaches could further profit from proximal soil sensing methods such as vis-NIR to reduce the required amount of laboratory analysis.

1.3.1 Pedogenesis

According to Hudson (1992), all soil survey approaches can be seen as a strategy that is based on the factors of soil formation, combined with the relationship between soil and landscape.
Soil development is basically dependant on decomposition, conversion and reloca-

tion of organic as well as inorganic material. Soil properties that change during soil formation are relatively stable. On the other hand, properties that change in cyclic ways, e.g. on a annual basis are not part of the pedogenesis (Van Breemen & Buurman, 2002).
All soil properties are determined in the soil forming process, consisting of five soil forming factors. These were first described by Dokuchaev (1883) and then proposed as a formula by Jenny (1941) as follows in equation 1:

$$S = f(cl, o, r, p, t, ...) \tag{1}$$

In this equation, S is the soil property, that is developing within environmental conditions (cl for climate, o for organisms, r for relief, p for parent material and t for time). Predominant climate influences the soil forming process by precipitation, movement of water and temperature effects, resulting e.g in shrinking and swelling of soil aggregates. Organisms impact the processes in form of fauna and vegetation by input of litter, decomposition and bioturbation processes. The relief causes erosion and reallocation while parent material determines mineralogy, soil chemistry and particle size distribution. The factor time controls the amount of time in which all other factors are taking effect (Rentschler, 2021; Van Breemen & Buurman, 2002).

1.3.2 Digital soil mapping using proximal soil sensing

New procedures of soil sensing have emerged and become popular through the last decades in soil science. In particular methods of proximal soil sensing have been investigated, tested and applied to estimate soil properties. Amongst these methods, spectroscopy is already proven to be an important and useful method. It has been applied in numerous studies, especially on agricultural areas for measuring various chemical and also physical soil properties. The prediction of soil properties is possible either by direct interaction with specific absorbance bonds or by indirect correlation with soil properties that are directly linked to soil spectra (Askari et al., 2015; Soriano-Disla et al., 2014). According to Ben-Dor and Banin (1995), properties with direct spectral assignment are, for example, C content and particle size. Other properties like pH value and cation exchange capacity can be predicted through indirect assignments resulting from correlations to other properties (Stenberg et al., 2010; Zornoza et al., 2008).
Often, the visual and near-infrared (vis-NIR) as well as the mid-infrared regions of the electromagnetic spectrum are used for the investigation of soil. While the mid-infrared range relies on fundamental absorption, the vis-NIR is limited to

overtone and combination bands (Hutengs et al., 2019; Rossel et al., 2006; Stenberg et al., 2010). However, mid-infrared spectra are more affected by moisture and sensitive to sample preparation. Therefore, the soil material has to be ground to avoid disturbances in the spectra caused by soil aggregates bigger than 1-2 mm (Reeves III, 2010). The usage of the vis-NIR regions only requires dried and sieved sample material. This facilitates the data acquisition process and reduces the necessary effort for sample preparation. Furthermore, the development of portable devices is more advanced in the vis-NIR region. Portable devices have been available for decades, while they are only becoming available in the last years for mid-infrared measurements (Hutengs et al., 2019). For soil analysis, vis-NIR devices are more widely used due to their suitability for remote sensing approaches and lower economic cost (Haghi et al., 2021).

Chang et al. (2001) used vis-NIR spectroscopy and more than 800 samples from various sites in the USA for estimating C and N content, cation exchange capacity, moisture, sand, silt and extractable Ca, and reached R^2 higher than 0.8. For other properties like exchangeable cations, sum of exchangeable bases, acidity, respiration rate and pH value, they reported R^2 values between 0.5 and 0.8.

Fystro (2002) predicted C and N content including their mineralisation in three agricultural regions in Norway. Mouazen et al. (2007) managed to measure C content, moisture content, pH values and phosphorus using soil samples collected on agricultural fields from France and Belgium. On soils of three representative agro-ecosystems in Italy, Leone et al. (2012) investigated the prediction of numerous soil properties, including particle size, organic carbon, nitrogen, cation exchange capacity and calcium carbonate.

In Australia, Rossel et al. (2006) examined the prediction of the properties soil pH, Ca, lime requirement, organic carbon, clay, silt, sand, cation exchange capacity, exchangeable calcium, exchangeable aluminium, nitrate–nitrogen, available phosphorus, exchangeable potassium and electrical conductivity. Santra et al. (2009) was able to estimate soil hydraulic properties when investigating a watershed in India. In summary, vis-NIR spectroscopy can already be seen as a standard procedure in agricultural soil sensing.

Studies in this field already tend to focus on further developments. For example, the feasibility of in-situ measurements was investigated by Rossel et al. (2009) by comparing field and laboratory spectra to make predictions of soil mineral composition and clay content. In another study, Zhang et al. (2017) predicted soil organic matter, water and clay content as well as pH, Mg, Ca, and K in different depths up to one meter on field scale in a study area based in Canada.

Other studies focused on data fusion approaches, such as Mahmood et al. (2012), and broadened the application cases, e.g. to detect toxins instead of nutrients or soil texture (Gholizadeh et al., 2020). Additionally commercial offers based on spectroscopy are already emerging, promising to provide nutrient information on soil within short time without chemical analysis.

On forest soils however, a different picture can be drawn. Due to the permanent vegetation cover, it is not possible to pass over the soil using vehicles. Soil samples must be collected by manual field work. This increases the amount of cost and effort needed to obtain the needed samples and data for investigations. In addition, on forest soils there is an organic humus layer present.

This uppermost layer has high organic carbon content and consists of plant residuals and humified litter, often in the form of complex humic substances. It is therefore chemically different from mineral soil samples. Previous studies have already examined the possibilities of using vis-NIR spectroscopy to predict properties of forest soils as well.

For example, Ludwig et al. (2002) reported promising results when predicting C and N content on two experimental sites in the Central Highlands of Victoria, Australia. In an investigation that took place in the Calabria region, Italy, Conforti et al. (2018) investigated mineral soil samples from forests and predicted soil organic C, total N, pH value and particle size. Pietrzykowski and Chodak (2014) used vis-NIR spectroscopy to estimate, amongst other properties, organic C, total N, cation exchange capacity and base saturation on four different afforested former mining sites in Central and South Poland. They reported high prediction accuracy with R^2 values above 0.8.

These studies have proven that it is generally possible to use vis-NIR spectroscopy to analyse soils from forests. They showed that several important soil properties can be estimated, but were conducted using only soil samples taken from mineral horizons. For the assessment of humus of forest soils however, the organic layer needs to be investigated as well. So far, few studies have applied vis-NIR spectroscopy on samples originating from the humus layer.

One of the first broad studies on forest soils focusing on organic layers was conducted by Chodak et al. (2002) on two sites in Lower Saxony covered by Norway spruce, beech and mixed stands. They reported that vis-NIR predicted the contents of C, N, P, S, Ca, Na, K, Fe, and Al and C/N and C/P ratios in organic layers with satisfying accuracy. In another study Coûteaux et al. (2003) investigated C and N content of organic layers from coniferous forests on study sites located in France and Sweden. More recently, on an investigation across

China, Liu et al. (2019) established a Chinese forest soil spectral library and estimated soil organic C on large-scale. They sampled soil material in 0-10 cm depth, but C contents distribution in the data set revealed that samples with high values up to 99.6% were included in the modelling process. Assessing soil organic C using vis-NIR spectra on national scale in the Czech Republic, Gholizadeh, Viscarra Rossel, et al. (2021) included soil samples from organic horizons, separated by litter, fragmented and humus layer. They reported successful models for the estimation of organic C, with the most accurate results originating from organic soil layers.

The studies including investigations of the organic layer mainly focus on (organic) C content. For other properties that are crucial for the assessment of current humus conditions, like pH value, cation exchange capacity and base saturation, vis-NIR spectra have so far not been investigated regarding their prediction ability. Furthermore, recent development in the field of sensor techniques have made portable devices increasingly available (Sharififar et al., 2019). Micro electro mechanical systems allows for the production of smaller, lighter and cheaper devices (Hintschich et al., 2014).

These devices often cover a smaller spectral range and also have lower spectral resolution when compared to conventional devices. Current research often focuses on the feasibility of possible application scenarios for the micro electro mechanical system devices (Beć et al., 2021). First examples of studies investigating their suitability for soil properties prediction are already published (Sharififar et al., 2019).

Due to their size and costs, these devices offer new opportunities regarding a wider range of applications also for the investigation of forest soil and humus properties. When investigating the possibilities of using vis-NIR spectroscopy for the estimation of humus properties, it is therefore of great interest to assess the possibilities of these sensors and compare the results to other devices.

Solely the applicability of vis-NIR spectroscopy for the estimation of humus properties does, however, not yield information about the usefulness of the procedure for forest soil mapping.

The logical next step is therefore the integration of the achieved results into a framework using digital soil mapping approaches for spatial prediction of humus properties. Such an approach would aim to derive spatial maps displaying humus properties and therefore close the current data gap on forest stand level. The provided information would be ready to use for management purposes and enhance decision-making in order to face the described challenges that silviculture is

currently exposed to in Saxony and other states of Germany. The derivation of possible courses of action regarding forestry and soil management could profit from the enhanced data basis.

2 Objectives

As previously described, the usage of vis-NIR spectroscopy for the determination of humus properties of forest soil could help to increase data availability with reasonable cost and effort. Furthermore, spatial prediction using digital soil mapping approaches has the potential to provide information about humus properties at the forest stand scale.
Therefore, the overall objective of this work is to investigate the potential of vis-NIR spectroscopy to determine properties of forest soils relevant for silviculture. In addition, the usage of digital soil mapping methods to provide spatially available information at the forest stand scale was researched. The focus of the research is on the humus layer and mineral topsoil and on the assessment of the results regarding possible application and usage for forest management.
In particular, these goals are accomplished by:

- investigating the use of vis-NIR spectroscopy for humus properties estimation on forest soils with a focus on the humus layer and mineral topsoil with high percentage of organic carbon (manuscript 1, 2, 3)
- compare the prediction performance of different regression models and machine learning methods (manuscript 1, 2)
- assess novel MEMS Vis-NIR spectrometers operating in different wavelength ranges regarding their applicability for assessing humus properties and compare the results to full-range devices (manuscript 2)
- investigate if and how model accuracy depends on spatial scale of the study area (manuscript 2)
- present a digital soil mapping framework for spatial prediction of humus properties of forest soils in order to close a current data gap in forest management (manuscript 3)
- the integration of vis-NIR spectroscopy data and model results into the digital soil mapping framework (manuscript 3)
- assess the results regarding their potential usage and advantages for forest management, including the identification of a possible course of action based on the findings

3 Material and Methods

3.1 Proximal soil sensing and vis-NIR spectroscopy

Proximal soil sensing is defined as the usage of sensors that obtain signals from the soil when being in direct contact or close (< 2 m) to the soil (Rossel et al., 2011; Rossel & McBratney, 1998). The collected signals are determined by physical measures, which are related to soil properties. Proximal soil sensing methods are known to be non-destructive, fast and therefore offer the possibility to replace or support expensive and time-consuming chemical laboratory analysis.
In general, different techniques can be characterized in the way they measure (in-situ or ex-situ), by the source energy that is used (active or passive), regarding their operation mode (stationary or mobile) and by inference (direct or indirect). Different frequencies of the electromagnetic spectrum can be used for soil sensing purposes. For example, according to Rossel et al. (2011), γ-ray is used to investigate spatial variability and parent material (Priori et al., 2014), X-ray fluorescence for elemental analysis (Towett et al., 2013), radar for soil water content (Weihermüller et al., 2007) and electromagnetic induction to measure electrical conductivity (Saey et al., 2013).
Vis-NIR spectroscopy is an optical method, and the visual (400-760 nm) and near-infrared region (760 - 2500 nm) of the electromagnetic spectrum are used to investigate the soil. In general, vis-NIR spectroscopy can be operated in-situ and ex-situ. Active (e.g. a light bulb) or passive energy (sun light) can be used, and the inference can be direct or indirect, depending on the soil properties that are being investigated (Rossel et al., 2011). As forests, in contrary to agricultural areas, can not be passed over by vehicles, soil spectra were collected under laboratory conditions. In this case, the measuring procedure can be defined as ex-situ and active due to the usage of an artificial light source. It is also referred to as laboratory spectroscopy (Rossel et al., 2006). The usefulness of vis-NIR spectroscopy in soil science is based on correlations of the collected spectra to contents of the soil. The absorption consists of a physical and a chemical component. Physical absorption mechanisms are mainly formed by particle size and shape. Surface roughness and mass density further cause spectral differences. Bowers and Hanks (1965) found that the most important particles for reflectance are smaller than 0.4 mm. Furthermore, penetration depth determining the soil volume recorded during measurement is important. It is dependant on the wavelength and is highest between 600 and 1000 nm (Gubler, 2011; Siesler et al., 2008). In the chemical absorption mechanisms, electronic and vibrational processes can be distinguished

(Hunt, 1977). Electronic processes are caused by molecules changing energy states causing absorbance or emittance at specific wavelengths. These are mainly caused by iron, but can be caused by other elements as well (Gubler, 2011; Hunt, 1977). The vibrational processes originate from molecules that are held together by chemical bonds. The atoms within these molecules are stretching and bending and are excited to vibrate by electromagnetic radiation. This process is absorbing energy in the corresponding regions of the spectra (Gubler, 2011). Absorption in the vis-NIR is often depending on overtones and mainly caused by O-H, C-H and N-H groups that have high fundamental frequencies (Hunt, 1977). Different soil compounds have important absorption assignments in different regions of the vis-NIR spectrum. The characteristics of the vis-NIR spectrum are based on the overtones and combinations of fundamental vibrational bands for each of the chemical bonds, which in general strongly absorb in the mid-infrared region (Burns & Ciurczak, 2007; Zornoza et al., 2008). The most important correlations of soil properties and their corresponding spectral region can be seen in figure 1.

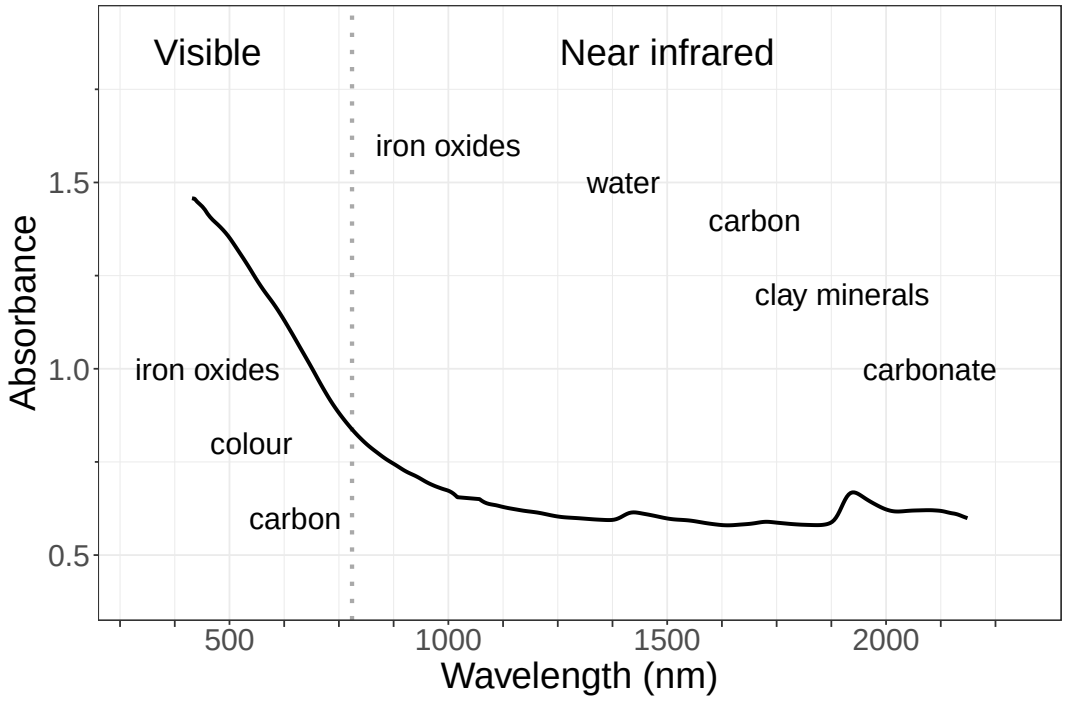


Figure 1: Overview of visual (left) and near infrared (right) regions of the electromagnetic spectrum and known correlations to various soil properties, example based on own data from Saxon forests, information by Rossel et al. (2011)

The procedure can not be used as a stand-alone analytical method and is always dependant on a regression model. These need established reference methods, in this case in form of chemical analysis in the laboratory (Gubler, 2011). The

rapidly growing field of machine learning offers new possibilities of prediction, including soil research purposes. Various investigations test the possible usage of new machine learning algorithms in addition to established regression methods. Therefore, several methods are often used at the same time, allowing us to compare the performance of the algorithms for different scenarios. In this work, three regression algorithms were used to calibrate the models for estimating humus properties based on vis-NIR data. Partial least squares regression can be seen as a standard procedure for predicting soil properties based on vis-NIR spectra (Ramirez-Lopez et al., 2013). There are various studies using Partial least squares regression successfully to predict physical and chemical soil properties using vis-NIR spectra, on a variety of study areas of different sizes (Gogé et al., 2014; Jiang et al., 2016; Leone et al., 2012; Xu et al., 2018). It was developed by Wold et al. (1983) as a method to solve multivariate calibration problems and is usually used when there is a high number of collinear predictors. During the procedure, a group of factors that describes the maximum correlation between predictors and target variables is created based on the initial data. For the actual regression, these factors are used instead of the initial predictors. This further results in a reduction of the amount of data and therefore also reduces the computation time. More recently, methods from the field of machine learning are also being used for proximal soil sensing purposes, including the estimation of soil properties based on vis-NIR spectra. For this purpose, supervised models that are trained with example data are used. Support vector machines originate from the theory of statistical learning. They were first introduced by Cortes and Vapnik (1995). Support vector machines were already used in various studies investigating vis-NIR spectra and soil properties, e.g. by de Santana et al. (2021) and Dotto et al. (2017) for soil organic matter and particle size, by Morellos et al. (2016) for nitrogen and moisture content and by Guo et al. (2021) for potassium and phosphorus. Furthermore, Cubist as a rule-based algorithm was used for modelling humus properties. It was first presented by Quinlan et al. (1992). Yang et al. (2019) used it to predict soil organic carbon an pH values of paddy soil in the Yangtze plain, China. In another study, Silva et al. (2019) were able to estimate sand and clay content. At the large scale, Liu et al. (2019) predicted soil organic carbon, including forested areas and humus samples with high carbon content.

3.2 Spatial prediction of soil properties

Sanchez et al. (2009) describe digital soil maps as a spatial database of soil properties. Field sampling is the basis to describe the spatial distribution of soil

properties, normally determined in the laboratory. This information is then used to map soil properties in areas that have not been sampled before. According to Sanchez et al. (2009), digital soil mapping approaches are consisting of three main steps. In the beginning, the input data is assembled in the form of base maps. Then, the covariates are selected based on factors of soil formation. In this work, the SCORPAN model (Jenny, 1941; McBratney et al., 2003) is used as a basis for our approach.
It includes the already in section 1.3.1 described factors of soil formation. In addition, already available information about the soil (s) and the geographic location (n) are added as covariates for the soil prediction. The second step consists of model calibration or training by deriving quantitative relationships between the desired soil properties (dependent target variable) and the available and selected spatially continuous covariates. This results in spatial maps of soil properties, and information is subsequently available for so far unsampled areas. Further steps consist of the derivation of soil management practices based on the maps produced with the soil mapping workflow. The provision of the gained information can then be used for decision making (Sanchez et al., 2009).

3.3 Application of vis-NIR spectroscopy for estimation of humus properties (manuscript 1)

This study was based on data originating from retained samples of the periodic forest soil inventory in the federal state of Saxony, Germany, covering an area of 17400 km^2 of which 5209 km^2 are covered by forests. The collection of the sample material was conducted between 2006 and 2014, following a grid-based approach. The data was supplemented with samples from a previous study focusing on natural areas (lowland, hilly terrain and middle mountain range) (Wellbrock et al., 2015). The data collection was done following the German sampling standard designed for the forest soil inventory. This method consists of collecting sample material on eight points around the sampling center point at a radius of 10 m. Soil material from the organic layer (Oh horizon) and mineral soil (0-5 cm, Ah horizon) was collected. The chemical analysis was done by the standards of forest soil chemical analysis (Gutachterausschuss Forstliche Analytik, 2014). From a total of 727 retained soil samples, conditioned Latin hypercube sampling was used in order to optimize the number of samples. They represent the dominant vegetation types Norways spruce (*Picea abies*) and Scots pine (*Pinus sylvestris*) as well as mixed stands.
For spectral data acquisition we used a Veris vis-NIR Spectrophotometer by Veris

Technologies Inc. (Salina, KS, USA). It operates with two sensors, an Ocean Optics USB4000 (340 to 1100 nm) and a Hamamatsu Minispectrometer TG series (1100 to 2220 nm), working with a spectral resolution of five and six nanometres. Data collection was conducted by means of a self-developed measuring protocol. In order to assure a proper recording of each samples variability, two petri dishes were measured five times while being shifted after every measurement. The spectrophotometer was calibrated after every sample. Pre-processing was performed to increase data quality (Rinnan et al., 2009). The spectral data was smoothed by the Savitzky-Golay-Filter (Savitzky & Golay, 1964) and normalized using standard normal variate (Rinnan et al., 2009; Stevens et al., 2013). Furthermore, outliers were removed using principal component analysis and Mahalanobis distance (Filzmoser et al., 2005).

For the modelling process and the calibration of the regression models, we used partial least squares regression, support vector machine and cubist. These methods can be seen as especially suitable for modelling soil properties based on spectral data as they are robust towards numerous collinear independent variables. The spectral bands used for the prediction are highly correlated, and this has to be taken into account when selecting suitable algorithms. As dependant variables, C and N content, C/N ratio, pH value, cation exchange capacity and base saturation were selected. The models were trained for Oh and Ah horizon separately. To select the hyperparameters resulting in the best prediction values, model tuning was done by means of a grid search procedure. Model calibration and validation was done using a nested cross validation, which allows for robust tuning and independent validation while using all available data (Müller, Guido, et al., 2016). Furthermore, partial least squares regression models were calibrated using all available data in order to identify the most important wavelengths for model building for each of the humus properties.

In addition, the results were evaluated regarding their usefulness for mapping purposes. For this, we classified the samples on the basis of measured and predicted pH values and calculated a confusion matrix to compare the model output with chemically measured values.

3.4 Application of low-cost MEMS spectrometers for forest topsoil properties prediction (manuscript 2)

This study focused on the usage of micro-electro-mechanical system (MEMS) devices and their suitability for prediction of humus properties. For the evaluation, a comparison to a full-range device was conducted. Two different data sets were

used, representing two different spatial scales.
As a data set for the regional scale, again the retained soil samples from the periodic forest soil inventory in Saxony between 2006 and 2014 were used. Focusing on C and N content of the soil samples, we created a sample selection from the available 727 samples, representing all abundant vegetation types in Saxony. Conditioned Latin hypercube sampling was performed to select a representative subsample. In total, the data set consisted of 176 samples from Oh horizon and 186 samples from Ah horizon, respectively. Main parent materials in this data set were sand, loess loam, gneiss, granite shale and phyllite, with cambisols, gley and podsols being the most abundant soil types.
The data for the local scale was collected at the forest size "Zellwald", also located in Saxony. It has a size of 2336 ha, with an annual precipitation of 750 mm and a mean annual temperature of 9.5 °C. Parent material in the study area is loess loam. Dominant soil types are luvisols and stagnic luvisols. The vegetation consists mainly of coniferous stands of Norway Spruce (*Picea abies*) and Scots Pine (*Pinus sylvestris*), with smaller deciduous areas formed by oak (*Quercus spp.*), birch (*Betula pendula*) and few other broadleaf species.
During a field campaign carried out in June and July 2019, 50 samples from Oh horizon and 60 samples from 0-5 cm depth were collected. In accordance with the sampling procedure from the periodic forest soils inventory, eight samples were taken per point.
The chemical analysis of samples from both data sets was conducted in the laboratory of the Sachsenforst public enterprise in accordance to the German standard for forest soil analysis (Gutachterausschuss Forstliche Analytik, 2014).
For the spectral analysis, two MEMS devices were used, one operating in the visual range by Hamamatsu Photonics K.K. and one in the NIR range by Si-Ware Systems Inc., Menlo Park, CA, USA. In addition, a Veris Spectrophotometer by Veris Technologies Inc., Salina, KS, USA was used as full-range device and benchmark. Specifications of all devices can be seen in table 1.
As it is important to consider the different wavelength ranges, the spectra from the two MEMS devices were used separately and combined, to ensure that the comparison of the results is based on sensor differences rather than the diverging wavelength range.
For the regression analysis partial least squares regression and Cubist regression were used in this study. Model calibration was done using a ten-fold cross validation, and the models were tuned by means of a grid search procedure to optimize the hyperparameters. The outcome of the model approaches was assessed

Device	Veris Spectrophotometer	NeoSpectra SWS62231	Hamamatsu C12880MA
Wavelength	400 - 2220 nm	1350-2550 nm	340 - 850 nm
Spectral Resolution	6 nm @ 350–1000 nm, 5 nm @ 1100–2220 nm	16 nm	15 nm
SNR	300:1 @ 400-1000 nm, NA @ 1100–2220 nm	2000:1	NA
Wavelength reproducibility	NA @ 350–1000 nm, ±0.4 @ 1100-2000 nm	± 0.15 nm	± 0.5 nm
Weight	24kg	17g	5g

Table 1: Overview of technical specifications for the selected MEMS and conventional devices used for spectral data acquisition

using an independent test set. This set consisted of 30% of the data points that were excluded from model calibration procedure.
Models were established based on both regional and local data set as basis. In each case, Oh horizon and Ah horizon or 0-5 cm depth were investigated separately. Using the larger regional data set, we also carried out a modelling approach using both data sets together. In this comparison of different vis-NIR sensors, investigated humus properties were limited to C and N content.

3.5 Integrated framework for the assessment and spatial prediction of humus properties (manuscript 3)

In this study, the focus lay on the presentation of an integrated framework for spatial prediction of humus properties at forest stand level. In addition, the possibilities of including the results of vis-NIR spectroscopy into such a framework were investigated. This work presents the results of the joint project DIGI-Humus (Detection and spatial prediction of humus properties using vis-NIR spectroscopy and digital soil mapping), conducted by Sachsenforst public enterprise and Helmholtz Centre for environmental research. It consisted of two sub-projects, investigating (i) the applicability of vis-NIR spectroscopy for the estimation of humus properties and (ii) the possibilities of spatial prediction of these properties using digital soil mapping approaches (2). The framework combines methods and results developed within both sub-projects.

The basis of the framework is the input data selected according to the soil forming factors. For every factor, a corresponding predictor variable was selected based on information spatially available in forest management. Therefore, soil form classes were used to represent the factor soil. They were aggregated to 23 classes. To represent climate, temperature, evapotranspiration, precipitation, climatic water balance and grass reference evaporation were used. Organisms in form of vegetation were covered by normalized difference vegetation index values derived from SENTINEL2 satellite imagery. Normalized difference vegetation index values aggregated to represent eight different dates during the vegetation period were used.
The relief was represented by height above sea level, aspect (Roberts, 1986), curvature (Zevenbergen & Thorne, 1987) and SAGA wetness index (Böhner et al., 2001). To include information about the parent material, the geological information from the forest soil map was used. In order to provide reasonable sampling locations within the study area, conditioned Latin hypercube sampling was applied (Minasny & McBratney, 2006). This way it is ensured that the sample distribution is covering the covariate space properly. To enhance soil material collection in the field, the Gowers similarity index was calculated to allow for the selection of similar sampling points in case of obstacles restraining the sampling. For the next step, the samples were taken in the designated sampling locations, prepared by drying and sieving and then analyzed in the laboratory for the desired properties. In addition, vis-NIR spectra of the samples were taken following the protocol described in section 3.3.
Next, the selected humus properties were estimated in the first modelling step on basis of the recorded spectra. Model calibration was done using partial least squares regression. In order to use all available soil samples, a nested cross validation procedure was applied. More information on the modelling can be found in the methods chapter of the manuscript in the appendix.
For the final part, the acquired data is used for spatial prediction of the humus properties. For this modeling step, the Random Forest algorithm was used (Breiman, 2001). It is known for its high prediction power, can be used for small sample sizes (Scornet et al., 2015) and is already commonly used in other studies for soil mapping procedures (Behrens et al., 2014).
The predictor values at all sampling locations in the study area were extracted from the input data sets and built to the basis of the model.
For model calibration, a leave-one-out cross-validation in combination with a grid search to optimize hyperparameters was used. Samples from Oh horizon and 0-5

cm depth were investigated separately. Furthermore, models were established using humus property values originating from chemical analysis as well as from spectral modelling. For each case, the importance of the single predictor variables for model calibration was investigated. The final models were then used to predict the humus properties on the whole area to get spatial information on forest stand level. The proposed framework was hereby tested in the form of a case study on the site "Zellwald". More general information regarding the study area is already given in section 3.4.

4 Results and Discussion

4.1 Application of vis-NIR spectroscopy for estimation of humus properties (manuscript 1)

The investigation of the recorded vis-NIR spectra revealed differences between the horizons. Generally, samples from Oh horizon showed higher absorbance levels within the whole spectrum. We further detected deviations in four regions of the spectrum, present in the visible range, around 1400 nm, at 1900 nm and as well in the region above 2000 nm. The spectra and their first derivative, separated by horizons, are shown in figure 2. The main differences found are marked using the letters A-D.

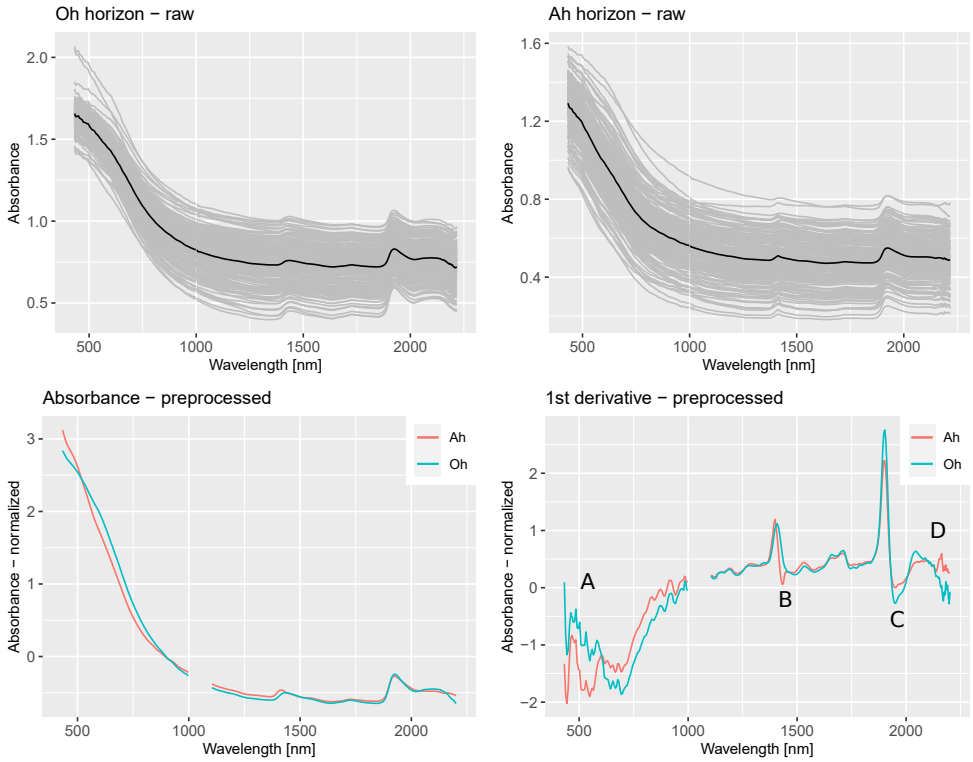


Figure 2: Absorbance and its first derivative of specra from Oh and Ah soil samples, raw and pre-processed (standard normal variate and Savitzky-Golay-Filter), remarkable differences are marked by letters A-D

We assume that the differences in the recorded spectra are a direct result of the distinct composition of the sample material originating from the investigated horizons. All wavelength regions that are showing differences between the horizons are known to be sensitive for organic matter compounds. Therefore, the much higher amount of organic matter in Oh samples are likely the cause for the different spectral behaviour. The generally higher absorbance values can as well

be explained by the high organic matter percentage. Differences in the features around 1400 and 1900 nm could also be caused by the different amount of clay that is found in these regions.
The observations had direct impact on the model calibration processes. Regarding C content prediction, important spectral regions for Oh horizons were in the visual range while for Ah horizons, features above 2000 nm were most important.
The modeling results of the nested cross-validation procedure were various and highly dependant of the investigated property and horizon. The models reached R^2 values between 0.44 and 0.9. Therefore, the recorded spectra held information that was able to explain between 44% and 90% of the variance in the humus property values. Predicted and observed values for all properties and both horizons are shown in figure 3.
For samples from Oh horizon, the models for C and N content reached R^2 values of between 0.46 and 0.58, with ratio of performance to interquartile distance (RPIQ) values up to 2.06. Important regions of the spectrum were in the visual range between 500 and 600 nm. The complex structure of humic material seemed to reduce the model accuracy, as numerous examples report better model performance.
Highest precision was achieved for pH values with R^2 values up to 0.9. C/N ratio and base saturation were next, with R^2 around 0.7. In both cases, most important wavelengths for model calibration were around 1900 and 2200 nm.
Less accurate predictions were found for the cation exchange capacity. Here, R^2 values of all algorithms were 0.54 and most important features at 570 and 690 nm. A possible reason could be the absence of clay that could act as indirect spectral assignment (Ben-Dor & Banin, 1995).
Base saturation was predicted with R^2 up to 0.71 and RPIQ up to 2.61 with most important wavelengths found at 1900 and 2200 nm. The predictions are likely based on indirect assignments of hydroxy and carbonyl groups (Rossel & Behrens, 2010).
Other studies achieved more accurate results for estimation of C content of samples from organic layers. Nocita et al. (2014) reported R^2 of 0.78, but also included other land use forms. Only investigating Oh samples, Gholizadeh, Viscarra Rossel, et al. (2021) reached $R^2 = 0.63$, which is more comparable to the results of this study. For the other properties, no comparable studies focusing on the humus layer of forest soils could be found, highlighting the importance of the investigation in this manuscript.
The model results for Ah horizon achieved different results for the investigated properties. Here, prediction accuracy was higher for C and N content with R^2

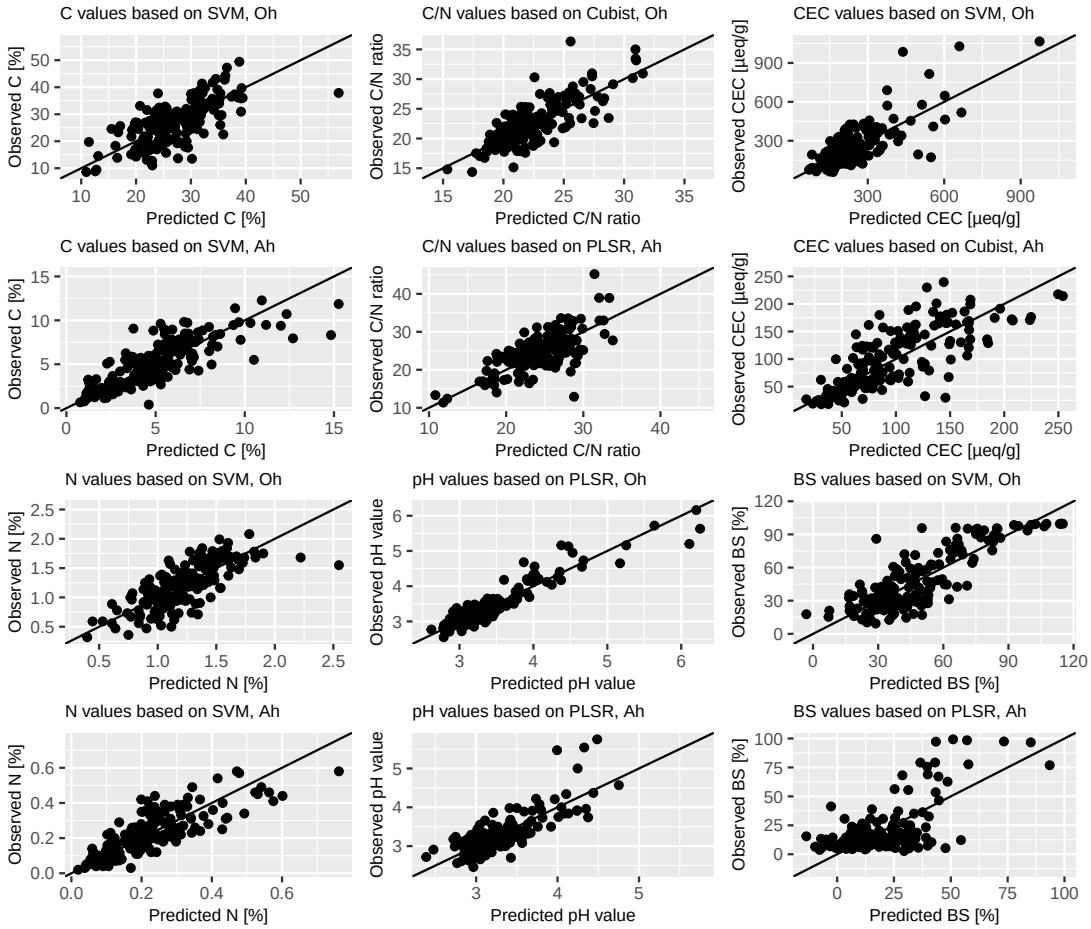


Figure 3: Best predicted and observed values of humus properties based on vis-NIR data for Oh and Ah horizon, SVM = support vector machine, plsr = partial least squares regression, CEC = cation exchange capacity, BS = base saturation

between 0.59 and 0.72 and RPIQ values of 2.22-2.54. Important features in the spectrum lay in the visual region and around 2150 and 2200 nm. For C content, the results lay within the range of similar approaches reported by Gholizadeh, Coblinski, et al. (2021) and Coûteaux et al. (2003). Investigating other land use forms, Shi et al. (2013) and Fystro (2002) reported comparable model performance for N content prediction.

Results for C/N ratio showed R^2 values of 0.5, with most important wavelengths at 450 and 2050 nm. Other studies also showed remarkable differences when comparing model results of C/N ratio to the estimation of C and N separately.

Prediction of pH values achieved R^2 values up to 0.56. Most important features in the spectrum were in the visual range and around 1900 nm. Other studies report better (Conforti et al., 2018) as well as worse (Cohen et al., 2005) model performances, leaving our results in between.

Models for cation exchange capacity reported R^2 up to 0.67 and RPIQ values up to

2.81, with most important features laying around 1900 nm as well. In comparison, Leone et al. (2012) achieved R^2 between 0.59 and 0.85. The estimation of base saturation values of the Ah horizon resulted in the lowest R^2 and RPIQ values. It is important to mention that many of the studies used for comparison here were working with samples from other land use forms (agricultural areas, grassland) or from different depths. The direct comparison to investigations focusing on upper mineral soil of forested areas only was difficult due to lack of existing studies, again emphasizing the importance of the study itself.
For the assessment of the results with respect to practical application, the Oh samples were classified based on measured and predicted pH values, and a confusion matrix was calculated. The balanced accuracy was between 0.5 and 0.87. Therefore, we conclude that the predicted values can be used for classification purposes. However, acidic conditions are over-represented in our data set and the majority of the samples belonged to two of the classes. This limits the meaningfulness of the results of the less acidic classes.

4.2 Application of low-cost MEMS spectrometers for forest topsoil properties prediction (manuscript 2)

The data collected with the different devices showed distinct spectra. The investigation showed that the Hamamatsu and Veris spectra both showed the expected steady ascent of reflectance in the visual range. In the NIR-range, the important feature dips around 1400 as well as around 1900 nm could be detected in both measured spectra using the Neospectra as well as in the full-range device spectra. Raw and pre-processed spectra from all soil samples collected with the different devices can be seen in figure 4. The pre-processing procedure emphasized the described trends for spectra from all devices.
The data recorded with the different devices was used to predict total C and N content based on regional and local data using partial least squares regression and Cubist.
The regional models for C content were most accurate using Cubist regression. Furthermore, approaches using the combination of the visual and near-infrared range outperformed the models that only used solely one of the available ranges. Model results achieved RPIQ values between 1.48 and 1.96 for Oh horizon. The models for Ah horizon were more precise with RPIQ values between 1.67 and 2.05. The usage of the visual range solely did result in the least accurate model predictions.
In direct comparison, models based on visual and NIR range data recorded using

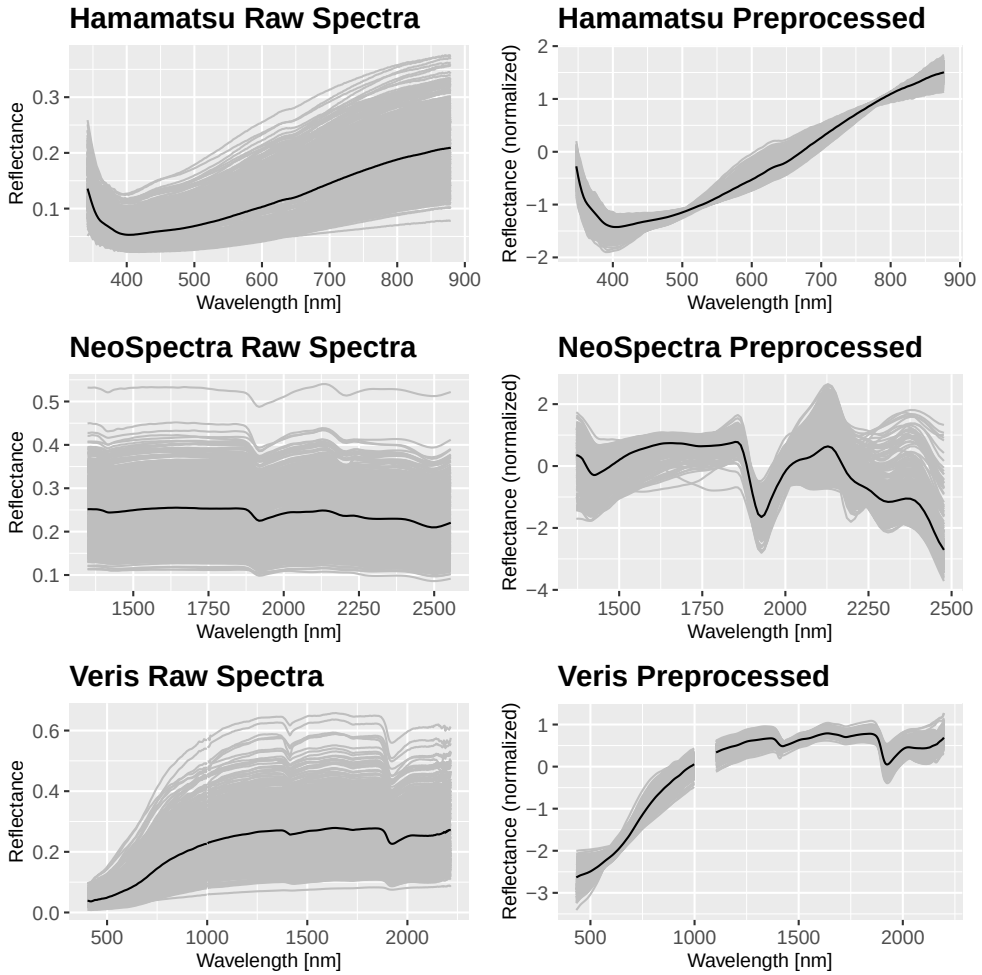


Figure 4: Raw and pre-processed reflectance spectra of forest soil samples collected with MEMS (Hamamatsu, Neospectra) and conventional spectrometer (Veris) devices

MEMS devices were able to reach 105% of the full-range models R^2 value for Oh horizon. For Ah horizon, 89% of the full-range devices R^2 value was reported. For the models based on the visual range only, these values were lower with 69% (Oh) and 58% (Ah), respectively.

The models using data from both horizons combined for calibration achieved much better model performance indicated by the error measure values. However, the difference can be explained with the larger data ranges resulting from combining the horizons. Improvements in root mean square error (RMSE) values were less remarkable. Here, RPIQ values ranged from 3.47 for partial least squares regression models based on the visual range, up to 4.6 for Cubist regression using Neospectra data, and 5.38 when using the full-range device. In direct comparison, the models based on MEMS devices were able to reach 95% of the full range models R^2 (combined: $R^2 = 0.84$, Veris: $R^2 = 0.89$). Surprisingly, the approach

based solely on NIR data performed better and the addition of spectra form the visual range resulted in less accuracy. For the local data set, similar observations could be made regarding the used wavelength ranges. Models based on visual range were less precise than models including the NIR region. For Ah horizon, RPIQ values reached between 1.66 and 4.22, with R^2 values up to 0.89. No preference regarding the applied algorithms could be made. For the Ah horizon, the data from combined MEMS devices resulted in comparable accuracy when using Cubist for C content prediction. In fact, both models reported R^2 of 0.68. Therefore 100 % of the full range devices accuracy was achieved by models built on spectra recorded by the MEMS devices.

Regarding the prediction of N content on regional scale, the Cubist models for Oh horizon based on the full range data resulted in the most precise results (RMSE = 0.25, R^2 = 0.66, RPIQ = 2.64). Models based on the MEMS device in the visual range showed least accuracy while the results including NIR data were comparably, with R^2 of 0.61 and 0.57, respectively. In direct comparison, 85% of the R^2 of the full-range model were reached. For the mineral soil samples, the full range data yielded the most precise results with R^2 = 0.78. Models based on the NIR data recorded with the MEMS device achieved R^2 = 0.54, which corresponds to 69%. In both cases, the addition of data from the visual range did not improve model results. In the approach modeling both horizons together, Cubist regression outperformed partial least squares regression. Best results were achieved by the full-range device (R^2 = 0.88), the combination of both MEMS spectrometers showed similar results (R^2 = 0.85). In direct comparison, this means that 96% of the full-range devices precision could be reached using data from MEMS devices. On the local scale at the study site Zellwald, the predictions for N content of mineral samples showed slightly more deviation in the model results. The combined data of the MEMS devices showed R^2 = 0.71, while the R^2 of the full range data was 0.84. This equals 85% of the full range R^2 values.

Regarding the Oh horizon of the local data set, no meaningful model could be calibrated. One reason could be the small size of the validation set. More elaborate validations techniques could help overcome this problem.

Our results indicated that the MEMS spectrometers can be used to substitute common full-range devices. For the investigated data sets and properties, especially the combination of visual and NIR range data measured with MEMS devices showed predictive performance comparable with the full-range device. In three cases, estimations even outperformed the conventional approach. Additionally, for some approaches the results achieved by usage of the NIR range solely reported

more accurate predictions, and interestingly the addition of the visual range of the spectrum reduced the precision.
The scale seemed to influence the model performance based on samples from the mineral horizons. More precise predictions could be achieved for the local study site "Zellwald" than for the regional scale using samples from the state of Saxony. It could further be observed that this difference in model performance is bigger for models built with spectra from MEMS devices. There are several reasons that could explain these deviations, for example the greater heterogeneity caused by the much larger area. In addition, the data acquisition took place during a longer period of time (years compared to one month) in different campaigns and also by different persons taking samples and measurements. Other studies came to ambiguous results in this matter. While Grunwald et al. (2018) reported increasing precision with scale, Seidel et al. (2019) and Ramirez-Lopez et al. (2013) stated that diverse geographic origins decreases model accuracy. At the time of the publication of the manuscript, only few studies were investigating the usage of MEMS devices to predict soil properties. Sharififar et al. (2019) reported results that were more precise than our results separated by horizon, but less accurate than our results based on combined horizons. Since then, more research articles came to similar results regarding the application of MEMS devices for the prediction of soil properties, but on other land use forms. Priori et al. (2022) achieved comparable results and stated that difference in performance can be explained mainly by the used wavelength range. Karyotis et al. (2021) as well stated that MEMS can be used for soil properties, reporting R^2 values of 0.8 for organic C content.
Based on the findings, a future application for in-situ measurements of forest soils seems feasible. However, the effects of water present in the samples, and the usage of unprepared sample material have to be investigated. The MEMS devices could then enhance the derivation of information about humus properties, for example as part of systematic and periodic monitoring systems. The usage could help to reduce the costs of spectral data acquisition procedures.

4.3 Integrated framework for assessment and spatial prediction of humus properties (manuscript 3)

The manuscript reports on the application of the proposed framework in a case study on the test site "Zellwald" and further presents the obtained results. The approach was implemented stepwise and was found to be suitable to obtain spatial information about humus properties on forest stand level.

The determination of sample points by conditioned Latin hypercube sampling and the data collection could be carried out successfully with the sampling design. The usage of Gowers similarity index facilitated the collection of soil material.
Chemical analysis of the collected samples was conducted in the laboratory of public enterprise Sachsenforst and revealed depleted humus conditions and very acidic pH values.
The spectral data acquisition using the protocol was found to be easy to use and robust. The collected data has been used to predict humus properties based on vis-NIR spectra using partial least squares regression and a nested cross validation procedure. The results of the chemical analysis of the soil samples as well as the predictions based on vis-NIR data can be seen in form of Box-Whisker-Plots in figure 5.

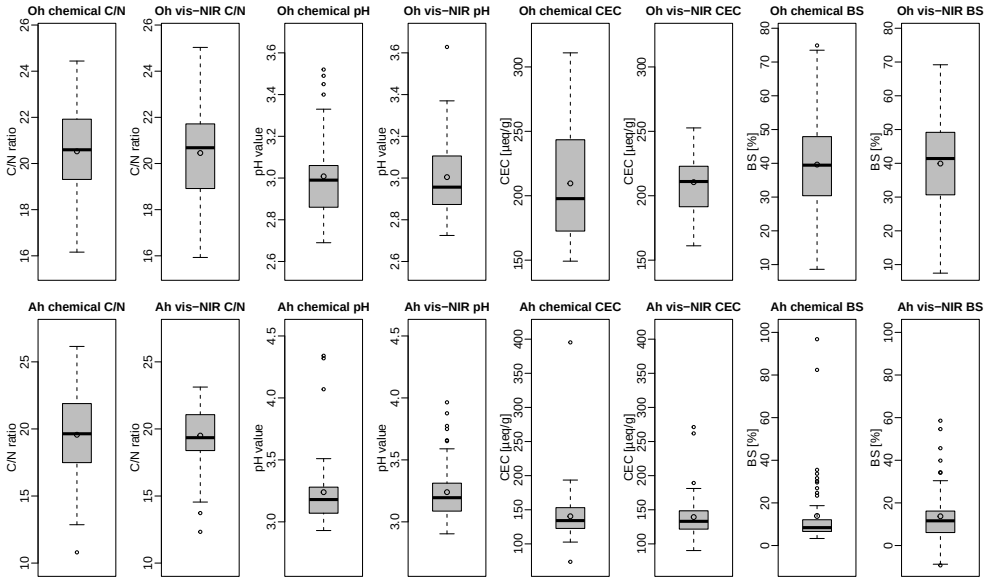


Figure 5: Data distribution of C/N, pH values, cation exchange capacity (CEC) and base saturation (BS) of chemical measurement and vis-NIR based estimations

For the Oh horizon, mean and standard deviation values of the predictions were in the same range as the chemically determined values for C/N, pH and base saturation.
Similar results were reported for samples from 0-5 cm depth. Mean of the predicted values were close to the chemically measured values. Deviations could be found in the data ranges of cation exchange capacity and base saturation, indicating inaccuracies in extreme values.
The last and most important step of the framework was the spatial prediction and creation of maps in order to provide information about humus properties at forest

stand level. Random Forest models were calibrated based on chemically measured values and vis-NIR predictions and covariates based on the SCORPAN-model. Based on chemically measured values, the R^2 values of the model achieved between 0.92 (pH) and 0.94 (cation exchange capacity) in the Oh horizon and 0.91 (pH) and 0.96 (cation exchange capacity) in 0-5 cm depth.
The results of the models using vis-NIR predictions of the humus properties were similar (Oh: 0.94 - 0.95, 0-5 cm 0.9 - 0.95). As an example, the final spatial predictions of C/N ratio and pH value in the case study area can be seen in figure 6, together with the input data.
The prediction maps for C/N ratio and pH values show similar value patterns within the area, independent from the used data basis. However, the vis-NIR results show less distinct minima and maxima values, which results in a smoothed effect across the map. In the Oh layer, the normalized difference vegetation index was the most important predictor while in 0-5 cm depth, also climate variables were amongst the covariates with the most influence.
In accordance with the most important predictors, the observable patterns in the prediction maps match with the spatial distribution of coniferous and deciduous tree species. Areas forested with deciduous trees show lower C/N ratios and higher pH values.
For cation exchange capacity, the predicted values showed less distinct values, the pattern resemble more to the climate based predictors. These are also the most important covariates. In the 0-5 cm depth, the data range is narrow, with little differences between the chemical and predicted data basis.
Base saturation maps in Oh horizon showed similar patterns for both approaches as well, with climate data being most important. In the 0-5 cm depth, the predictions resulted in little variation. Important predictors were different depending on the data basis. Here, more investigations focusing on the existing correlations should be done.
If used within the framework, vis-NIR spectroscopy has the potential to reduce the required amount of chemical analysis. In this case, it is not necessary to use all data for model calibration. Instead, a small percentage could be used for calibration, and the rest of the samples properties can then be estimated. If the procedure is repeated, it is also possible to make use of the previously built spectral database. The performance of the spectral modelling step using partial least squares regression was satisfying for C/N ratio, pH value and base saturation. The prediction resulted in RMSE values that are reasonable in context of data range and study area. Higher uncertainties were found for cation exchange

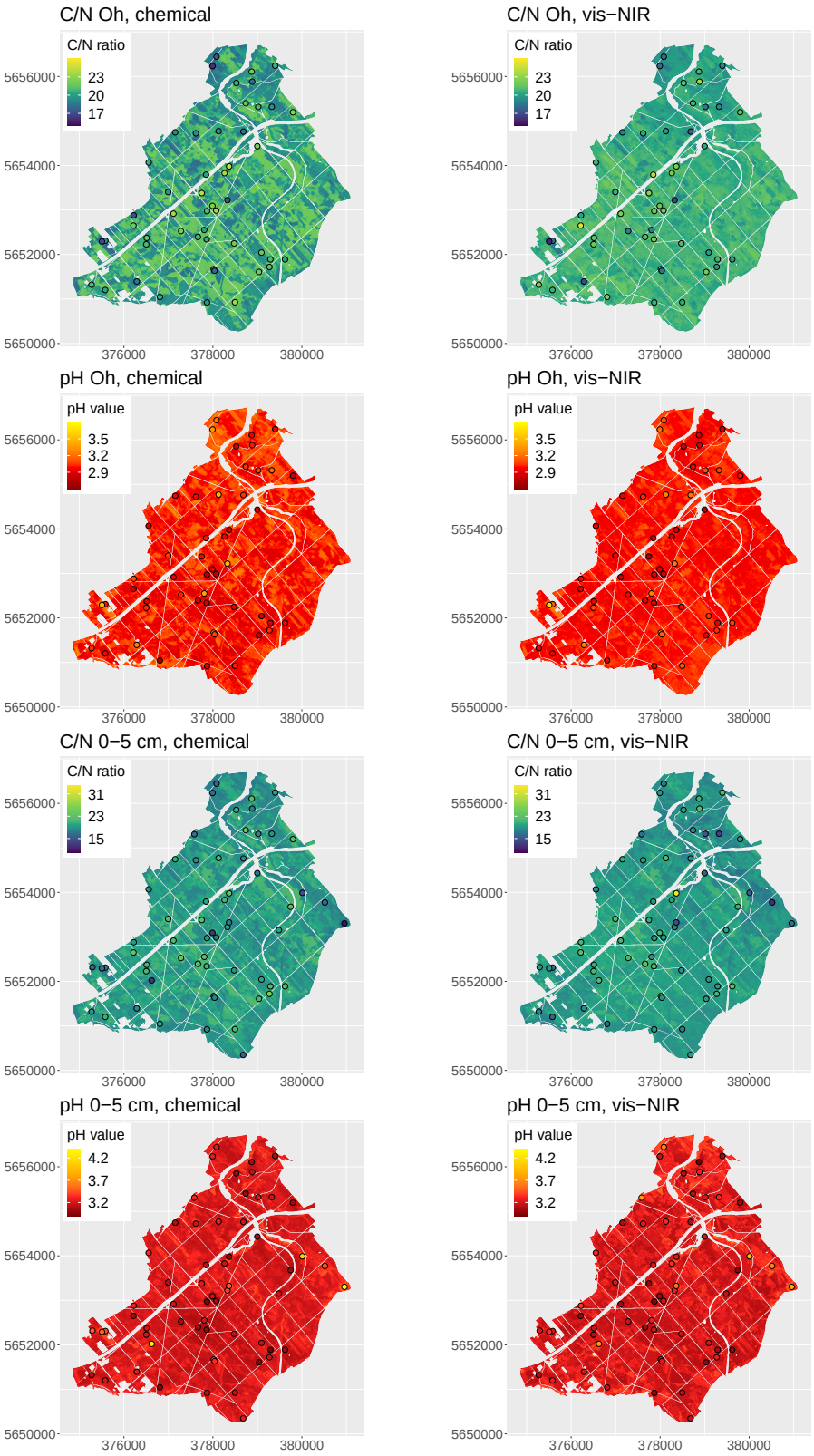


Figure 6: Final map of C/N ratio and pH values of Oh horizon and 0-5 cm depth at forest stand level in the case study area "Zellwald", including measured input values at the sampling points

capacity in the Oh horizon, where R^2 values were low and deviations to the chemically measured values were higher. We expected a stronger correlation to the vis-NIR spectra. The underlying correlations seem to be complex and are not fully understood.

More research is needed, investigating the correlations to the spectra or to other soil properties that could act as proxy. The correlation could also depend on particle size, which was not investigated in this work.

Only a few other studies focus on the spatial prediction of humus properties and the provision of data at the forest stand level. Using digital soil mapping approaches, Zirlewagen et al. (2007) assessed forest health conditions based on soil topography and vegetation data. Focusing on soil, Heitkamp et al. (2020) mapped soil nutrient regimes, Blackford et al. (2021) predicted soil moisture regime and textural class while Hanes et al. (2022) focused on organic layer thickness. However, all these studies had objectives different from our study but highlight the beginning usage of digital soil mapping for various fields of forest assessment. As the presented framework is able to provide information about humus properties at the forest stand level, it could increase data availability, whilst produced maps could be used to facilitate forest management decisions. Current schemes do not provide information at this spatial scale. Based on the computed information, direct recommendations for a possible course of action in the case study area can be derived. For example, the spatially available pH values make conclusions about acidification processes possible, which have impact on fine root systems and plant germination procedures. As we found very depleted conditions, the most important recommendation is to focus on mitigation strategies in order to restore natural soil quality. This could be done by improving rooting conditions by strip milling and initial liming. With longer perspective, unwanted low pH and high C/N values can be handled by tree species selection.

The framework can be seen as ready to use when data from chemical laboratory is available. In order to reduce the amount of laboratory work, the usage of vis-NIR predictions was investigated. It is however important to mention that uncertainty introduced by the vis-NIR modelling step could not be quantified. It would be beneficial to test the approach while using larger spectral libraries as additional data sources as well as use larger study areas to further assess the framework.

We conclude that the presented workflow is feasible and can be used to close data gaps regarding the provision of spatial information on humus properties at the forest stand scale. It was additionally applied in a case study, including the derivation of recommendations for forest management based on the findings.

The possibility of using vis-NIR predictions within the framework in order to reduce the amount of needed laboratory work showed that it is principally possible to substitute parts of the chemical analysis. The possible cost reduction however comes with less precise predictions and smoothed pattern in the produced maps. Finally, we demonstrated the potential usage of the derived data to show an exemplary course of action for the management of the case study area. By this, we were able to highlight the value of the provided information for the practical application.

5 Conclusion

This thesis main objectives were to investigate the application of vis-NIR spectroscopy to estimate humus properties of forest soils. The presented studies analyzed different aspects of the topic, covering several properties, the performance of different algorithms, the usage of various devices as well as possible utilisation for practical application in forest management strategies.

In manuscript 1, we could demonstrate that vis-NIR spectra can be used to predict humus properties of forest soils in Saxony. Distinct absorbance features could be detected when comparing the recorded spectra from Oh and Ah horizons. These differences primary lay in regions known for their sensitivity regarding organic matter. This highlights the relevance of the samples composition regarding the usage of vis-NIR for the estimation of properties. In Oh horizon, predicted values were most useful for N content, C/N ratio, pH value and base saturation, while C content and cation exchange capacity showed less prediction accuracy. In Ah horizons, satisfying accuracy in predictions could be found for C and N content as well as pH value and cation exchange capacity, but less precise results for C/N ratio and base saturation.

Within the conducted studies, we had the opportunity to compare the prediction performance of different regression models and machine learning methods (manuscript 1 and 2). However, no clear result could be achieved in favour for one of the used algorithms. The best performing method was often dependent on the investigated properties and soil horizons. In manuscript 2, Cubist performed better at the regional scale. Generally, the prediction performance was often comparable as the achieved model accuracy lay within the same range. It seems to be useful to apply several methods to be able to select the most precise results, especially when investigating several properties at different depths.

Manuscript 2 assessed novel MEMS spectrometers with regards of their applicability for predicting humus properties (C and N content), using different wavelength ranges and comparing the results to conventional devices. It could be shown that MEMS spectrometer can be successfully used to predict C and N content of humus samples from forest soils. Especially the combination of spectra from both MEMS devices, covering the visual and the NIR range can compete with data collected with a conventional spectrometer. The usage of the visual range solely was not sufficient.

The influence of the spatial scale on the model performance was investigated as well. It could be shown that the estimated properties were more precise for the local data set when compared to the regional scale covering the state of Saxony,

possibly due to the greater variability in the data set and differences in data acquisition.

Furthermore, manuscript 3 presented a digital soil mapping framework to spatially predict humus properties at forest stand level. It was tested and assessed in a case study on a study site in Saxony. We conclude that the procedure is feasible and can be used to derive spatial information about humus conditions. The provision of this data is a great improvement regarding data availability, as current mapping schemes do not provide any information about humus properties at this spatial scale.

To get a more profound assessment of the usage of vis-NIR spectroscopy for practical applications, prediction based on vis-NIR spectra were integrated into the framework, as this could reduce the amount of needed chemical analysis. Reasonable results were achieved for C/N, pH value and base saturation. The reduction of laboratory analysis however comes with less precise spatial prediction results, and the variation of the properties appears to be smoothed in comparison to the output of the models based on chemically measured values.

The results of the spatial prediction were exemplary assessed with respect to their potential use to support decision making in forest management. Our results showed degraded humus conditions within the area of the case study. Based on the derived findings, we were able to propose a possible course of action to face the situation and to restore more favourable soil conditions. This underlines the potential value of the work from a practical point of view.

Things to keep in mind are the difficulties that occurred within the investigations presented in the manuscripts. In some of the approaches, the model results included a wide range of predictive performance, dependant on the humus property. Especially for more complicated properties with no direct spectral assignment (cation exchange capacity, base saturation), the accuracy of the results varied. Further research regarding correlations between spectral signatures and humus properties could be helpful in order to improve the accuracy of the predictions. It could also be helpful to further look into correlations between the humus properties to detect if some predictions are based on the correlation to another spectral active substance of content. For this, information about particle size and distribution could be useful as well.

The usage of bigger data sets and new approaches like spiking existing spectral libraries with few samples of local study areas could as well improve the general quality of predictions and reduce the amount of field and laboratory work. Recently published investigations presented new innovative ways of using large libraries for

predictions at local scale (Luce et al., 2022) and new methods to reduce noise in spectra, reduce their dimensionality while increasing interpretability of model results (Behrens et al., 2022). The fast developments in the field of machine learning will result in more accurate results in the future due to increasingly powerful information extraction from the soil spectra (Viscarra Rossel et al., 2022).

Similar conclusion can be drawn for the spatial prediction of the humus properties. The SCORPAN model is widely used for digital soil mapping, but more research regarding correlations between predictors and humus properties especially of forest soils could be helpful in order to improve the quality of the spatial predictions in forest stands. Investigations on larger scales would also be desirable as they could cover more soil and vegetation types and therefore allow for more general assessment of the procedure.

Finally, this work shows that vis-NIR spectroscopy has great potential and can be used to predict humus properties of forest soils. Linked with digital soil mapping approaches, it can increase the data availability, especially on forest stand level, and its application could complement current mapping schemes. This can be helpful to face current challenges of implementing reliable monitoring systems for forest soils. Such systems are dependant on reliable data sources and can profit from the possibilities that vis-NIR spectroscopy and digital soil mapping are offering. The results can furthermore be useful to support management decisions in order to deal with the challenges that forestry in Europe is currently facing.

References

Anderegg, W. R., Trugman, A. T., Badgley, G., Konings, A. G., & Shaw, J. (2020). Divergent forest sensitivity to repeated extreme droughts. *Nature Climate Change*, *10*(12), 1091–1095.

Askari, M. S., O'Rourke, S. M., & Holden, N. M. (2015). Evaluation of soil quality for agricultural production using visible–near-infrared spectroscopy. *Geoderma*, *243*, 80–91.

Augusto, L., Bonnaud, P., & Ranger, J. (1998). Impact of tree species on forest soil acidification. *Forest Ecology and Management*, *105*(1-3), 67–78.

Baruck, J., Nestroy, O., Sartori, G., Baize, D., Traidl, R., Vrščaj, B., Bräm, E., Gruber, F. E., Heinrich, K., & Geitner, C. (2016). Soil classification and mapping in the alps: The current state and future challenges. *Geoderma*, *264*, 312–331.

Beć, K. B., Grabska, J., & Huck, C. W. (2021). Principles and applications of miniaturized near-infrared (nir) spectrometers. *Chemistry–A European Journal*, *27*(5), 1514–1532.

Becker, C., Thomas, F., Petzold, R., & Werban, U. (2022). *Räumliche prognose der humuseigenschaften von waldböden mittels vis-nir-spektroskopie und digitaler bodenkartierung* (tech. rep.).

Behre, K.-E. (1988). The role of man in european vegetation history. *Vegetation history* (pp. 633–672). Springer.

Behrens, T., Schmidt, K., Ramirez-Lopez, L., Gallant, J., Zhu, A., & Scholten, T. (2014). Hyper-scale digital soil mapping and soil formation analysis. *Geoderma*, *213*, 578–588.

Behrens, T., Rossel, R. A. V., Ramirez-Lopez, L., & Baumann, P. (2022). Soil spectroscopy with the gaussian pyramid scale space. *Geoderma*, *426*, 116095.

Ben-Dor, E., & Banin, A. (1995). Near-infrared analysis as a rapid method to simultaneously evaluate several soil properties. *Soil Science Society of America Journal*, *59*(2), 364–372.

Binkley, D., & Fisher, R. F. (2020). *Ecology and management of forest soils* (5th edition). Wiley: Hoboken, NJ, USA.

Blackford, C., Heung, B., Baldwin, K., Fleming, R. L., Hazlett, P. W., Morris, D. M., Uhlig, P. W., & Webster, K. L. (2021). Digital soil mapping workflow for forest resource applications: A case study in the hearst forest, ontario. *Canadian Journal of Forest Research*, *51*(1), 59–77.

Böhner, J., Koethe, R., Conrad, O., Gross, J., Ringeler, A., & Selige, T. (2001). Soil regionalisation by means of terrain analysis and process parameterisation. *Soil classification*, *7*, 213.

Borůvka, L., Mládková, L., Penížek, V., Drábek, O., & Vašát, R. (2007). Forest soil acidification assessment using principal component analysis and geostatistics. *Geoderma*, *140*(4), 374–382.

Bowers, S., & Hanks, R. (1965). Reflection of radiant energy form soil. *Soil Science*, *100*, 130–138.

Breiman, L. (2001). Random forests. *Machine learning*, *45*(1), 5–32.

Burns, D. A., & Ciurczak, E. W. (2007). *Handbook of near-infrared analysis*. CRC press.

Chang, C.-W., Laird, D. A., Mausbach, M. J., & Hurburgh, C. R. (2001). Near-infrared reflectance spectroscopy–principal components regression analyses of soil properties. *Soil Science Society of America Journal*, *65*(2), 480–490.

Chodak, M., Ludwig, B., Khanna, P., & Beese, F. (2002). Use of near infrared spectroscopy to determine biological and chemical characteristics of organic layers under spruce and beech stands. *Journal of Plant Nutrition and Soil Science*, *165*(1), 27–33.

Cohen, M. J., Prenger, J. P., & DeBusk, W. F. (2005). Visible-near infrared reflectance spectroscopy for rapid, nondestructive assessment of wetland soil quality. *Journal of environmental quality*, *34*(4), 1422–1434.

Conforti, M., Matteucci, G., & Buttafuoco, G. (2018). Using laboratory vis-nir spectroscopy for monitoring some forest soil properties. *Journal of soils and sediments*, *18*(3), 1009–1019.

Cortes, C., & Vapnik, V. (1995). Support-vector networks. *Machine learning*, *20*(3), 273–297.

Coûteaux, M.-M., Berg, B., & Rovira, P. (2003). Near infrared reflectance spectroscopy for determination of organic matter fractions including microbial biomass in coniferous forest soils. *Soil Biology and Biochemistry*, *35*(12), 1587–1600.

De Vries, W., Dobbertin, M., Solberg, S., Van Dobben, H., & Schaub, M. (2014). Impacts of acid deposition, ozone exposure and weather conditions on forest ecosystems in europe: An overview. *Plant and Soil*, *380*(1), 1–45.

de Santana, F. B., Otani, S. K., de Souza, A. M., & Poppi, R. J. (2021). Comparison of pls and svm models for soil organic matter and particle size using vis-nir spectral libraries. *Geoderma Regional*, *27*, e00436.

Dokuchaev, V. (1883). *The russian chernozem*. Report to the freee economic society, St. Petersburg.

Dotto, A. C., Dalmolin, R. S. D., Grunwald, S., ten Caten, A., & Pereira Filho, W. (2017). Two preprocessing techniques to reduce model covariables in soil property predictions by vis-nir spectroscopy. *Soil and Tillage Research*, *172*, 59–68.

Filzmoser, P., Garrett, R. G., & Reimann, C. (2005). Multivariate outlier detection in exploration geochemistry. *Computers & geosciences*, *31*(5), 579–587.

Food and Agriculture Organization of the United Nations. (2020). *Global forest resources assessment 2020: Main report*. Food & Agriculture Organization of the UN.

Fystro, G. (2002). The prediction of c and n content and their potential mineralisation in heterogeneous soil samples using vis–nir spectroscopy and comparative methods. *Plant and soil*, *246*(2), 139–149.

Gholizadeh, A., Coblinski, J. A., Saberioon, M., Ben-Dor, E., Drábek, O., Demattê, J. A., Borůvka, L., Němeček, K., Chabrillat, S., & Dajčl, J. (2021). Vis–nir and xrf data fusion and feature selection to estimate potentially toxic elements in soil. *Sensors*, *21*(7), 2386.

Gholizadeh, A., Saberioon, M., Rossel, R. A. V., Boruvka, L., & Klement, A. (2020). Spectroscopic measurements and imaging of soil colour for field scale estimation of soil organic carbon. *Geoderma*, *357*, 113972.

Gholizadeh, A., Viscarra Rossel, R., Saberioon, M., Borůvka, J. K., Luboš Ktatina, & Pavlů, L. (2021). National-scale spectroscopic assessment of soil organic carbon in forests of the czech republic. *Geoderma*, *385*, 114832.

Gogé, F., Gomez, C., Jolivet, C., & Joffre, R. (2014). Which strategy is best to predict soil properties of a local site from a national vis–nir database? *Geoderma*, *213*, 1–9.

Grunwald, S., Congrong, Y., & Xiong, X. (2018). Transferability and scalability of soil total carbon prediction models in florida, usa. *Pedosphere*, *28*(6), 856–872.

Gubler, A. (2011). *Quantitative estimations of soil properties by visible and near infrared spectroscopy: Applications for laboratory and field measurements* (Doctoral dissertation). University of Bern, Bern, Switzerland.

Guo, P., Li, T., Gao, H., Chen, X., Cui, Y., & Huang, Y. (2021). Evaluating calibration and spectral variable selection methods for predicting three soil nutrients using vis-nir spectroscopy. *Remote Sensing*, *13*(19), 4000.

Gutachterausschuss Forstliche Analytik. (2014). Handbuch Forstliche Analytik. Eine Loseblatt-Sammlung der Analysemethoden im Forstbereich.

Haghi, R., Pérez-Fernández, E., & Robertson, A. (2021). Prediction of various soil properties for a national spatial dataset of scottish soils based on four different chemometric approaches: A comparison of near infrared and mid-infrared spectroscopy. *Geoderma*, *396*, 115071.

Hanes, C., Wotton, M., Woolford, D., Martell, D., & Flannigan, M. (2022). Mapping organic layer thickness and fuel load of the boreal forest in alberta, canada. *Geoderma*, *417*, 115827.

Heitkamp, F., Ahrends, B., Evers, J., Steinicke, C., & Meesenburg, H. (2020). Inference of forest soil nutrient regimes by integrating soil chemistry with fuzzy-logic: Regionwide application for stakeholders of hesse, germany. *Geoderma Regional*, *23*, e00340.

Hintschich, S., Pügner, T., Knobbe, J., Schröder, J., Reinig, P., Grüger, H., & Schenk, H. (2014). Mems-based miniature near-infrared spectrometer for application in environmental and food monitoring. *International Journal on Smart Sensing and Intelligent Systems*, *7*(5), 1–5.

Hudson, B. D. (1992). The soil survey as paradigm-based science. *Soil Science Society of America Journal*, *56*(3).

Hunt, G. R. (1977). Spectral signatures of particulate minerals in the visible and near infrared. *Geophysics*, *42*(3), 501–513.

Hutengs, C., Seidel, M., Oertel, F., Ludwig, B., & Vohland, M. (2019). In situ and laboratory soil spectroscopy with portable visible-to-near-infrared and mid-infrared instruments for the assessment of organic carbon in soils. *Geoderma*, *355*, 113900.

Jandl, R., Spathelf, P., Bolte, A., & Prescott, C. E. (2019). Forest adaptation to climate change—is non-management an option? *Annals of forest science*, *76*(2), 1–13.

Jenny, H. (1941). Factors of soil formation: A system of quantitative pedology new york. *Macgraw Hill*.

Jiang, Q., Chen, Y., Guo, L., Fei, T., & Qi, K. (2016). Estimating soil organic carbon of cropland soil at different levels of soil moisture using vis-nir spectroscopy. *Remote Sensing*, *8*(9), 755.

Karyotis, K., Angelopoulou, T., Tziolas, N., Palaiologou, E., Samarinas, N., & Zalidis, G. (2021). Evaluation of a micro-electro mechanical systems spectral sensor for soil properties estimation. *Land*, *10*(1), 63.

Kazda, M., & Zvacek, L. (1989). Aluminium and manganese and their relation to calcium in soil solution and needles in three norway spruce (picea abies, l. karst.) stands of upper austria. *Plant and Soil*, *114*, 257–267.

Keenan, R. J. (2015). Climate change impacts and adaptation in forest management: A review. *Annals of forest science*, *72*, 145–167.

Lechner, A. M., Foody, G. M., & Boyd, D. S. (2020). Applications in remote sensing to forest ecology and management. *One Earth*, *2*(5), 405–412.

Leone, A., Viscarra-Rossel, R., Amenta, P., & Buondonno, A. (2012). Prediction of soil properties with plsr and vis-nir spectroscopy: Application to mediterranean soils from southern italy. *Current Analytical Chemistry*, *8*(2), 283–299.

Lindner, M., Maroschek, M., Netherer, S., Kremer, A., Barbati, A., Garcia-Gonzalo, J., Seidl, R., Delzon, S., Corona, P., Kolström, M., et al. (2010). Climate change impacts, adaptive capacity, and vulnerability of european forest ecosystems. *Forest ecology and management*, *259*(4), 698–709.

Liu, S., Shen, H., Chen, S., Zhao, X., Biswas, A., Jia, X., Shi, Z., & Fang, J. (2019). Estimating forest soil organic carbon content using vis-nir spectroscopy: Implications for large-scale soil carbon spectroscopic assessment. *Geoderma*, *348*, 37–44.

Luce, M. S., Ziadi, N., & Rossel, R. A. V. (2022). Global-local: A new approach for local predictions of soil organic carbon content using large soil spectral libraries. *Geoderma*, *425*, 116048.

Ludwig, B., Khanna, P., Bauhus, J., & Hopmans, P. (2002). Near infrared spectroscopy of forest soils to determine chemical and biological properties related to soil sustainability. *Forest Ecology and Management*, *171*(1-2), 121–132.

Mahmood, H. S., Hoogmoed, W. B., & van Henten, E. J. (2012). Sensor data fusion to predict multiple soil properties. *Precision Agriculture*, *13*, 628–645.

McBratney, A. B., Santos, M. M., & Minasny, B. (2003). On digital soil mapping. *Geoderma*, *117*(1-2), 3–52.

Meesenburg, H., Riek, W., Ahrends, B., Eickenscheidt, N., Grüneberg, E., Evers, J., Fortmann, H., König, N., Lauer, A., Meiwes, K. J., et al. (2019). Soil acidification in german forest soils. *Status and Dynamics of Forests in Germany: Results of the National Forest Monitoring*, 93–121.

Minasny, B., & McBratney, A. B. (2006). A conditioned latin hypercube method for sampling in the presence of ancillary information. *Computers & geosciences*, *32*(9), 1378–1388.

Morellos, A., Pantazi, X.-E., Moshou, D., Alexandridis, T., Whetton, R., Tziotzios, G., Wiebensohn, J., Bill, R., & Mouazen, A. M. (2016). Machine learning based prediction of soil total nitrogen, organic carbon and moisture content by using vis-nir spectroscopy. *Biosystems Engineering*, *152*, 104–116.

Mouazen, A., Maleki, M., De Baerdemaeker, J., & Ramon, H. (2007). On-line measurement of some selected soil properties using a vis–nir sensor. *Soil and Tillage Research*, *93*(1), 13–27.

Müller, A. C., Guido, S. et al. (2016). *Introduction to machine learning with python: A guide for data scientists* (1st Edition). O'Reilly Media, Inc.: Newton, MA, USA.

Nocita, M., Stevens, A., Toth, G., Panagos, P., van Wesemael, B., & Montanarella, L. (2014). Prediction of soil organic carbon content by diffuse reflectance spectroscopy using a local partial least square regression approach. *Soil Biology and Biochemistry*, *68*, 337–347.

O'Hara, K. L. (2016). What is close-to-nature silviculture in a changing world? *Forestry: An International Journal of Forest Research*, *89*(1), 1–6.

Pietrzykowski, M., & Chodak, M. (2014). Near infrared spectroscopy—a tool for chemical properties and organic matter assessment of afforested mine soils. *Ecological engineering*, *62*, 115–122.

Priori, S., Bianconi, N., & Costantini, E. A. (2014). Can γ-radiometrics predict soil textural data and stoniness in different parent materials? a comparison of two machine-learning methods. *Geoderma*, *226*, 354–364.

Priori, S., Mzid, N., Pascucci, S., Pignatti, S., & Casa, R. (2022). Performance of a portable ft-nir mems spectrometer to predict soil features. *Soil Systems*, *6*(3), 66.

Qian, H., & Klinka, K. (1995). Spatial variability of humus forms in some coastal forest ecosystems of british columbia. *Annales des sciences forestières*, *52*(6), 653–666.

Quinlan, J. R. et al. (1992). Learning with continuous classes. *5th Australian joint conference on artificial intelligence*, *92*, 343–348.

Ramirez-Lopez, L., Behrens, T., Schmidt, K., Stevens, A., Demattê, J. A. M., & Scholten, T. (2013). The spectrum-based learner: A new local approach for modeling soil vis–nir spectra of complex datasets. *Geoderma*, *195*, 268–279.

Reeves III, J. B. (2010). Near-versus mid-infrared diffuse reflectance spectroscopy for soil analysis emphasizing carbon and laboratory versus on-site analysis: Where are we and what needs to be done? *Geoderma*, *158*(1-2), 3–14.

Rentschler, T. (2021). *Explainable machine learning in soil mapping: Peeking into the black box* (Doctoral dissertation). Universität Tübingen.

Richter, D. (1986). Sources of acidity in some forested udults. *Soil Science Society of America Journal*, *50*(6), 1584–1589.

Rinnan, Å., Van Den Berg, F., & Engelsen, S. B. (2009). Review of the most common pre-processing techniques for near-infrared spectra. *TrAC Trends in Analytical Chemistry*, *28*(10), 1201–1222.

Roberts, D. W. (1986). Ordination on the basis of fuzzy set theory. *Vegetatio*, *66*(3), 123–131.

Rossel, R. V., Adamchuk, V., Sudduth, K., McKenzie, N., & Lobsey, C. (2011). Proximal soil sensing: An effective approach for soil measurements in space and time. *Advances in agronomy* (pp. 243–291). Elsevier: Amsterdam, The Netherlands.

Rossel, R. V., & Behrens, T. (2010). Using data mining to model and interpret soil diffuse reflectance spectra. *Geoderma*, *158*(1-2), 46–54.

Rossel, R. V., Cattle, S., Ortega, A., & Fouad, Y. (2009). In situ measurements of soil colour, mineral composition and clay content by vis–nir spectroscopy. *Geoderma*, *150*(3-4), 253–266.

Rossel, R. V., & McBratney, A. (1998). Laboratory evaluation of a proximal sensing technique for simultaneous measurement of soil clay and water content. *Geoderma*, *85*(1), 19–39.

Rossel, R. V., Walvoort, D., McBratney, A., Janik, L. J., & Skjemstad, J. (2006). Visible, near infrared, mid infrared or combined diffuse reflectance spectroscopy for simultaneous assessment of various soil properties. *Geoderma*, *131*(1-2), 59–75.

Saey, T., De Smedt, P., De Clercq, W., Meerschman, E., Monirul Islam, M., & Van Meirvenne, M. (2013). Identifying soil patterns at different spatial scales with a multi-receiver emi sensor. *Soil Science Society of America Journal*, *77*(2), 382–390.

Sanchez, P. A., Ahamed, S., Carré, F., Hartemink, A. E., Hempel, J., Huising, J., Lagacherie, P., McBratney, A. B., McKenzie, N. J., Mendonça-Santos, M. D. L., et al. (2009). Digital soil map of the world. *Science*, *325*(5941), 680–681.

Santra, P., Sahoo, R. N., Das, B. S., Samal, R. N., Pattanaik, A. K., & Gupta, V. K. (2009). Estimation of soil hydraulic properties using proximal spectral reflectance in visible, near-infrared, and shortwave-infrared (vis–nir–swir) region. *Geoderma*, *152*(3-4), 338–349.

Savitzky, A., & Golay, M. J. (1964). Smoothing and differentiation of data by simplified least squares procedures. *Analytical chemistry*, *36*(8), 1627–1639.

Schöpp, W., Posch, M., Mylona, S., & Johansson, M. (2003). Long-term development of acid deposition (1880–2030) in sensitive freshwater regions in europe. *Hydrology and Earth System Sciences*, *7*(4), 436–446.

Schuldt, B., Buras, A., Arend, M., Vitasse, Y., Beierkuhnlein, C., Damm, A., Gharun, M., Grams, T. E., Hauck, M., Hajek, P., et al. (2020). A first assessment of the impact of the extreme 2018 summer drought on central european forests. *Basic and Applied Ecology*, (45), 86–103.

Schulze and Kopp. (2013). Anleitung für die forstliche Standortserkundung im nordostdeutschen Tiefland. *Standortserkundungsanleitung 95*.

Scornet, E., Biau, G., Vert, J., et al. (2015). Consistency of random forests. *The Annals of Statistics*, *43*(4), 1716–1741.

Seidel, M., Hutengs, C., Ludwig, B., Thiele-Bruhn, S., & Vohland, M. (2019). Strategies for the efficient estimation of soil organic carbon at the field scale with vis-nir spectroscopy: Spectral libraries and spiking vs. local calibrations. *Geoderma*, *354*, 113856.

Senf, C., Buras, A., Zang, C. S., Rammig, A., & Seidl, R. (2020). Excess forest mortality is consistently linked to drought across europe. *Nature communications*, *11*(1), 6200.

Sharififar, A., Singh, K., Jones, E., Ginting, F. I., & Minasny, B. (2019). Evaluating a low-cost portable nir spectrometer for the prediction of soil organic and total carbon using different calibration models. *Soil Use and Management*, *35*(4), 607–616.

Shi, T., Cui, L., Wang, J., Fei, T., Chen, Y., & Wu, G. (2013). Comparison of multivariate methods for estimating soil total nitrogen with visible/near-infrared spectroscopy. *Plant and soil*, *366*(1-2), 363–375.

Siesler, H. W., Kawata, S., Heise, H. M., & Ozaki, Y. (2008). *Near-infrared spectroscopy: Principles, instruments, applications*. John Wiley & Sons.

Silva, E. B., Giasson, É., Dotto, A. C., Caten, A. t., Demattê, J. A. M., Bacic, I. L. Z., & Veiga, M. d. (2019). A regional legacy soil dataset for prediction of sand and clay content with vis-nir-swir, in southern brazil. *Revista Brasileira de Ciencia Do Solo*, *43*.

Soriano-Disla, J. M., Janik, L. J., Viscarra Rossel, R. A., Macdonald, L. M., & McLaughlin, M. J. (2014). The performance of visible, near-, and mid-infrared reflectance spectroscopy for prediction of soil physical, chemical, and biological properties. *Applied Spectroscopy Reviews*, *49*(2), 139–186.

Stenberg, B., Rossel, R. A. V., Mouazen, A. M., & Wetterlind, J. (2010). Visible and near infrared spectroscopy in soil science. *Advances in agronomy* (pp. 163–215). Elsevier: Amsterdam, The Netherlands.

Stevens, A., Nocita, M., Tóth, G., Montanarella, L., & van Wesemael, B. (2013). Prediction of soil organic carbon at the european scale by visible and near infrared reflectance spectroscopy. *PloS one*, *8*(6), e66409.

Towett, E. K., Shepherd, K. D., & Cadisch, G. (2013). Quantification of total element concentrations in soils using total x-ray fluorescence spectroscopy (txrf). *Science of the Total Environment*, *463*, 374–388.

Van Breemen, N., & Buurman, P. (2002). *Soil formation*. Springer Science & Business Media.

Viscarra Rossel, R. A., Behrens, T., Ben-Dor, E., Chabrillat, S., Demattê, J. A. M., Ge, Y., Gomez, C., Guerrero, C., Peng, Y., Ramirez-Lopez, L., et al. (2022). Diffuse reflectance spectroscopy for estimating soil properties: A technology for the 21st century. *European Journal of Soil Science*, *73*(4), e13271.

Weihermüller, L., Huisman, J., Lambot, S., Herbst, M., & Vereecken, H. (2007). Mapping the spatial variation of soil water content at the field scale with different ground penetrating radar techniques. *Journal of hydrology*, *340*(3-4), 205–216.

Wellbrock, N., Grüneberg, E., Ziche, D., Eickenscheidt, N., Holzhausen, M., Höhle, J., Gemballa, R., & Andreae, H. (2015). *Entwicklung einer methodik zur stichprobengestützten erfassung und regionalisierung von zustandseigenschaften der waldstandorte* (Thünen Report No. 36). Johann Heinrich von Thünen-Institut. Braunschweig, Germany, Johann Heinrich von Thünen-Institut.

Wold, S., Martens, H., & Wold, H. (1983). The multivariate calibration problem in chemistry solved by the pls method. *Matrix pencils* (pp. 286–293). Springer: Cham, Siwtzerland.

Xu, D., Ma, W., Chen, S., Jiang, Q., He, K., & Shi, Z. (2018). Assessment of important soil properties related to chinese soil taxonomy based on vis–nir reflectance spectroscopy. *Computers and electronics in agriculture*, *144*, 1–8.

Yang, M., Xu, D., Chen, S., Li, H., & Shi, Z. (2019). Evaluation of machine learning approaches to predict soil organic matter and ph using vis-nir spectra. *Sensors*, *19*(2), 263.

Zevenbergen, L. W., & Thorne, C. R. (1987). Quantitative analysis of land surface topography. *Earth surface processes and landforms*, *12*(1), 47–56.

Zhang, Y., Biswas, A., Ji, W., & Adamchuk, V. I. (2017). Depth-specific prediction of soil properties in situ using vis-nir spectroscopy. *Soil Science Society of America Journal*, *81*(5), 993–1004.

Zirlewagen, D., Raben, G., & Weise, M. (2007). Zoning of forest health conditions based on a set of soil, topographic and vegetation parameters. *Forest Ecology and Management*, *248*, 43–55.

Zornoza, R., Guerrero, C., Mataix-Solera, J., Scow, K., Arcenegui, V., & Mataix-Beneyto, J. (2008). Near infrared spectroscopy for determination of various physical, chemical and biochemical properties in mediterranean soils. *Soil Biology and Biochemistry*, *40*(7), 1923–1930.

Acknowledgements

First of all i want to thank Dr. Ulrike Werban for the opportunity to work on this interesting and challenging topic within the DIGI-Humus project and for her supervision, encouragement and constructive feedback during the conduction of the measurements, the writing of the manuscripts and the peer reviewing processes.
I also thank Dr. Rainer Petzold, for his supervision within the project and his valuable suggestions and insights on forest site survey and soil science.
I am grateful to Prof. Dr. Peter Dietrich and Prof. Dr. Thomas Scholten for the supervision and evaluation of this thesis, and to Prof. Dr. Volker Hochschild, and Prof. Dr. Yvonne Oelmann for being referees in the thesis defense.
Special thanks go to Solveig Landmark for the hours of measurements in the darkness of the optical lab, and to Frankie Lehmann and his adventures which made the data acquisition a lot easier.
I appreciate the support of my colleagues of the Department Monitoring and Exploration Technologies, Hannes Mollenhauer, Marco Pohle, Helko Kotas and Paul Remmler during difficulties in the laboratory, especially with devices that were sometimes unwilling to cooperate. Further thanks to the chemical laboratory of Sachsenforst public enterprise for the chemical analysis of the soil samples collected within the project.
I also thank Daniel, Patricia, Lisa and Tristan for reviewing this thesis and helping me find inconsistencies and improve the spelling.
Last but not least, I thank my family and friends for their support, and especially Montse for always listening and encouraging me during the whole time.

Appendix

Manuscript 1

Estimating Forest Soil Properties for Humus Assessment—Is Vis-NIR the Way to Go?

Remote Sensing 14.6 (2022): 1368

Felix Thomas[1*], Rainer Petzold[2], Solveig Landmark[1], Hannes Mollenhauer[1], Carina Becker[2], Ulrike Werban[1]

[1] Department Monitoring & Exploration Technologies, Helmholtz Centre for Environmental Research—UFZ, Permoser Straße 15, 04318 Leipzig, Germany
[2] Public Enterprise Sachsenforst, Unit Site Survey, Soil Monitoring and Laboratory, Bonnewitzer Straße 34, 01796 Pirna, Germany

* Corresponding author
E-mail: felix.thomas@ufz.de

Received; 26 Januar 2022; Accepted: 9 March 2022; Published: 11 March 2022

Abstract

Recently, forest management faces new challenges resulting from increasing temperatures and drought occurrences. For sustainable, site-specific management strategies, the availability of up to date soil information is crucial. Proximal soil sensing techniques are a promising approach for rapid and inexpensive collection of data, and could facilitate the provision of the necessary information. This study evaluates the potential of visual and near-infrared spectroscopy (vis-NIRS) for estimating soil parameters relevant for humus mapping in Saxon forests. Therefore, soil samples from the organic layer are included. So far there is little knowledge about the applicability of vis-NIRS in the humus layer of forests. We investigate the spectral behaviour of samples from organic (Oh) and mineral (0–5 cm, Ah) horizons, pointing out differences in the occurring absorption features. Further, we identify and assess the accuracy of selected soil properties based on vis-NIRS for forest sites, compare the outcome of different regression methods, investigate the implications for forest soils due to the presence and different composition of the humus layer and organic horizons and interpret the results regarding their usefulness for soil mapping and monitoring purposes. For this, we used retained humus soil samples of forests from Saxony. Regression models were built with Partial Least Squares Regression, Support Vector Machine and Cubist. Investigated properties were carbon (C) and nitrogen (N) content, C/N ratio, pH value, cation exchange capacity (CEC) and base saturation (BS) due to their importance for assessing humus conditions in forests. In organic Oh horizons, prediction results for C and N content achieved R^2 values between 0.44 and 0.58, with corresponding RPIQ ranging from 1.58 to 2.06 depending on the used algorithm. Estimations of C/N ratio were more precise with $R^2 = 0.65$ and RMSE = 2.16. Best results were reported for pH value, with $R^2 = 0.90$ and RMSE = 0.20. Regarding BS, the best model accuracy was $R^2 = 0.71$, with RMSE = 13.97. In mineral topsoil, C and N content models achieved higher values of $R^2 = 0.59$ to 0.72, with RPIQ values between 2.22 and 2.54. However, prediction accuracy was lower for C/N ratio ($R^2 = 0.50$, RMSE = 3.52) and pH values ($R^2 = 0.62$, RMSE = 0.29). Models for CEC achieved $R^2 = 0.65$, with RPIQ = 2.81. In general, prediction precision varied dependent on the used algorithm, without showing clear tendencies. Classification into pH classes was exemplified since this offers a new perspective for humus mapping on forest soils. Balanced accuracy for the defined classes ranged from 0.50 to 0.87. We show that vis-NIR spectroscopy is suitable for assessing humus conditions in Saxon forests (Germany), in particular not only for mineral horizons but also for organic Oh horizons.

keywords: forest soils; vis-NIR spectroscopy; humus; machine learning; partial least squares regression; proximal soil sensing; support vector machine; cubist

Introduction

Forests in Europe are highly affected by changing environmental conditions caused by increasing annual temperatures and drought events. As a result, tree mortality increased and forest stands remain vulnerable to further impacts like insect or fungal attacks [1]. This can lead to rapidly altering forest ecosystems [2]. Further, persistently high nitrogen inputs shift the nutrient balance of forests. In order to avoid decreasing resilience of forests and loss of forest ecosystem services, this has to be addressed by management strategies. For sustainable and site-specific forest management, the availability of up to date soil information is crucial. Hereby, information is needed at desired spatial scale [3], as soil properties such as carbon content are spatially highly variable [4].

This information can support management decisions regarding tree species selection, silvicultural treatments, timber harvesting and soil protection measures [5]. However, forest soils are complex systems and it is challenging to properly describe and classify their properties and functions, in particular in the organic and the uppermost mineral soil layer [6, 7]. In the methodological approach of forest site mapping in Eastern Germany, it is common to subclassify soil properties in stable and variable components [8]. Soil properties which are stable over a time span of at least one rotation period or 100 years are mainly vinculated to parent material, physical properties and typical sequence of pedogenetic soil horizons. These properties are summarized in so called soil forms.

In contrary to this, variable properties in particular of the organic layers and upper mineral soil are defined by chemical properties, C/N-ratio, pH-value, cation exchange capacity (CEC) and base saturation (BS). Variable soil properties are consolidated in humus forms. Currently, a vegetation scheme consisting of indicator plants is used to map humus properties according to the mapping field guide for the Northeastern Lowland of Germany [8]. Element input, anthropogenic overprint in vegetation as a result of forest management and changing climate cause fast changing base conditions. Thus, the current methods have weaknesses and are increasingly questioned.

There is a substantial need for inexpensive and viable methods for periodic mapping of the variable soil properties in particular [3]. The National Forest Soil Inventory in Germany (NFSI) provides periodic information about the conditions of forest soils [9]. Its focus lies on long term observations and monitoring of the same sampling points. Its sampling raster is too coarse to assess forest stands.

Proximal soil sensing (PSS) is an interesting approach for rapid and inexpensive collection of data, and could facilitate the provision of the necessary information at

desired scale. It can be used for a better understanding of soils spatial variability [10], and for meaningful statistical analyses. One PSS technique which arouses widespread interest to provide data for soil mapping purposes is diffuse visual and near-infrared reflectance spectroscopy (vis-NIRS). It is known to be fast, cost efficient and non-destructive. Further, it does not require complex soil preparation and is suitable for estimation of several soil properties [11, 12].

Despite the widespread use on agricultural sites and mineral soils (e.g., [13, 14, 15, 16]), there are so far only few examples for applications on forest soils and humus layers. Pietrzykowski and Chodak [17] evaluated the potential of vis-NIRS to estimate, amongst other properties, soil organic carbon content (SOC), N content, C/N ratio on mineral soil samples from afforested former mining sites. They report the development of successful models for prediction, even though the studied soils differed from natural conditions in chemical and microbial properties. Ludwig et al. [18] investigated the applicability of spectroscopy to predict SOC, N content and pH value along with enzyme activities on mineral horizons in two forest sites in Germany. They used partial least squares regression (PLSR) approaches and confirmed the usefulness for SOC and N contents, but had variable results for pH-values dependent on the data range. Comparing different sensors for acquiring spectral data, Thomas et al. [19] found useful results for C and N content in Saxon forests.

On a large-scale approach across Chinese forests, Liu et al. [20] built the Chinese forest soil spectral library with high spatial heterogeneity. Samples were taken from different depths, but horizons were not separated during analysis. They were able to accurately predict SOC and confirmed the feasibility of estimating forest soil parameters based on vis-NIR spectra. Pinheiro et al. [21] reported good prediction for SOC and reasonable results for other properties including CEC in a study in the Brazilian Central Amazon. Investigating forest soils of the Czech Republic, Gholizadeh et al. [22] were able to accurately estimate SOC in organic horizons, also using material from whole soil profiles instead of investigating a specific horizon. As separation of horizons can be challenging during sample collection, an approach with sample collection at defined depths might be a solution to face this problem, as done in agriculture.

To our knowledge, there are so far no other studies investigating the applicability of vis-NIRS for prediction of N content, C/N ratio, pH value, CEC and BS on organic surface layers of forest soils. Most studies focus on mineral soil and investigate samples from other land use forms. However in terms of forest soil mapping the organic surface layer has a major role and its condition has impact on

management decisions. For humus assessment in forest management, the selected properties, including CEC and BS, are important to assess current soil conditions. Previous studies show that vis-NIR spectra are sensitive to differences in soil organic matter from different land use and vegetation forms [23]. We therefore investigate organic and mineral layers separately.
Nutrient availability is part of the basis for decision making when developing site-specific management strategies. It shall supplement or enhance current methods of vegetation-based mapping of humus properties as well as grid based periodic soil inventory. If successful, vis-NIRS raises the possibility to predict desired soil parameters without expensive chemical analyses of all collected samples. In this study, we focus on using vis-NIRS to predict selected forest soil properties that are relevant for the periodic mapping of humus properties of forest soils in Saxony. We investigate C and N content, C/N ratio, pH, CEC and BS. We apply the method to samples from the organic layer (Oh horizon, mainly humic material and decomposed plant residues with at least 30% organic substance) and mineral soil samples (0–5 cm, Ah horizon with less than 30% organic substance). Within this scope, the objectives are (i) to identify and assess the accuracy of estimations of selected soil properties based on vis-NIRS for forest sites in the state of Saxony (Germany) using different algorithms, (ii) investigate the implications for forest soils due to the different composition of the humus layer and organic horizons and (iii) discuss options for the usage of vis-NIRS predictions for classification and soil monitoring purposes.

Methods

Study Area

For this study, retained soil samples from forest sites in Saxony (Germany, approx. 17,400 km^2, with 5209 km^2 covered by forests) were used. Data collection took place within the periodic NFSI between 2006 and 2014 in a grid-based approach and during a previous study at forest sites representing the typical natural areas lowland, hilly terrain and middle mountain range [24].
An overview of the locations of the sampling sites and the corresponding natural areas can be seen in Figure 1.

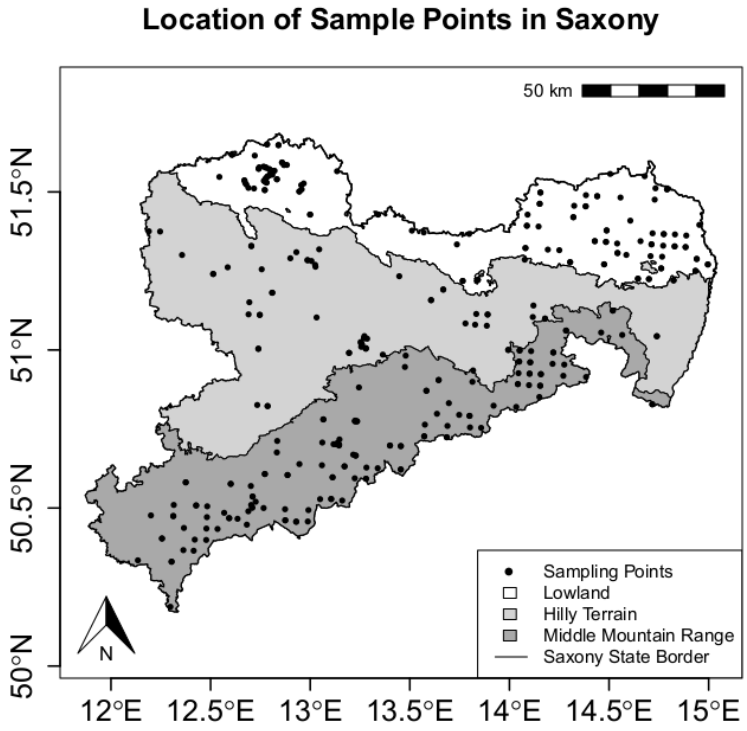


Figure 1: Location of sampling points in Saxony, Germany.

Vis-NIR Spectroscopy

Vis-NIR spectra are sensitive to mineral and organic soil substances [25] and reflectance spectroscopy is a well-known method in soil science to predict chemical and physical soil properties, even on a global scale [26]. Reflectance spectra are obtained by measuring scattered light from an illuminated soil sample. The light causes molecular vibrations, which absorb parts of the radiated energy. A comparison of emitted and reflected light holds information about molecules present in the sample [27]. As molecules consists of chemically bonded atoms, the exposition to electromagnetic radiation results in excited atoms and therefore in vibrational processes, e.g., in changing length (stretching) or changing angle of the bonds. As this absorbs energy, the absorptions are visible in the measured spectra [28]. In the visual range, the spectra is mainly related to iron oxides [29] and soil organic matter due to the darkness of organic compounds and humic acid which is caused by absorption of organic compounds in the visual range [25, 30]. The predominant absorbers in the NIR region are overtones of the C–H, N–H and O–H functional groups, making the NIR region ideal for quantifying forms of carbon and nitrogen [31, 27]. A short overview of spectrally active molecules can be seen in Table 1.

Table 1: Spectral Assignments.

Wavelength	**Suggested Molecules/Compounds**	**Source**
400–700 nm	humic acids	[25]
517, 665 nm	iron oxides	[29]
1400 nm	O-H	[31]
1450, 1730 nm	C-H	[32]
1520 nm	N-H	[32]
1900 nm	O-H	[29]
1904, 2097, 2185 nm	clay	[33]
1824, 1904, 1930, 2014, 2033, 2060, 2137, 2208 nm	organic matter components	[25]
2200 nm	O-H, Al-OH	[34]

It is important to notice that especially C-H, N-H and O-H molecules imply correlations to organic compounds present in upper soil layers, like hemicellulose, cellulose, lignin, proteins and sugar [32]. Regarding our selected properties, Xu et al. [35] states that the spectral active wavelength ranges for C and N content are similar. For pH value, e.g., Xu et al. [35] found high correlations in the ranges of 480, 780, 1120, 1910, 2200 and 2390 nm. However, Stenberg et al. noted that pH value has no direct relationship to vis-NIR spectra, but can be predicted through co-variations with buffering capacity of organic matter, clay and mineralogy [34]. For CEC, Ben-Dor and Banin [33] suggest important spectral assignments around 2000 as well as around 1400 nm. As they also mention a high correlation of CEC to clay minerals, these assignments are probably caused by the correlation and therefore indirect. BS has no direct spectral assignment as well. However, Xu et al. [35] found good prediction results, suggesting indirect assignments due to its strong correlations to clay, salt and iron oxide.

Soil Samples and Laboratory Analysis

All soil material was collected based on the German sampling standard for the NFSI [9]. In brief, this method consists of the sampling on eight points around each sampling center point with a radius of 10 m. A schematic presentation of the sampling design is shown in Figure 2. If one or more points could not be probed due to specific site conditions, they were shifted two meters in- or outwards the circle. At all points, soil material from organic layer (Oh) as well as mineral soil (0–5 cm, Ah) was collected and then mixed, resulting in one organic and one mineral sample per point. The separation of the organic and mineral horizons was

carried out via visual assessment (see Figure 2 on the right). In this procedure, the soil horizons are separated manually based on the distinguishable colour and structure.

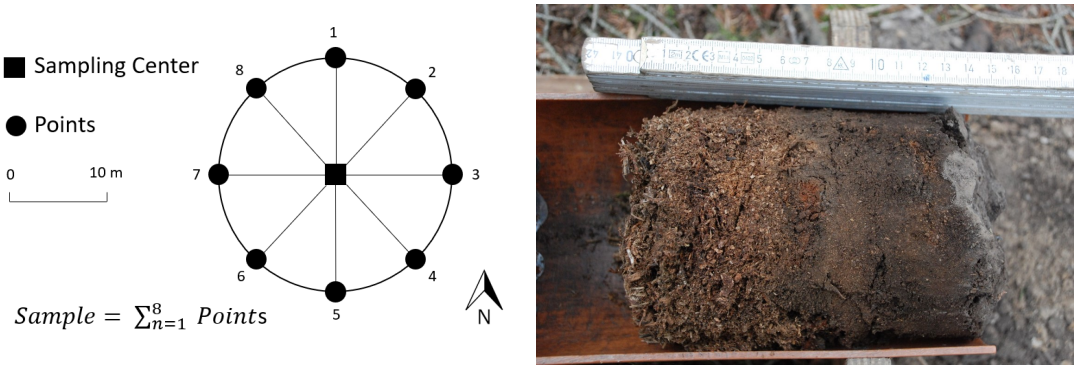


Figure 2: Schematic presentation of the sampling design (**left**) and humus sample during data collection (**right**).

Chemical analysis of all samples was performed by the laboratory of Sachsenforst public enterprise, following German-wide standards of forest soil chemical analysis [36]. The pH value was analyzed on the basis of the norm DIN-ISO-10390 (2005) [37] using KCl solution, as recommended for soils in Germany [38]. To quantify total carbon content the dry combustion method with elementary analysis was applied (DIN10694, 1996) [39]. As we focused on humus properties, we used the soil samples and legacy lab data from both Oh-horizon and Ah-horizon.
From a total of 727 retained samples, we stratified the population into the dominant two classes: spruce (*Picea abies*) and pine (*Pinus sylvestris*) stands. Within these classes we performed conditioned Latin hypercube sampling (clhs) in order to optimize the number of samples. Samples from mixed stands were then added manually due to their smaller number. In order to cover the full range of observed values and represent humus conditions in Saxony, the minima, maxima and median values of C/N ratio, pH value and CEC were added per horizon and vegetation type as these properties are also used for humus assessment. A graphical illustration of the sample selection procedure can be seen in Figure 3.

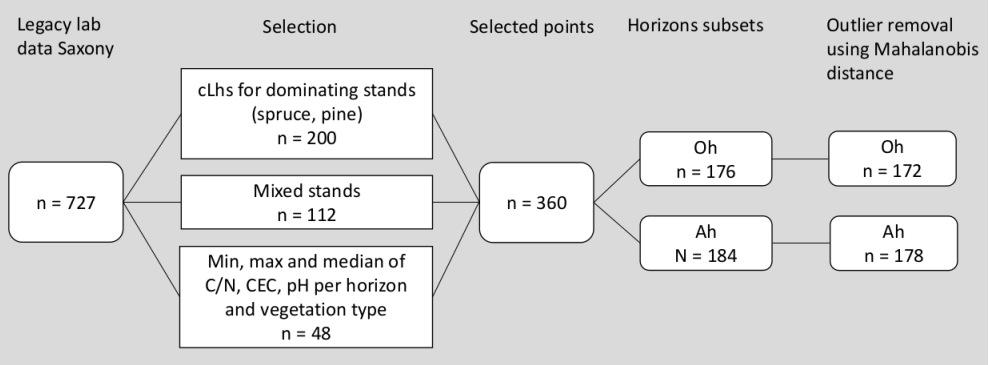


Figure 3: Graphical illustration of the sample selection procedure.

In total, the procedure resulted in a data set consisting of 360 soil samples (176 from Oh and 184 from Ah, with 287 samples originating from NFSI and 73 from Wellbrock et al. [24]). The most abundant parent materials were sand, loess loam, gneiss, granite, shale and phyllite, main soil types were cambisols, gley and podsols. Prior to the spectral analysis, the samples have been dried. To avoid changes or loss of structures or volatile compounds, all soil material was dried according to laboratory standards [36]. Samples from Oh were dried at 60 °C, mineral samples at 40 °C. Further, the dry samples were sieved with a two mm mesh in order to homogenize the soil material.

Spectral Measurements and Pre-processing

For data collection, we used a Veris vis-NIR Spectrophotometer by Veris Technologies Inc. (Salina, KS, USA). It contains two sensors, an Ocean Optics USB4000 (340 to 1100 nm) and a Hamamatsu Minispectrometer TG series (1100 to 2220 nm), working with a spectral resolution of five and six nanometres. Calibration of the spectrometer was done using four Fluorillon grey scale standards as external references [40]. Based on the protocol, two petri dishes have been filled per soil sample, and each dish was measured five times in direct contact. To homogenize the measured surface, it was softly pressed using the lid of the dishes. Samples were rotated and shifted between the measures to capture more of the sample variability. This procedure also balances the values within the measured area [41]. The chosen method results in ten spectra for each soil sample. Vis-NIR spectra can be influenced by light scatter during data acquisition, causing, e.g., baseline shifts and non-linearities. Suitable preprocessing is able to largely eliminate these unwanted effects [42]. Selected methods for spectral preprocessing were applied to the spectra. To smooth the data without distorting the signal trend, the Savitzky–Golay filter [43] was applied, using a window size of 11 and a polynomial

order of three. It operates as a weighted sum over a given window, computed as follows in Equation (1):

$$s_i* = \frac{1}{N} \sum_{h=-k}^{k} c_h s_{i+h} \tag{1}$$

where s_i* is the new signal value, s_i the old signal value, N is a normalizing coefficient, k is the gap size on each side of i and c_h are pre-computed coefficients, that depend on the chosen polynomial order and degree [44].
Light scatter and multiplicative interference correction as well as adjusting base line shifts was done using standard normal variate (SNV) [45, 42]. It is calculated as shown in Equation (2):

$$SNV_i = \frac{s_i - \bar{s_i}}{sd_i} \tag{2}$$

where s_i is the signal of a sample i, $\bar{s_i}$ is its mean and sd_i its standard deviation. All preprocessing steps were carried out by means of the R package prospectr [46]. Measurements taken below 430 nm and above 2205 nm and data between the ranges of the sensors (1000 to 1100 nm) were removed due to occurring noise at the sensors edges. We then formed the mean of ten single measurements per sample. Outlier detection was performed on the data set by means of the R package mvoutlier [47] for both horizons separately. In this approach, a principal component analysis (PCA) builds the basis for the outlier detection. The first two principal components are used to identify outliers based on Mahalanobis distance. Filzmoser et al. [48] states that the Mahalanobis distance of gaussian distributed data follows a chi-square distribution. Data points laying beyond a defined threshold of the chi-square distribution were flagged and removed from the data set. After this procedure, ten samples (four Oh and six Ah) were removed from the data set. The R language for Statistical Computing was used for all processing and calculation steps in this study [49].

Regression Approaches

Numerous studies use PLSR to calibrate regression models to estimate soil properties based on vis-NIR spectra (e.g., [50, 51, 52]). However, new methods from the field of machine learning are applied recently. Stevens et al. [44] and Shi et al. [53] used Support Vector Machine (SVM) to estimate organic C and total N, respectively. Cubist regression was also already successfully used, e.g., for prediction of SOC, total N and pH value [54].
PLSR was introduced by Wold et al. [55] as one way to solve multivariate

calibration problems. Today, PLSR is widely known as a standard algorithm to calibrate models for predicting soil properties [56]. PLSR constructs a set of linear combinations of the input data by producing a sequence of derived, orthogonal directions [57]. These combinations have high variance as well as high correlation with the response variable. For the regression, these components are used instead of the original data, resulting in a remarkable data reduction.
SVM is based on the idea of non-linearly mapping the data into very high dimensional feature space. A linear decision boundary is then constructed in this space, ensuring high generalization ability [58]. The data points lying on the edge between classes are important for the creation of the boundary. These are called support vectors. For predicting on new data, the distance to the support vectors is calculated and used as basis for the decision [59]. In this study, a radial basis function kernel was used for the calculation of the distances.
As another algorithm from the field of machine learning, we calibrated Cubist regression models. This algorithm was introduced by Quinlan [60] and can be used for learning tasks with high dimensionality. It is based on a regression tree, where intermediate linear models at each step are the basis of the predictions. Contrary to other tree based models, it retrieves a set of rules associated with sets of multivariate models [61]. The rules are then connected using if/else statements. If a condition is fulfilled, the regression rule for this subset is applied, otherwise, the next rule is probed [62]. The predictions can further be improved by creating several models ("committees"), where each new model corrects the previous one to reduce the error [63]. It was already used for soil property estimations in previous studies [19].

Spectral Model Tuning and Validation

To predict forest soil properties relevant for humus mapping, we calibrated regression models based on samples from Oh and Ah horizon separately. However, the separation of the horizons was challenging during the sampling of soils. Disturbances can alter the sequential arrangement of the horizons.
Model calibration and validation was done using a nested cross validation. In a cross-validation procedure, the data is randomly split into n subsets of approximately same size. The model is calibrated with $n - 1$ folds and then used to predict on the holdout data. This procedure is repeated until every fold was treated as validation set once. In total, n models are built with different parts of the data being used to train and test the performance, resulting in n estimates of the model performance and in predicted values for every sample in the data set.

Then, the mean of the n individual prediction error estimates is formed [57].
In a nested cross-validation, there is an inner and an outer loop over the splits of the data into training and test sets. For each of the inner splits, a grid search is done and the inner test set performance using the best tuning parameters is reported for the outer left out validation set with the final model [59]. For the calibration part using the inner splits and a grid search, the models were built using a 10-fold inner cross validation to ensure a robust tuning of hyperparameters. In a grid search procedure, models are trained using different combinations of values of the hyperparameters. The best combination resulting in the lowest prediction error is then used to predict on the test set from the outer cross validation. PLSR was tuned using one up to 20 components. For SVM, sigma values lay between 0.00001 and one, cost values between one and 10,000. Regarding the Cubist models, we probed values between one and 50 for committees and between zero and seven neighbours. The evaluation during the model tuning process was based on the root mean square error (RMSE) of the output of each parameter combination. Model tuning and validation procedure was performed by means of the R package caret [64]. We were working in a closed system as validation does not include prediction on new sampling sites. For all properties except BS, logarithmized values were used.
We computed different error measures to evaluate the model performance: RMSE, coefficient of determination (R^2), and ratio of performance to interquartile (RPIQ). The RMSE is computed as described in Equation (3):

$$RMSE = \sqrt{\frac{1}{n}\sum_{i=1}^{n}(y_i - x_i)^2} \tag{3}$$

where y_i are the predicted, x_i are the observed values. Apart from the deviations of the predictions to the actual observed values, overall model performance was assessed using the model efficiency coefficient developed by Nash [65]. It is shown in Equation (4).

$$R^2 = 1 - \frac{\sum(x_i - y_i)^2}{\sum(y_i - \bar{x})^2} \tag{4}$$

where x_i are the observed values, y_i are the predicted values and $\bar{x}$ is the observed mean value.
As complementary quality criteria for performance assessment for data without Gaussian distribution, the RPIQ was calculated as described below in Equation (5) [66]:

$$RPIQ = \frac{Q3_{obs} - Q1_{obs}}{RMSE} \tag{5}$$

where $Q1$ and $Q3$ are the first and the third quantile of the observed values. In order to rank the RPIQ values, we used the system suggested by Chang et al. [67] for ratio of performance to deviation (RPD) values. Transformation was done by multiplying the values with 1.34896 (as the interquartile range of a Gaussian distribution equals 1.34896 × SD). Thus, the threshold for good models is ¿2.70, moderate models are between 1.89 and 2.69 and poor performance is for values ¡ 1.89. Nevertheless, the usefulness of a model should be assessed regarding its context. Generally, large values for R^2 and RPIQ and low RMSE values are desired.

We further calibrated PLSR models using all points as training data in order to identify the most important wavelength ranges for the regression models for each property. The cross-validation procedure results in numerous models per property and is therefore not suitable to identify important wavelengths as they can differ between the different splits.

Evaluate Feasibility for Soil Mapping

Apart from calculating soil parameter estimations based on spectral data, the results are evaluated with respect to their usefulness for soil mapping purposes. For practical applications, simple classes of values are desirable, as they are more easy to interpret as basis for decision making when compared to continuous values. Therefore, we classify our samples to see how well the predictions can be used for such classification purposes.

Schulze and Kopp [8] proposed a classification scheme for humus of forest soils. It is to be used for evaluating nutrients availability. We use this example to present a possible way to classify the soil samples and evaluate the usefulness of the predicted values. The measured and predicted pH values build the basis for the classification. As examples of application of vis-NIRS for organic layers are scarce, the samples from Oh horizon and predictions from SVM are used as basis for the classification.

A confusion matrix is then calculated to compare the outcome of the classifications based on chemically measured and predicted values. This opens up the possibility to see which classes are robust in both classifications and where confusion between defined classes is present. The defined class thresholds can be see in Table 2 (modified after Schulze and Kopp [8]).

For each class, balanced accuracy is used to assess the outcome of the classification. It is calculated as shown in Equation (6):

$$\frac{sensitivity + specificity}{2} \tag{6}$$

where sensitivity is the true positive rate while specificity is the true negative rate. The calculation of the confusion matrix and their evaluation was done as well by means of the R package caret [64].

Table 2: Classes and corresponding pH values, (modified from Schulze and Kopp (2013) [8]).

Class	Strongly Acidic	Very Acidic	Moderate Acidic	Weakly Acidic	Neutral
pH values	≤3.3	3.4–4.1	4.2–4.9	5–6	≥6

Results

Descriptive Statistics of Soil Properties

A summary of descriptive statistics for the observed soil parameters investigated in this study, separated by horizon, is presented in Table 3. In the organic layer, values for C content range from 8.60 to 49.43%. The mean is 27.47% , representing large variation due to the use of sampling locations across whole Saxony. The standard deviation is 7.83%. For 18 samples from Oh horizon, C content lay below 17.5%. Therefore, these samples do theoretically not contain enough organic matter to be counted to the organic horizon.
In the Ah samples, C content ranged from 0.40 to 12.27% with a mean 5.05%, showing the big differences in C content between the horizons. Similar remarks can be done on the N percentages, ranging from 0.32 to 2.08% in the Oh horizon and from 0.02 to 0.58% in the Ah. The C/N ratio is more evenly distributed, with mean values of 22.77 (Oh) and 24.55 (Ah). The mean of the samples pH-values is 3.39 (Oh) and 3.32 (Ah). It is notable that the majority of the samples have acidic pH-values below 4 and that samples from basic soils are not present in the data set. Values for CEC range from 59.07 to 1065.50 µeq/g in the Oh and are much higher than in the Ah (18.16 to 239.60 µeq/g). Measured values for BS are higher in the Oh as well, with a mean of 46.63% compared to 20.08% in the Ah. A correlation matrix of the soil parameters for both horizons is shown in Figure 4. Significant correlations are marked. In Oh horizons, C and N show the

Table 3: Summary statistics of investigated soil properties for Oh (n = 172) and Ah (n = 178) horizon, Pctl = percentile.

Horizon	Parameter	Mean	St. Dev.	Min	25. Pctl	75. Pctl	Max
Oh	C [%]	27.47	7.83	8.60	22.37	32.67	49.43
	N [%]	1.23	0.37	0.32	0.97	1.55	2.08
	C/N	22.77	3.67	14.36	20.59	24.46	36.33
	pH	3.39	0.62	2.55	3.03	3.48	6.16
	CEC [µeq/g]	261.58	160.22	59.07	166.71	309.91	1,065.50
	BS [%]	46.63	26.01	9.34	27.28	63.30	99.80
Ah	C [%]	5.05	2.60	0.40	2.90	6.94	12.27
	N [%]	0.22	0.13	0.02	0.11	0.31	0.58
	C/N	24.55	4.87	11.36	22.13	26.90	45.20
	pH	3.32	0.48	2.46	3.07	3.40	5.75
	CEC [µeq/g]	100.05	54.70	18.16	53.41	143.52	239.60
	BS [%]	20.08	20.66	2.77	8.86	20.38	99.28

strongest positive correlation. C is moreover correlated with CEC only. N content is positively correlated with CEC and BS and shows negative correlation to C/N ratio. The C/N ratio is moreover negatively correlated with pH, CEC and BS. CEC shows correlations to all other properties and BS only shows no dependence to C content. In comparison, results for Ah horizons differ from these observations. Here, C content shows positive correlations to N content and CEC, but also negative correlation to C/N and pH value. N has dependence to all other properties, also including pH value. In contradiction to Oh samples, C/N shows no correlation to pH value, and pH value is correlated with C content. CEC correlation with pH is negative. The correlations regarding BS do not differ from the Oh samples, even though they are less strong. The different observations regarding the correlations between the selected soil properties for Oh and Ah horizons reveal differences between organic and mineral horizon.

Spectral Differences between Horizons

The raw spectra, the mean and the 1st derivative of preprocessed spectra, separated by horizon can be seen in Figure 5. The mean absorbance is shown on the left, the 1st derivative on the right. The absorbance shows the characteristic decline through the visible range up to 1000 nm. The raw spectra show that samples from Oh horizons have higher absorbance values through all measured wavelengths. Further, the most obvious features can clearly be seen in the absorbance around

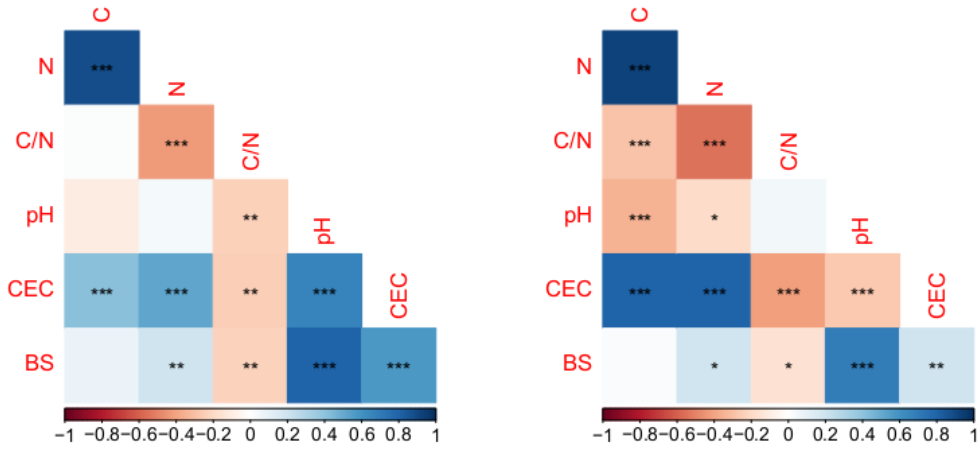


Figure 4: Significance of Pearsons correlation coefficients between investigated soil properties for Oh (**left**) and Ah (**right**) horizon (* , ** and *** indicates a p-value < 0.05, < 0.01 and < 0.001, respectively).

1400 and 1900 nm in both horizons. However, the 1st derivative allows a more detailed qualitative analysis. Smaller features in the visual range as well as around 1550 and 1700–1800 nm become more visible. Further, differences in the absorption of both horizons were more clear. We identified four ranges with remarkable differences, and marked them with letters inside the plot. In the visual range (A), mineral horizons have two peaks at around 470 and 600 nm, the Oh samples behaved differently here and show several smaller peaks inside a general decline of values. The next difference (B) can be detected at the dip following the peak at 1400 nm, which is stronger for the mineral samples. On the other hand, the peak and dip at 1900 nm are stronger for samples form Oh horizons (C). The last distinction takes place above 2000 nm. Here, the Oh samples show another higher peak with a following decline, while Ah samples show no corresponding dip.

Predicting Oh Properties

The results of the selected model approaches for all investigated soil properties can be seen in Table 4. The models results for the Oh samples are shown on the left, performance measures for Ah horizon on the right side. Predicted vs. observed values for all investigated soil properties and both horizons are shown in Figure 6. The plots show the prediction results of the best performing algorithm per property and horizon.

For C content, values for R^2 lay between 0.46 and 0.54, with corresponding RMSE values ranging from 5.59% to 6.16% and RPIQ between 1.58 and 1.75.

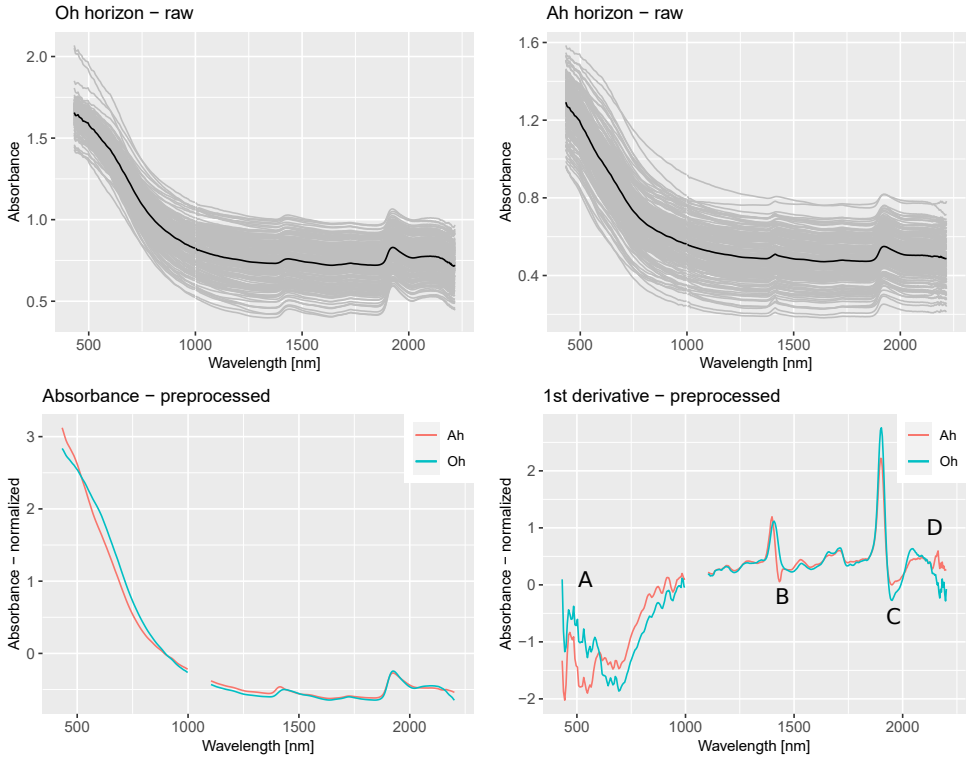


Figure 5: Raw spectra (black line represents the mean) and preprocessed absorbance and 1st derivative spectra of samples from Oh and Ah samples, ranges with remarkable differences are marked by letters A–D.

Wavelengths important for model building lay between 500 and 600 nm.
The prediction of N content showed similar accuracy and achieved R^2 values ranging from 0.48 to 0.58, with RPIQ values between 1.82 and 2.06.
For both C and N content, the plot showed no patterns as the points cluster around the x = y line. Regarding the C/N ratio of the Oh horizon, the predictions resulted in higher R^2 values of 0.64–0.66. For this property, RMSE lay between 2.16 and 2.26, with Cubist yielding the most accurate results. RPIQ was calculated between 1.73 and 1.81. The features around 2200 and 1900 nm were most important.
For pH value, we found little differences between the used algorithms. R^2 were between 0.88 and 0.9 and RMSE ranged from 0.2 to 0.21, with corresponding RPIQ values of 2.39–2.47. The scatterplot of the predictions also shows that even the underrepresented high pH values show small deviation and cluster tightly to the x = y line. Again wavelength ranges around 1900 and 2200 nm were most important for model calibration.
The predictions derived for CEC were less precise, with R^2 being 0.54. Relevant spectral ranges were identified between 570 and 690 nm.
Regarding BS, again little differences between the used algorithms are reported.

Table 4: Model results for selected soil properties and algorithms for Oh (left) and Ah (right) samples from Saxony.

	Horizon	Oh			Ah		
Property	**Method**	**RMSE**	**R^2**	**RPIQ**	**RMSE**	**R^2**	**RPIQ**
C	PLS	6.16	0.46	1.58	1.77	0.61	2.22
	SVM	5.59	0.54	1.75	1.56	0.72	2.54
	Cubist	6.14	0.44	1.58	1.71	0.59	2.31
N	PLS	0.28	0.48	1.82	0.08	0.63	2.27
	SVM	0.25	0.58	2.06	0.07	0.71	2.44
	Cubist	0.26	0.52	1.97	0.08	0.63	2.32
C/N	PLS	2.19	0.66	1.75	3.51	0.45	1.35
	SVM	2.26	0.64	1.73	3.52	0.50	1.37
	Cubist	2.16	0.65	1.81	3.58	0.45	1.31
pH	PLS	0.20	0.90	2.47	0.29	0.62	1.22
	SVM	0.21	0.88	2.38	0.31	0.56	1.14
	Cubist	0.21	0.89	2.38	0.34	0.45	1.05
CEC	PLS	102.47	0.54	1.36	33.94	0.67	2.67
	SVM	99.69	0.54	1.43	39.04	0.58	2.34
	Cubist	103.60	0.54	1.43	33.16	0.65	2.81
BS	PLS	14.56	0.69	2.51	15.75	0.39	0.71
	SVM	13.97	0.71	2.61	16.66	0.33	0.67
	Cubist	14.52	0.69	2.53	17.98	0.29	0.63

R^2 values ranged from 0.69 to 0.71, RPIQ lay between 2.51 and 2.61. Important spectral features lay around 1900 and 2200 nm.
The scatter plot reveals that especially high BS values close to 100% seem to have bigger deviation from the observed values as they form a visible cluster.
Regarding the used algorithms, none of the chosen methods was superior among all investigated properties, while SVM resulted in the most accurate predictions for C and N content, the differences were minor for the other properties, with no clear trends in favour for one of the algorithms.

Predicting Ah Properties

Models results for samples from Ah horizon showed different trends. Prediction of C and N content was more precise for mineral samples. For C content we achieved R^2 values between 0.59 and 0.72 and corresponding RPIQ values of 2.22–2.54. The calculated RMSE ranged from 1.56% to 1.77%. SVM regression outperformed PLSR and Cubist. The models for N content reached R^2 values between 0.63 and 0.71 and RPIQ values from 2.27 to 2.44. Again, SVM regression yielded the most

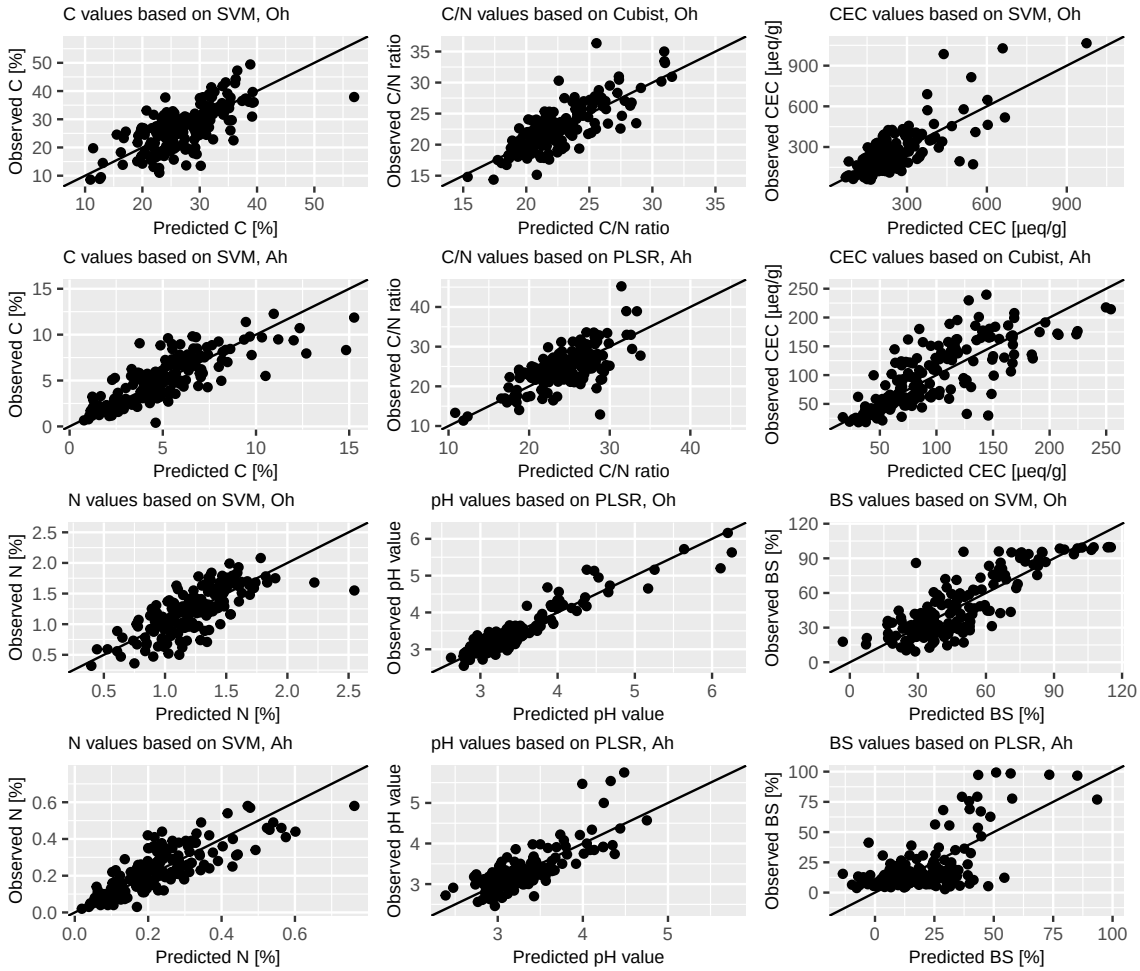


Figure 6: Predicted vs. observed plots for the investigated properties separated by horizon, results of the most accurate algorithm per property.

accurate predictions. Important features for C and N content lay between 2150 and 2200 nm as well as in the visual range. Unlike for the Oh models, prediction for C/N ratio was less precise, with R^2 ranging from 0.45 to 0.5. The predicted values mostly lay between a C/N ratio of 20 and 30. Relevant spectral ranges were around 450 and 2050 nm.

Compared to predictions for Oh samples, accuracy decreased for pH values, with R^2 values between 0.45 and 0.56 and RMSE ranging from 0.29 to 0.34. For this property, PLSR outperformed the other algorithms. The visual interpretation reveals that some high values were underestimated. In contrary to Oh samples, most important wavelengths were in the visual range, but also around 1900 nm.

In contrast, results for CEC in Ah horizons achieved better model predictions. Depending on the algorithm, R^2 values ranged from 0.58 to 0.67, with RMSE values between 33.16 and 39.04 µeq/g. RPIQ was calculated from 2.34 to 2.81. The spectral feature around 1900 nm was identified to be most important.

Table 5: Error matrix of predicted and observed pH-classes.

	Reference					
Prediction	strongly acidic	very acidic	moderately acidic	weakly acidic	neutral	total
strongly acidic	95	10	0	0	0	105
very acidic	12	29	8	0	0	49
moderately acidic	0	1	8	3	0	12
weakly acidic	0	0	1	4	1	6
neutral	0	0	0	0	0	0
total	107	40	17	7	1	172
balanced accuracy	0.87	0.79	0.72	0.78	0.50	0.73

Prediction of BS based on mineral samples resulted in lowest R^2 and RPIQ values. The scatter plot shows that the model has difficulties in detecting a relationship between measured spectra and chemically obtained BS values.
Similar to the results for Oh horizon, SVM showed the most accurate predictions for C and N content. For the other investigated properties, again no clear trend was visible. Cubist was most accurate for CEC values. On the other hand, SVM and Cubist showed poorer results for pH, where PLSR was most precise.

Classification for Mapping Purposes

For a better assessment of the usefulness of the predicted soil property values, we classified both measured and estimated values based on pH value. We then calculated a confusion matrix to see if the defined classes are robust. This classification was done using the Oh samples and the prediction results from SVM. The results of the classification based on chemically determined and predicted pH values in form of a confusion matrix can be seen in Table 5. Based on the chemical values, 107 samples were classified as strongly acidic, 40 as very acidic, 17 as moderate acidic, seven as weakly acidic and one as neutral. When classified on basis of predictions, 107 samples ended up strongly acidic, 48 as very acidic, 11 as moderately acidic, 6 as weakly acidic and none as neutral. Balanced accuracy is highest for strongly acidic class with 0.87, while the accuracy for the other classes range from 0.5 to 0.79. In total, a value of 0.73 was reached.

Discussion

Data Ranges of Soil Properties

The data ranges of the investigated properties show typical conditions for Saxon forests. Remarkable are the acidic conditions. Reasons for the low measured pH values lie in the parent materials. Alkaline parent materials are scarce and many forest sites were further acidified by historical coniferous usage on unsuitable sites. In addition, industrial element input (mainly sulfur and nitrogen) also led to soil acidification.

Spectral Behaviour

The investigation of the spectra obtained from Oh and Ah horizons showed divergent absorbance features. The most remarkable differences occurred in the visual range between 500 and 700 mn, at 1400 nm, at 1900 nm and above 2000 nm. We assume that the differences in spectral behaviour are a result of the distinct composition of Oh horizons when compared to mineral Ah horizons. As the differences occurred in wavelength ranges that are known to be sensitive for organic matter, it is reasonable to assume that the much higher percentage of organic matter in organic layers leads to the observed differences. It also explains higher absorbance values through the whole spectrum and especially the differences in the visual range and above 2000 nm. The feature differences at 1400 nm and 1900 nm can be caused by differences in organic matter, but also due to divergent percentages of clay, which is active in this regions. The differences arelikeweise pronounced in the variable importance of the PLSR models. For example, relevant features for C content prediction for Oh samples lay in the visual range while features around 2200 nm were most important for Ah samples. Regarding pH values, features around 1900 and 2200 nm were most important for Oh samples. On the other hand, the visual range was relevant as well in Ah horizons. Similar observations could be made for CEC, were the visual range was important in Oh samples, but models for Ah horizons mostly relied on the feature around 1900 nm.

Predicting Oh Properties

Prediction results for soil properties based on samples from Oh horizon yielded diverse results. Accuracy for C content was weak, as no algorithm was able to reach the proposed threshold of RPIQ = 1.89. However, keeping in mind that C

content values were up to 49.43% in the Oh horizon, the RMSE values of 5.59 and R^2 of 0.54 could still indicate useful results. The identified important spectral ranges in the visual range point to humic acids.

Due to the numerous examples of successful C content prediction in various settings, we expected better results. Possible reasons for the low accuracy could lie in the complex and heterogeneous structure of humic material compared to mineral soil material. A more intensive soil preparation in form of milling could help to address this issue. In an approach using soil samples from all over Europe and PLSR, Nocita et al. [68] reported R^2 values of 0.76 for organic samples. However, they did not collect samples explicit from organic horizon, but selected samples with C content ¿ 18% from a larger data set. Further, the sample location also included other land use forms such as cropland and grassland. These differences may explain the differences in prediction accuracy. Investigating forest soils in the Czech Republic, Gholizadeh et al. [22] reported $R^2 = 0.78$ for combined organic horizons. They used material originating from L and F horizons as well. For Oh horizons, they reported $R^2 = 0.63$ and RMSE = 4.2. Using samples originating from forests across China, Liu et al. [20] reached $R^2 = 0.75$ for PLSR and $R^2 = 0.93$ using Cubist. In this case, samples were taken from different depths without separating the horizons and thus covering a much wider range of carbon content values (0.2–99.6 %).

We achieved moderate prediction results for N content using SVM and Cubist regression, with R^2 up to 0.58 and RPIQ ¿ 1.98 for SVM and Cubist. Thus, N content in humus samples can be estimated using vis-NIRS at sufficient accuracy. Relevant features in the visual range and around 2200 suggest humic acids and organic matter as spectral response. Vohland et al. [69] found similar spectral assignments for C and N content.

The model results of the used algorithms were quite similar for C/N ratio. However, no models reached results classified as moderate as RPIQ values were slightly below the proposed threshold.

Highest accuracy amongst investigated soil properties was found for pH value of Oh samples. Our models reached R^2 values of 0.88 to 0.9 and RPIQ ¿ 2.38. The relevant wavelengths around 1900 and 2200 nm point to indirect assignments via O-H and organic matter components. Thus, we conclude that pH value can be successfully predicted for Oh horizons using vis-NIR spectral data. It is remarkable that predictions are more accurate for pH than for C content, despite the high C content values. One reason might be the differences in wavelengths important for the predictions. In another study investigating vis-NIRS for SOM and pH

prediction, Yang et al. also found different relevant wavelengths [70]. The results underline that predictions through indirect spectral assignments can be useful as well.
The RMSE values for CEC prediction in the Oh horizon were high, with values around 100 µeq/g. As a result, RPIQ values do not reach the threshold of 1.89. One reason for the high values were the few sample points with high CEC values, which are not predicted precisely. Another explanation could be the absence of clay in the organic horizon, as CEC correlation to vis-NIR spectra is suggested to be indirect and due to the correlation of CEC and clay [33]. This is also likely as the model relies mostly on the visual range. Even though BS has no direct spectral assignment, the models achieved meaningful results with RPIQ between 2.51 and 2.61 and R^2 between 0.69 and 0.71. The important features around 2200 and 1930 nm suggest indirect assignments via hydroxy and carbonyl groups [25]. The scatter plot reveals a cluster of points at highest possible measured value. BS can not be greater than 100 per definition. However, some points were predicted to have values exceeding this threshold. The cluster therefore indicates that the defined valid values can be a problem for predictive modeling purposes. For the potential usage of predicted values in practical application, it is necessary to find a way on how to deal with such occurrences.

Predicting Ah Properties

Models calibrated for mineral Ah horizon achieved higher prediction accuracy for C and N content. The estimates of all algorithms resulted in RPIQ values ranging from 2.22 to 2.54 and R^2 values between 0.59 and 0.72. According to the generally lower C and N percentages in mineral soil, RMSE was also lower (C: 1.56–1.77%, N: 0.07–0.08%). Therefore, vis-NIRS is suitable for C and N prediction in Ah horizons of forest soils. The better results compared to Oh samples could lie in the more homogeneous soil material producing a clearer spectral response. Gholizadeh et al. [22] reported R^2 values of 0.53 when estimating C content of mineral horizons from Czech forests using SVM, which is less precise than our findings. However, they were using soil material from depths up to 40 cm. For A horizons, they reached an R^2 of 0.72. On the other hand, e.g., Coûteaux et al. [71] reached R^2 values of 0.8 for mineral soils. Therefore, our findings are in-between the results of other similar investigations.
Regarding N content, other studies reported similar prediction accuracy. Shi et al. [53] reached R^2 values of 0.68 for PLSR and 0.76 for SVM on soil samples from different land use forms. A study investigating N content on grasslands in Norway

reported models with R^2 between 0.68 and 0.8 [72]. Thus, our results are within the same prediction accuracy as similar studies. For C and N content, the visual range as well as features around 1900 and 2200 nm were found to be important. These ranges were also found relevant in other studies [69].
Despite the results for C and N content prediction, model accuracy was weaker for C/N ratio for the mineral samples, with RMSE values being higher compared to models for Oh horizon. This is surprising, as more accurate values for single C and N values should also result in precise estimations for C/N ratio.
Other research reported likewise results for estimating C/N ratio. Ludwig et al.[73] had comparable PLSR results on forest soils, with R^2 values C and N content being higher (¿0.9) than the ones for C/N ratio (0.57). On agricultural sites, Mutuo et al. [74] observed similar findings. In their predictions, R^2 for C (0.84) and N (0.87) was much more accurate than their attempt to estimate C/N ratio (0.37). Contrariwise, other studies indicate more precise predictions of C/N ratio. Chang et al. [51] obtained R^2 of 0.88 when predicting using PLSR. Their samples were originating from grassland and agricultural sites. This contradictions raise the question if N is measured by direct response to vis-NIR spectra or as a result of correlation with C content within the samples. Chang et al. [51] interpret their results in favour of direct measurement. Ludwig et al. [18] name possible error propagation within the single measurement as possible source for the poorer performance, whereas Mutuo et al. [74] did not suggest any reasons for the different outcomes.
Regarding pH value, models were as well less precise for the Ah samples. None of the used algorithms were able to reach the proposed RPIQ threshold. The relevant wavelengths in the visual range and around 1900 nm suggest a indirect assignment to humic acids and hydroxy groups. However, the small range in the data set and the majority of samples having low pH values also results in low RPIQ values for pH. Further, the underestimation of few high values increases the RMSE value. Thus, we conclude that the PLSR results with $R^2 = 0.62$ and RMSE = 0.29 could nevertheless be useful for forest soil mapping.
Investigating samples from 0 to 20 cm depth, Conforti et al. [75] calibrated models that reached higher prediction accuracy with $R^2 = 0.7$ and RMSE = 0.15. In another study using only 0–5 cm depth from wetlands, Cohen et al. [76] reported RMSE values of 0.36, which is less precise than our PLSR results. Again, our predictions are in between the results of other investigations.
CEC prediction was successful for mineral samples as all algorithms achieved RPIQ values > 1.89. RMSE values were much lower than for organic samples,

best R^2 was 0.67. The better results and the importance of spectral features around 1900 nm underline the indirect prediction through correlation with clay, as mineral horizon contain more clay than organic layers. In comparison, Chang et al. [67] reported models with $R^2 = 0.81$. Leone et al. [50] presented R^2 values between 0.59 and 0.85, depending on the study site. Reasons for the occurring differences in some cases could be the usage of deeper depths up to 30 and 60 cm. It was not possible to create meaningful models for BS in Ah horizons. Even though RMSE values were not much higher than for the Oh samples, predictions were unreliable as scatter was high and occurred through the whole range. One reason could be the different chemical analysis, which was carried out using ammonium chloride whilst Oh samples were analyzed using barium chloride. Another explanation could lie in the divergent percentages of organic compounds.

Classification Based on pH Values

To assess the prediction accuracy with regards to practical application for forest soil mapping, the Oh samples were classified based on predicted and observed pH values. Balanced accuracy for the different classes lay between 0.5 and 0.87. We conclude that the values obtained from vis-NIRS can therefore be used to classify the samples based on pH values to provide easy to interpret information for assessing humus conditions. This can be used to support silvicultural decision making regarding, e.g., selection of tree species or soil liming measures.
It is important to notice that the less acidic soils are highly underrepresented in the data. This impacts the classification result, as the majority of the samples ended up in the strongly and very acidic classes. Only a few samples have pH values high enough to be classified in the other classes. Especially the accuracy for the classes weakly acidic and neutral are therefore not very meaningful. However, we show how a classification could be implemented in future forest monitoring and the acidic conditions emphasize the need for management strategies. The approach should be repeated with samples that are more evenly distributed and not biased towards one class. One problem of this approach is that the location of the values within classification influences the precision. Unfortunately, there is no solution for this when a classification of the samples is desired.

Further Implications

We expected generally better prediction results for Ah horizons due to numerous examples for successful application on forest areas as well as other land use forms.

Despite the more complex and heterogeneous structure of the humic material, the prediction accuracy was higher for samples from Oh horizons regarding the properties C/N ratio, pH-value and BS. As the latter are likely to be predicted through indirect spectral assignments, the better results can be explained by the different composition of the horizons regarding organic compounds.
As already mentioned, 18 samples collected as Oh horizon do not contain enough C to be classified as organic samples. On the other hand, it is also not possible to assume that these samples originate from the Ah horizon, as the separation during the sample collection was erroneous.
One way to overcome this problem when applying vis-NIRS to assess forest soil humus could lie in a combined investigation of every sample point. This way, an unclear separation of the horizons during the sample collection could not interfere with the model result. This approach has already been applied, e.g., for mixed samples of whole soil profiles [22] as well as modelling samples from both Oh and A horizon with the same model [71]. On the other hand, this could imply further difficulties as the wider data range for C and N contents could result in overoptimistic error measures [19]. Another reason against combined modeling is the different spectral behaviour of the investigated horizons.
Further, our samples originate from various forest types and from soils with different parent material. However, deciduous stands are highly underrepresented. This, e.g., impacts the distribution of pH values, for which it leads to an over-representation of acidic conditions. In addition, forest management strategies vary through the stands. The heterogeneity of the data set can affect the model accuracy, and local modelling approaches may have higher prediction power [44]. It would therefore be of great interest to expand the investigations to other study areas covering different forest types, soil forms and parent materials. Our results indicate that vis-NIRS could also be applied for humus assessment in other regions.

Conclusions

In this study, we investigated the applicability of vis-NIRS to predict soil properties relevant for humus assessment for samples from Oh and Ah horizon in Saxony.
Applications of vis-NIRS for the prediction of properties of organic soil layers of forests soils were not investigated so far, and our findings enrich the knowledge about the feasibility of this scenario.
For the Oh samples, we found useful predictions for N content, C/N ratio, pH value and base saturation based on the proposed classification scheme. Model

results for C content and CEC did not reach the required threshold (RPIQ < 1.89).
Oh and Ah horizons showed distinct absorbance features in wavelength ranges that are known to be sensitive for organic matter. Thus, we assume that the much higher percentage of organic matter in organic layers leads to the observed differences. Therefore our results point to the relevance of the different composition of the humus layer and organic horizon for vis-NIRS. This is also reflected in the results.
In the Ah we achieved satisfying accuracy for C and N content, pH value and CEC. However, our results for C/N ratio were poor, and the predictions for BS turned out to be unreliable. We used calibrated regression models based on different algorithms. While SVM turned out to be most accurate for C and N content prediction, differences were minor for the other properties. None of the used algorithms clearly outperformed the others regarding the prediction of the investigated properties. With respect to its usefulness for forest soil mapping based on pH values, we compared classification into classes based on measured and predicted pH values and provided classification accuracy for the different classes, with satisfying results. We would like to emphasize the potential of retained soil samples for building spectral libraries. A great benefit for future studies can be achieved by adding samples from deciduous sites with less acidic conditions as well. We can conclude that our results indicate useful possibilities for the usage of vis-NIR spectroscopy for forest soil mapping and could help identifying areas in need for mitigation strategies to face soil degradation. Based on the feasibility of predictions and the comparably low effort and costs, we recommend the further development of the method to supplement the periodic forest soil mapping procedure.

Author contributions Conceptualization, F.T., U.W. and R.P.; methodology, F.T. and U.W. ; software, F.T.; validation, F.T., U.W., C.B. and R.P.; formal analysis, F.T.; investigation, F.T., S.L. and C.B ; resources, R.P., U.W. and H.M.; data curation, F.T, S.L. and C.B.; writing—original draft preparation, F.T.; writing—review and editing, R.P., H.M., C.B. and U.W.; visualization, F.T.; supervision, U.W. and R.P.; project administration, U.W. and R.P.; funding acquisition, U.W. and R.P. All authors have read and agreed to the published version of the manuscript.

Funding The study is part of the joint research project DIGI-Humus: "Verbundvorhaben: Erfassung und Regionalisierung von Humuseigenschaften mittels VIS-NIR und Digitaler Bodenkartierung" and was funded by the Federal Ministry of Food and Agriculure (project no. 22014417 and 22001316).

Data availability The data set from this study is available through the EUDAT online archive under `10.23728/b2share.20727e01b826450ebe59600c315925cb` (accessed on 25 January 2022)

Acknowledgements We want to thank the chemical laboratory of Public Enterprise Sachsenforst for analyzing the soil samples used in this study, and Marco Pohle and Helko Kotas for their technical support conducting the spectral measurements. We thank the Federal Ministry of Food and Agriculture (BMEL) and the Fachagentur Nachwachsende Rohstoffe (FNR) for permanent support of the project DIGI-Humus (Erfassung und Regionalisierung von Humuseigenschaften mittels VIS-NIR und Digitaler Bodenkartierung). This study received funding for F.T. (#22014417) and C.B. (#22001316) within the project DIGI-Humus.

Conflicts of interest The authors declare no conflict of interest. The funders had no role in the design of the study; in the collection, analyses, or interpretation of data; in the writing of the manuscript, or in the decision to publish the results.

Abbreviations

The following abbreviations are used in this manuscript:

vis	visual
NIR	near infrared
C	carbon
N	nitrogen
CEC	cation exchange capacity
BS	base saturation
NFSI	national forest soil inventory
PSS	proximal soil sensing
vis-NIRS	visual and near-infrared reflectance spectroscopy
SOC	soil organic carbon
PLSR	partial least squares regression
SVM	support vector machine
RMSE	root mean square error
RPIQ	ratio of performance to interquartile
RPD	ratio of performance to deviation

References

[1] B. Schuldt et al. “A first assessment of the impact of the extreme 2018 summer drought on Central European forests”. In: *Basic and Applied Ecology* 45 (2020), pp. 86–103.

[2] C. D. Allen et al. “A global overview of drought and heat-induced tree mortality reveals emerging climate change risks for forests”. In: *Forest ecology and management* 259.4 (2010), pp. 660–684.

[3] M. Nussbaum et al. “Evaluation of digital soil mapping approaches with large sets of environmental covariates”. In: *Soil* 4.1 (2018), pp. 1–22.

[4] F. Conen et al. “The carbon balance of forest soils: detectability of changes in soil carbon stocks in temperate and boreal forests”. In: *The carbon balance of forest biomes* 9 (2004), pp. 233–247.

[5] R. Petzold, R. Benning, and J. Gauer. “Bodeninformationen in den verschiedenen Standortserkundungssystemen Deutschlands: Gegenwärtiger Stand und Perspektiven”. In: *Waldökologie, Landschaftsforschung und Naturschutz* 16 (2016), pp. 7–17.

[6] C. E. Prescott, D. G. Maynard, and R. Laiho. “Humus in northern forests: friend or foe?” In: *Forest ecology and management* 133.1-2 (2000), pp. 23–36.

[7] D. Binkley and R. F. Fisher. *Ecology and management of forest soils*. 5th edition. Wiley: Hoboken, NJ, USA, 2020.

[8] Schulze and Kopp. “Anleitung für die forstliche Standortserkundung im nordostdeutschen Tiefland”. In: *Standortserkundungsanleitung 95* (2013).

[9] N. Wellbrock et al. “Concept and Methodology of the National Forest Soil Inventory”. In: *Status and Dynamics of Forests in Germany*. Springer: Cham, Switzerland, 2019, pp. 1–28.

[10] R. V. Rossel et al. “Proximal soil sensing: an effective approach for soil measurements in space and time”. In: *Advances in agronomy*. Vol. 113. Elsevier: Amsterdam, The Netherlands, 2011, pp. 243–291.

[11] R. Viscarra Rossel and R. Lark. “Improved analysis and modelling of soil diffuse reflectance spectra using wavelets”. In: *European Journal of Soil Science* 60.3 (2009), pp. 453–464.

[12] M. Nocita et al. “Soil spectroscopy: An alternative to wet chemistry for soil monitoring”. In: *Advances in agronomy* 132 (2015), pp. 139–159.

[13] J. Reeves, G. McCarty, and J. Meisinger. "Near infrared reflectance spectroscopy for the analysis of agricultural soils". In: *Journal of Near Infrared Spectroscopy* 7.3 (1999), pp. 179–193.

[14] B. Kuang and A. Mouazen. "Calibration of visible and near infrared spectroscopy for soil analysis at the field scale on three European farms". In: *European Journal of Soil Science* 62.4 (2011), pp. 629–636.

[15] R. V. Rossel et al. "Visible, near infrared, mid infrared or combined diffuse reflectance spectroscopy for simultaneous assessment of various soil properties". In: *Geoderma* 131.1-2 (2006), pp. 59–75.

[16] S. G. Ribeiro et al. "Soil Organic Carbon Content Prediction Using Soil-Reflected Spectra: A Comparison of Two Regression Methods". In: *Remote Sensing* 13.23 (2021), p. 4752.

[17] M. Pietrzykowski and M. Chodak. "Near infrared spectroscopy—a tool for chemical properties and organic matter assessment of afforested mine soils". In: *Ecological engineering* 62 (2014), pp. 115–122.

[18] B. Ludwig et al. "Estimation accuracies of near infrared spectroscopy for general soil properties and enzyme activities for two forest sites along three transects". In: *Geoderma* 288 (2017), pp. 37–46.

[19] F. Thomas et al. "Application of Low-Cost MEMS Spectrometers for Forest Topsoil Properties Prediction". In: *Sensors* 21.11 (2021), p. 3927.

[20] S. Liu et al. "Estimating forest soil organic carbon content using vis-NIR spectroscopy: Implications for large-scale soil carbon spectroscopic assessment". In: *Geoderma* 348 (2019), pp. 37–44.

[21] É. F. Pinheiro et al. "Prediction of soil physical and chemical properties by visible and near-infrared diffuse reflectance spectroscopy in the central Amazon". In: *Remote Sensing* 9.4 (2017), p. 293.

[22] A. Gholizadeh et al. "National-scale spectroscopic assessment of soil organic carbon in forests of the Czech Republic". In: *Geoderma* 385 (2021), p. 114832.

[23] D. Ertlen et al. "Discriminating between organic matter in soil from grass and forest by near-infrared spectroscopy". In: *European Journal of Soil Science* 61.2 (2010), pp. 207–216.

[24] N. Wellbrock et al. *Entwicklung einer Methodik zur stichprobengestützten Erfassung und Regionalisierung von Zustandseigenschaften der Waldstandorte*. Thünen Report 36. Braunschweig, Germany: Johann Heinrich von Thünen-Institut, 2015.

[25] R. V. Rossel and T. Behrens. "Using data mining to model and interpret soil diffuse reflectance spectra". In: *Geoderma* 158.1-2 (2010), pp. 46–54.

[26] R. V. Rossel et al. "A global spectral library to characterize the world's soil". In: *Earth-Science Reviews* 155 (2016), pp. 198–230.

[27] C. D. Christy. "Real-time measurement of soil attributes using on-the-go near infrared reflectance spectroscopy". In: *Computers and electronics in agriculture* 61.1 (2008), pp. 10–19.

[28] A. Gubler. "Quantitative Estimations of Soil Properties by Visible and Near Infrared Spectroscopy: Applications for Laboratory and Field Measurements". PhD thesis. University of Bern, Bern, Switzerland, 2011.

[29] M. Knadel et al. "Assessing soil water repellency of a sandy field with visible near infrared spectroscopy". In: *Journal of near infrared spectroscopy* 24.3 (2016), pp. 215–224.

[30] M. F. Baumgardner et al. "Reflectance properties of soils". In: *Advances in agronomy* 38 (1986), pp. 1–44.

[31] G. R. Hunt. "Spectral signatures of particulate minerals in the visible and near infrared". In: *Geophysics* 42.3 (1977), pp. 501–513.

[32] T. Fourty et al. "Leaf optical properties with explicit description of its biochemical composition: direct and inverse problems". In: *Remote sensing of Environment* 56.2 (1996), pp. 104–117.

[33] E. Ben-Dor and A. Banin. "Near-infrared analysis as a rapid method to simultaneously evaluate several soil properties". In: *Soil Science Society of America Journal* 59.2 (1995), pp. 364–372.

[34] B. Stenberg et al. "Visible and near infrared spectroscopy in soil science". In: *Advances in agronomy*. Vol. 107. Elsevier: Amsterdam, The Netherlands, 2010, pp. 163–215.

[35] D. Xu et al. "Assessment of important soil properties related to Chinese Soil Taxonomy based on vis–NIR reflectance spectroscopy". In: *Computers and electronics in agriculture* 144 (2018), pp. 1–8.

[36] Gutachterausschuss Forstliche Analytik. *Handbuch Forstliche Analytik. Eine Loseblatt-Sammlung der Analysemethoden im Forstbereich*. 2014.

[37] DIN ISO 10390: 2005. *Bodenbeschaffenheit—Bestimmung des pH-Wertes*. 2005.

[38] J. Höhle et al. *Bodenzustandserhebung im Wald-Dokumentation und Harmonisierung der Methoden*. Tech. rep. Johann Heinrich von Thünen-Institut: Braunschweig, Germany, 2018.

[39] DIN. "DIN 10694: Bestimmung des organischen Kohlenstoffgehaltes und des Gesamtkohlenstoffgehaltes nach trockener Verbrennung (Elementaranalyse)". In: *Deutsche Normen (ed. Fachnormenausschuß Wasserwesen, FNW, im DIN Deutsches Institut für Normung e.V.)* (1994).

[40] Avian Technologies. *Fluorilon Gray Scale Standards & Targets*. Online. accessed on 13.06.2019. 2019. URL: https://aviantechnologies.com/product/gray-scale-standards/.

[41] A. Mac Arthur, C. J. MacLellan, and T. Malthus. "The fields of view and directional response functions of two field spectroradiometers". In: *IEEE transactions on geoscience and remote sensing* 50.10 (2012), pp. 3892–3907.

[42] Å. Rinnan, F. Van Den Berg, and S. B. Engelsen. "Review of the most common pre-processing techniques for near-infrared spectra". In: *TrAC Trends in Analytical Chemistry* 28.10 (2009), pp. 1201–1222.

[43] A. Savitzky and M. J. Golay. "Smoothing and differentiation of data by simplified least squares procedures." In: *Analytical chemistry* 36.8 (1964), pp. 1627–1639.

[44] A. Stevens et al. "Prediction of soil organic carbon at the European scale by visible and near infrared reflectance spectroscopy". In: *PloS one* 8.6 (2013), e66409.

[45] R. Barnes, M. S. Dhanoa, and S. J. Lister. "Standard normal variate transformation and de-trending of near-infrared diffuse reflectance spectra". In: *Applied spectroscopy* 43.5 (1989), pp. 772–777.

[46] A. Stevens and L. Ramirez-Lopez. *An introduction to the prospectr package*. R package version 0.1.3. R Core Team: Vienna, Austria, 2013.

[47] P. Filzmoser and M. Gschwandtner. *mvoutlier: Multivariate Outlier Detection Based on Robust Methods*. R package version 2.0.9. R Core Team: Vienna, Austria, 2018. URL: https://CRAN.R-project.org/package=mvoutlier.

[48] P. Filzmoser, R. G. Garrett, and C. Reimann. "Multivariate outlier detection in exploration geochemistry". In: *Computers & geosciences* 31.5 (2005), pp. 579–587.

[49] R Core Team. *R: A Language and Environment for Statistical Computing*. R Foundation for Statistical Computing. Vienna, Austria, 2018. URL: `https://www.R-project.org/`.

[50] A. Leone et al. "Prediction of soil properties with PLSR and vis-NIR spectroscopy: application to mediterranean soils from Southern Italy". In: *Current Analytical Chemistry* 8.2 (2012), pp. 283–299.

[51] C.-W. Chang and D. A. Laird. "Near-infrared reflectance spectroscopic analysis of soil C and N". In: *Soil Science* 167.2 (2002), pp. 110–116.

[52] J. B. Reeves III. "Near-versus mid-infrared diffuse reflectance spectroscopy for soil analysis emphasizing carbon and laboratory versus on-site analysis: where are we and what needs to be done?" In: *Geoderma* 158.1-2 (2010), pp. 3–14.

[53] T. Shi et al. "Comparison of multivariate methods for estimating soil total nitrogen with visible/near-infrared spectroscopy". In: *Plant and soil* 366.1-2 (2013), pp. 363–375.

[54] P. T. Sorenson et al. "Monitoring organic carbon, total nitrogen, and pH for reclaimed soils using field reflectance spectroscopy". In: *Canadian Journal of Soil Science* 97.2 (2017), pp. 241–248.

[55] S. Wold, H. Martens, and H. Wold. "The multivariate calibration problem in chemistry solved by the PLS method". In: *Matrix pencils*. Springer: Cham, Siwtzerland, 1983, pp. 286–293.

[56] L. Ramirez-Lopez et al. "The spectrum-based learner: A new local approach for modeling soil vis–NIR spectra of complex datasets". In: *Geoderma* 195 (2013), pp. 268–279.

[57] T. Hastie, R. Tibshirani, and J. Friedman. *The elements of statistical learning: data mining, inference, and prediction*. Springer Science & Business Media: Chams, Switzerland, 2009.

[58] C. Cortes and V. Vapnik. "Support-vector networks". In: *Machine learning* 20.3 (1995), pp. 273–297.

[59] A. C. Müller, S. Guido, et al. *Introduction to machine learning with Python: a guide for data scientists*. 1st Edition. O'Reilly Media, Inc.: Newton, MA, USA, 2016.

[60] J. R. Quinlan et al. "Learning with continuous classes". In: *5th Australian joint conference on artificial intelligence*. Vol. 92. World Scientific, Canberra, ACT, Autralia. 1992, pp. 343–348.

[61] T. Appelhans et al. "Evaluating machine learning approaches for the interpolation of monthly air temperature at Mt. Kilimanjaro, Tanzania". In: *Spatial Statistics* 14 (2015), pp. 91–113.

[62] A. Morellos et al. "Machine learning based prediction of soil total nitrogen, organic carbon and moisture content by using VIS-NIR spectroscopy". In: *Biosystems Engineering* 152 (2016), pp. 104–116.

[63] J. T. Walton. "Subpixel urban land cover estimation". In: *Photogrammetric Engineering & Remote Sensing* 74.10 (2008), pp. 1213–1222.

[64] M. Kuhn. *caret: Classification and Regression Training*. R package version 6.0-81. R Core Team: Vienna, Austria, 2018. URL: `https://CRAN.R-project.org/package=caret`.

[65] J. E. Nash and J. V. Sutcliffe. "River flow forecasting through conceptual models part I—A discussion of principles". In: *Journal of hydrology* 10.3 (1970), pp. 282–290.

[66] V. Bellon-Maurel et al. "Critical review of chemometric indicators commonly used for assessing the quality of the prediction of soil attributes by NIR spectroscopy". In: *TrAC Trends in Analytical Chemistry* 29.9 (2010), pp. 1073–1081.

[67] C.-W. Chang et al. "Near-infrared reflectance spectroscopy–principal components regression analyses of soil properties". In: *Soil Science Society of America Journal* 65.2 (2001), pp. 480–490.

[68] M. Nocita et al. "Prediction of soil organic carbon content by diffuse reflectance spectroscopy using a local partial least square regression approach". In: *Soil Biology and Biochemistry* 68 (2014), pp. 337–347.

[69] M. Vohland et al. "Determination of soil properties with visible to near- and mid-infrared spectroscopy: Effects of spectral variable selection". In: *Geoderma* 223 (2014), pp. 88–96.

[70] M. Yang et al. "Evaluation of machine learning approaches to predict soil organic matter and pH using Vis-NIR spectra". In: *Sensors* 19.2 (2019), p. 263.

[71] M.-M. Coûteaux, B. Berg, and P. Rovira. "Near infrared reflectance spectroscopy for determination of organic matter fractions including microbial biomass in coniferous forest soils". In: *Soil Biology and Biochemistry* 35.12 (2003), pp. 1587–1600.

[72] G. Fystro. “The prediction of C and N content and their potential mineralisation in heterogeneous soil samples using Vis–NIR spectroscopy and comparative methods”. In: *Plant and soil* 246.2 (2002), pp. 139–149.

[73] B. Ludwig et al. “Near infrared spectroscopy of forest soils to determine chemical and biological properties related to soil sustainability”. In: *Forest Ecology and Management* 171.1-2 (2002), pp. 121–132.

[74] P. K. Mutuo et al. “Prediction of carbon mineralization rates from different soil physical fractions using diffuse reflectance spectroscopy”. In: *Soil Biology and Biochemistry* 38.7 (2006), pp. 1658–1664.

[75] M. Conforti, G. Matteucci, and G. Buttafuoco. “Using laboratory Vis-NIR spectroscopy for monitoring some forest soil properties”. In: *Journal of soils and sediments* 18.3 (2018), pp. 1009–1019.

[76] M. J. Cohen, J. P. Prenger, and W. F. DeBusk. “Visible-near infrared reflectance spectroscopy for rapid, nondestructive assessment of wetland soil quality”. In: *Journal of environmental quality* 34.4 (2005), pp. 1422–1434.

Manuscript 2

Application of Low-Cost MEMS Spectrometers for Forest Topsoil Properties Prediction

Sensors 2021, 21, 3927

Felix Thomas[1*], Rainer Petzold[2], Carina Becker[2], Ulrike Werban[1]

[1] Department Monitoring & Exploration Technologies, Helmholtz Centre for Environmental Research—UFZ, Permoser Straße 15, 04318 Leipzig, Germany
[2] Public Enterprise Sachsenforst, Unit Site Survey, Soil Monitoring and Laboratory, Bonnewitzer Straße 34, 01796 Pirna, Germany

* Corresponding author
E-mail: felix.thomas@ufz.de

Received: 30 April 2021; Accepted: 1 June 2021, Published: 7 June 2021

Abstract

Increasing temperatures and drought occurrences recently led to soil moisture depletion and increasing tree mortality. In the interest of sustainable forest management, the monitoring of forest soil properties will be of increasing importance in the future. Vis-NIR spectroscopy can be used as fast, non-destructive and cost-efficient method for soil parameter estimations. Microelectromechanical system devices (MEMS) have become available that are suitable for many application fields due to their low cost as well as their small size and weight. We investigated the performance of MEMS spectrometers in the visual and NIR range to estimate forest soil samples total C and N content of Ah and Oh horizons at the lab. The results were compared to a full-range device using PLSR and Cubist regression models at local (2.3 ha, n: Ah = 60, Oh = 50) and regional scale (State of Saxony, Germany, 184,000 km^2, n: Ah = 186 and Oh = 176). For each sample, spectral reflectance was collected using MEMS spectrometer in the visual (Hamamatsu C12880MA) and NIR (NeoSpetrac SWS62231) range and using a conventional full range device (Veris Spectrophotometer). Both data sets were split into a calibration (70%) and a validation set (30%) to evaluate prediction power. Models were calibrated for Oh and Ah horizon separately for both data sets. Using the regional data, we also used a combination of both horizons. Our results show that MEMS devices are suitable for C and N prediction of forest topsoil on regional scale. On local scale, only models for the Ah horizon yielded sufficient results. We found moderate and good model results using MEMS devices for Ah horizons at local scale ($R^2 \geq$ 0.71, RPIQ $\geq$ 2.41) using Cubist regression. At regional scale, we achieved moderate results for C and N content using data from MEMS devices in Oh ($R^2 \geq$ 0.57, RPIQ $\geq$ 2.42) and Ah horizon ($R^2 \geq$ 0.54, RPIQ $\geq$ 2.15). When combining Oh and Ah horizons, we achieved good prediction results using the MEMS sensors and Cubist ($R^2 \geq$ 0.85, RPIQ $\geq$ 4.69). For the regional data, models using data derived by the Hamamatsu device in the visual range only were least precise. Combining visual and NIR data derived from MEMS spectrometers did in most cases improve the prediction accuracy. We directly compared our results to models based on data from a conventional full range device. Our results showed that the combination of both MEMS devices can compete with models based on full range spectrometers. MEMS approaches reached between 68% and 105% of the corresponding full ranges devices R^2 values. Local models tended to be more accurate than regional approaches for the Ah horizon. Our results suggest that MEMS spectrometers are suitable for forest soil C and N content estimation. They can contribute to improved monitoring in the future as their

small size and weight could make in situ measurements feasible.

keywords: forest soil; humus; proximal soil sensing; vis-NIR spectroscopy; MEMS-spectrometer

Introduction

The drought events of 2003 and 2010 broke the 500 year record, and the probability of occurrence of extreme heat events is increasing in the future due to global climate change [1]. In 2018, this record was broken again [2], with immediate effects on vegetation growth and further causing soil moisture depletion [3]. As direct consequence, tree mortality increased in many species. As trees are highly vulnerable to other impacts such as insect calamities or fungal attacks after the drought, mortality is likely to go on for years [4].

In Europe, forest areas affected by mortality doubled since 1984, with increasing annual temperature being identified as one of the causes [5]. As a result of the extreme drought stress, the 2018 event caused unprecedented drought-induced tree mortality in many species throughout the region. Moreover, unexpectedly strong drought legacy effects were detected in 2019. This implies that the physiological recovery of trees was impaired after the 2018 drought event, leaving them highly vulnerable to secondary drought impacts. As a consequence, the whole extent of mortality of trees triggered by the 2018 events can not be foreseen yet. In North America, increased rates of forest dieback are reported, linked to drought and rising temperatures [6, 7]. Evidence for heat-induced tree mortality was found around the whole globe [8]. Forest ecosystems will be substantially altered by these ongoing effects, which will as well have a strong impact on forest soils. Gessler et al. [9] state that high nutrient availability in soils can increase water use efficiency. Further, organic substance can positively influence water storage capacity in soils [10, 11]. Therefore, apart from observation of soil moisture and forest vegetation, there is a clear need for improved soil monitoring to ensure proper detection of changes in soil nutrients availability. Methods of proximal soil sensing can be helpful for fast, non-invasive and cost-effective determination of soil properties [12].

On agricultural sites, numerous studies successfully applied vis-NIR spectroscopy to predict soil properties on field scale, e.g., [13, 14, 15, 16]. There are examples for application of the method on different larger scales as well, e.g., for Australia [17], Europe [18] or Belgium and Luxembourg [19]. Some results proved that accuracy is decreasing with extension of the geographic range the samples were originating from [20]. Other studies also showed that local calibrations result in best prediction performance [21].

Regarding forest ecosystems, [22] used near-infrared spectroscopy to estimate total and exchangeable cations and [23] successfully predicted carbon and nitrogen content. The spectral ranges important for prediction of physical properties lie

around 480 and 580 nm in the visual range and around 1400, 1900 and 2200 nm in the NIR-range of the electromagnetic spectrum [24]. Unlike as in agricultural areas, satellites or airplanes can not be used to gain spectral information of forest soils due to the permanent vegetation cover. Using information gained from vegetation as proxy remains difficult and inapplicable. Even most recent approaches show poor results when compared to predictions based on bare soil data [25]. Measurements of forest soils are therefore mostly taken after sample collection under laboratory conditions. Due to the big size and heavy weight of the available devices, successful in situ measurements are scarce.

Recently, low-cost microelectromechanical system (MEMS) spectrometer with reduced spectral range are becoming available. Due to their size and weight, these devices are portable and possibly suitable for in situ measurements. This could reduce field campaign cost and make small-meshed recording of soil properties more feasible.

First studies show that these devices can as well be used for soil properties prediction. Ref. [26, 27] report model performances comparable to standard full-range devices. Their applicability for fertilizer recommendations are investigated as well [28]. However, there are so far no investigations evaluating their performance on forest soil humus and topsoil layers. In addition, information about the influence of the size of the study area on model predictions for forests are rare. Investigations comparing local and regional scales were mainly carried out on agricultural soils. Forest soils are different as they have an organic surface layer called O-horizon. It consists of organic matter in different states of decomposition. Within this layer, the Oh horizon consists of humus and amorphous organic material. Below this horizon, the Ah horizons lies as mineral layer, containing less than 30% organic matter. For forests, retained soil samples of the National Forest Soil Inventory (BZE) in Germany are highly suitable as they cover a wide range of parent material and soil types. The objectives of this work are (i) to assess the accuracy of forest humus properties prediction in Oh and Ah horizons based on MEMS-spectrometers using solely the visual, the near-infrared range and a combination of both, (ii) to compare the results to models build using data from full-range devices and (iii) see if and how model accuracy depends on the different spatial scale the samples originate from.

Methods

Study Area and Sampling Design

In this study, we used data sets collected at two different spatial scales. On one hand, we used retained samples from the periodic BZE in the federal state of Saxony, Germany, supplemented with data from sites representing typical natural areas of Saxony (see [29]). The BZE Saxony sampling was conducted from 2006 to 2014. Samples in this data set originate from all over Saxony (18.400 km^2). More information on the methodology of the periodic BZE sampling can be found in [30]. From all 727 available retained samples, we selected a subsample that represents abundant vegetation types and parent materials in Saxony. The focus lay on dominating forest stands. Conditioned Latin hypercube sampling (clhs) was used for samples from spruce and pine stands to get the optimal number of samples. Further, samples from mixed stands, and minima, median and maxima per horizon and humus form were added, resulting in 362 samples. This data set includes samples from organic and mineral horizons, with 176 samples from Oh-horizon (humified plant material) and 186 samples from Ah horizon (mineral layer with less than 30% organic matter). The main parent materials are sand, loess loam, gneiss, granite, shale and phyllite. Cambisols, gley and podsols are the most abundant soil types. This data set is referred to as "BZE Saxony".
On the other hand, we collected 110 (50 from Oh and 60 from Ah horizon) further samples for a second data set at forest stand scale in a field campaign that took place in June and July 2019 at the forest site "Zellwald" (2.3 ha), located in Middle Saxony. Parent material is loess loam, dominant soil types are luvisols and stagnic luvisols. For this data, the sampling points were selected using clhs sampling beforehand to ensure data collection at representative points and a good representation of the areas soil properties variability. Therefore, all collected samples were used. The data set is referred to as "Zellwald". The location of the sampling points in Saxony and at the forest site "Zellwald" can be seen in Figure 1.

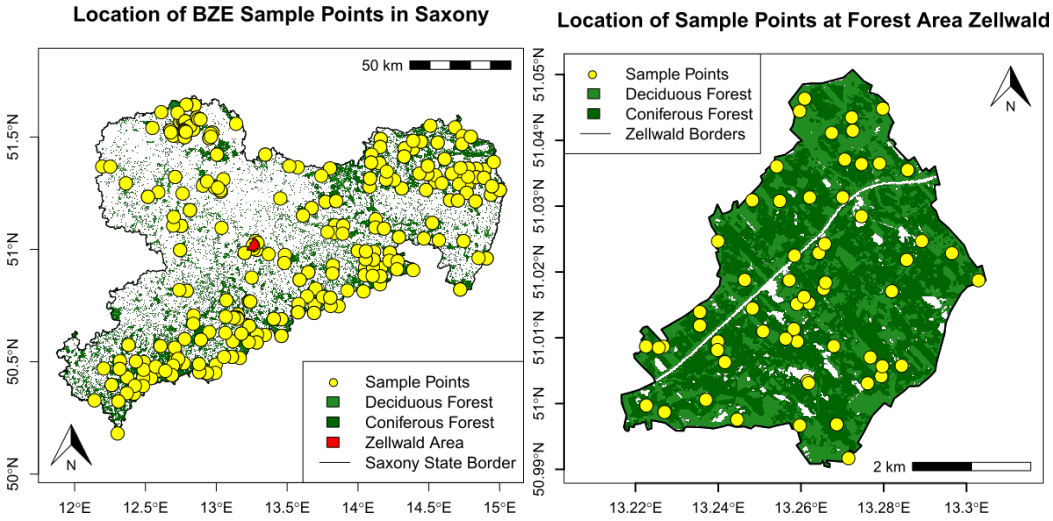


Figure 1: Location of BZE Sample Points in Saxony with Forest Area Zellwald (left), Location of the Sampling Points within the Zellwald Area (right), vegetation data provided by [31].

The study design described in the sampling standard for the BZE was used as basis for the acquisition [32]. The samples were collected using a satellite sampling scheme with eight satellites per point. In case that, due to the site conditions, one or more satellites could not be probed, it was shifted inwards or outwards the circle to facilitate the collection. At every satellite, soil material from Ah horizon and, if present, from organic Oh-horizon was collected and mixed for each horizon. This procedure results in one sample per horizon per sampling point.

Laboratory Analysis

All chemical analysis was performed by the laboratory of Sachsenforst public enterprise, following german-wide standards for forest soil chemical analysis [33]. Total carbon (C) and nitrogen (N) fractions were determined. For total carbon content the dry combustion method with elementary analysis was applied [34].
Before the spectral analysis was conducted, all samples were dried and sieved with a 2 mm mesh to ensure homogeneous material. To protect volatile compounds of the soil during the drying process, the temperature for the samples was set to 40 °C.
The spectral measurements were acquired following a self-developed protocol, which was created based on literature research and several trial measures. Aims of the protocol were to capture each samples variability, to enable a fail-safe procedure and ensure comparability of the measurements. Per soil sample, two petri dishes were filled with soil material. Each dish was then measured five times,

rotating the dish after every measure to increase the acquired variability. Further, this procedure balances the values within the measured area [35]. According to the protocol, the procedure results in ten spectra per sample.
The R language for statistical computing was used for all processing and calculation steps in this study [36].
During the spectral measuring, light scatter can result in effects like baseline shifts or other anomalies. To antagonize these effects, numerous suitable preprocessing techniques exist [37]. First, we smoothed our data using the Savitzky–Golay-Filter. It calculates the sum over a given window, computed as follows in Equation (7):

$$x_j* = \frac{1}{N} \sum_{h=-k}^{k} c_h x_{j+h} \tag{7}$$

where x_j* is the new value, N is a normalizing coefficient, k is the gap size on each side of j and c_h are pre-computed coefficients, that depend on the chosen polynomial order and degree [38, 39]. We used the third polynomial and a window size of 11.
We further normalized our spectra using standard normal variate (SNV). It is calculated as displayed in Equation (8):

$$SNV_i = \frac{x_i - \bar{x_i}}{s_i} \tag{8}$$

where x_i is the signal of a sample i, $\bar{x_i}$ is its mean and s_i its standard deviation [40, 37]. The above described and applied pre-processing steps were carried out by means of the the R package prospectr [39].

Sensors

We used three different spectrometers in our study: one full-range vis-NIR devices (Veris Technologies Inc., Salina, KS, USA), one MEMS-spectrometer for measuring in the visible range (Hamamatsu Photonics K.K.) and one MEMS-spectrometer capturing the NIR range only (Si-Ware Systems Inc., Menlo Park, CA, USA). An overview of the devices and their technical specifications can be seen in Table 1.

Table 1: Overview of technical specifications for the selected devices.

Device	**Veris Spectrophotometer**	**NeoSpec SWS62231**	**Hamamatsu C12880MA**
Wavelength	400–2220 nm	1350–2550 nm	340–850 nm
Spectral Resolution	6 nm @ 350–1000 nm, 5 nm @ 1100–2220 nm	16 nm	15 nm
SNR	300:1 @ 400–1000 nm, NA @ 1100–2220 nm	2000:1	NA
Wavelength reproducibility	NA @ 350–1000 nm, ±0.4 @ 1100-2000 nm	±0.15 nm	±0.5 nm
Weight	24kg	17g	5g

The Veris device uses two internal spectrometers (Ocean Optics USB4000 and Hamamatsu C9914GB). At the beginning and end of the spectra of the Hamamatsu C12880MA device some bands were cut off to match the transition range of the used optical fibre.

Furthermore, for the Veris spectromters bands were cut of at the beginning and end due to a known high amount of noise. Data between the ranges of the two Veris spectrometers (1000 to 1100 nm) were removed. Calibration of the Veris spectrometer was done using four Fluorillon grey standards as external references [41]. The other devices were calibrated by means of a Spektralon plate. In our study, we investigated the performance of each single device and moreover, the data from the Hamamatsu and NeoSpectra device were merged into one vis-NIR data set to evaluate combined performance of the MEMS-spectrometers using the visual and near-infrared range at the same time. This data fusion results in a gap between the ranges of devices from 850 to 1350 nm and therefore still contains less spectral information than the full-range device.

Regression Analysis

For forest soil properties predictions, we selected two regression approaches. First, partial least square regression (PLSR) was applied, which can be seen as widely known standard method to for soil properties prediction using vis-NIR spectral data [42]. It was initially introduced as a solution for multivariate calibration problems using spectroscopy [43]. PLSR constructs a set of linear combinations

of the input data by extracting a sequence of derived, orthogonal directions [44]. These so called factors have high variance as well as high correlation with the response variable and are used for the regression instead of the original data. In this way, the amount of data and therefore the computation time are reduced considerably.
As second method from the field of machine learning, we used the Cubist regression model. The technique is based on the M5 algorithm. It constructs tree-based linear models and is suitable for learning tasks with high dimensionality [45]. It is based on a regression tree, where intermediate linear models at each step are the basis of the predictions. By using subsets of the original data with similar attributes, rules for regression are set by selecting the best predictor, which is used as regression variable. The rules are then connected using if/else statements. If a condition is fulfilled, the regression rule for this subset is applied, otherwise, the next rule is probed [46]. The advantage of this approach is the capability of detecting non-linear relationships [47]. Recently, it was successfully applied for soil properties prediction. Ref. [48] used cubist amongst other methods to predict soil organic carbon (SOC), total nitrogen (TN) and pH values and found it to be superior amongst different algorithms. Similar results were reported by [27] when estimating SOC and total C of agricultural soils based on spectra recorded with different devices.

Model Tuning and Validation

Model calibration was done by means of a ten-fold cross validation and independent validation was performed using parts of the data as test set. Accordingly, we split our data into a calibration and validation set using a ratio of 70:30. In this way, 70% of the data is used to calibrate the model. The remaining 30% are held back and used for independent validation of the prediction performance after the regression models are calibrated.
We calibrated models for Oh and Ah horizons for the regional BZE data and local Zellwald data separately. For the regional BZE data, we also carried out an approach using samples from both horizons. This can be reasonable as the separation of the horizons can be difficult during the sampling. In this case, soil samples of the two horizons from the same sampling point were always kept together as spatial dependence between the horizons my otherwise led to overoptimistic results. The accuracy of the selected algorithms for regression analysis can be improved by tuning specific hyperparameters. In case of PLSR, the number of used components has to be optimized. For Cubist regression,

we have to select the ideal number of committees and neighbours. To ensure a robust selection of values for the hyperparameters of each approach, we used a 10-fold cross validation during the model calibration. In this procedure, we randomly split the data into ten subsets of the same size. Again, samples from the same point were kept in the same splits. Then, model calibration is performed with nine of the subsets, and the remaining subset is used for validation of the model. This procedure is repeated ten times, until each of the ten subsets was used as validation for the model performance once. By this, in total ten models are built, always using different parts of the training data and thus resulting in ten estimates of the model performance using all the data in the calibration set. The estimated prediction errors of all ten models is then combined [44]. This ten-fold cross validation was repeated several times, using different values for the hyperparameters of the algorithms. The tuning was done by a grid-search. Regarding PLSR, one up to 20 components were used to optimize the results. For Cubist, we selected the ideal combination of hyperparameters while searching between values of 1 and 50 for committees, values for neighbours ranged from zero to nine. The values resulting in the lowest error were then chosen and used to evaluate the performance on the test data set, which consists of data the model has not seen yet. For regression model calibration, log-transformed values of C and N content were used. All values were back-transformed prior to model performance validation. For assessing the models performance on the test data, we used different error measures. To evaluate the deviation of the predicted from the measured values, we used the root mean squared error (RMSE). The RMSE is computed as can be seen in Equation (9):

$$RMSE = \sqrt{\frac{1}{n}\sum_{i=1}^{n}(y_i - x_i)^2} \tag{9}$$

where y_i are the predicted, x_i are the observed values.
Apart from error measures based on the deviations of the predictions to the actual observed values, overall model performance was assessed using the coefficient of determination, R^2, described in Equation (10):

$$R^2 = 1 - \frac{\sum(y_i - \hat{y}_i)^2}{\sum(y_i - \bar{y})^2} \tag{10}$$

where y are the observed, $\hat{y}$ are the predicted values and $\bar{y}$ is the mean value of the observed values.
We computed the ratio of performance to interquartile distance in addition. It is

calculated as follows in Equation (11) [49]:

$$RPIQ = \frac{Q3_{obs} - Q1_{obs}}{RMSE} \tag{11}$$

where $Q1$ and $Q3$ are the first and the third quantile of the observed values.
Chang et al. Chang et al. [50] suggested a system to rank RPD values. We adapted it for RPIQ (transformation was done by multiplying the values with 1.34896 (as the interquartile range of a Gaussian distribution equals 1.34896 × SD)). Model with RPIQ > 2.70 are considered good, models with 1.89 < RPIQ < 2.70 are moderate and the threshold for poor performance is RPIQ < 1.89.
In general, the models accuracy is indicated by low RMSE and high R^2 and RPIQ values. All calculations were carried out by means of the R language for statistical computing [36] and the caret package for classification and regression training [51].

Results

Results of Chemical and Spectral Data Analysis

The summary of the results of the chemical analysis of the soil samples from both data sets are shown in Table 2, separated by horizon. The BZE Saxony data consisted of 362 samples in total, with 176 samples from Oh horizons and 186 samples from Ah horizons. In the organic horizon, values for total C content ranged from 8.60 to 49.4%, with a mean of 27.15%. Percentage of nitrogen in the sample lay between 0.32 and 2.08%. Mean value was 1.22%. For the Ah horizon, C content values lay between 0.40 and 17.22, with a mean of 5.12. The mean of the N content was 0.23, with values ranging from 0.02 to 1.06.
Regarding the data set collected in the forest area Zellwald, values for C content in the Oh horizon were measured to be between 18.81 and 41.36 %, with a mean of 33.99 %. The N content in these samples ranged from 0.2 to 2.11 %. The mean was 1.66 %. In the Ah horizon, C content lay between 3.16 and 13.88 with a mean value of 6.43. Measured values for N content ranged from 0.17 to 1.08, mean value was 0.34.
Graphs of the spectra obtained with the different devices can be seen in Figure 2. It shows all measured samples (mean of ten single measurements) of both data sets per spectrometer, with the mean of all measurements. The raw spectra is shown on the left, while pre-processed data can be seen on the right side. It clearly can be seen that remarkable trends in all measured spectra were emphasized by the applied pre-processing methods.

Table 2: Descriptive statistics for C and N content of Oh and Ah horizons for soil samples from both data sets.

Data Set	Horizon	Parameter	N	Mean	St. Dev.	Min	Pctl (25)	Pctl (75)	Max
BZE Saxony	Oh	C [%]	176	27.15	8.01	8.60	21.73	32.53	49.43
		N [%]	176	1.22	0.38	0.32	0.96	1.53	2.08
	Ah	C [%]	186	5.12	2.77	0.40	2.88	6.99	17.22
		N [%]	186	0.23	0.15	0.02	0.11	0.31	1.06
Zellwald	Oh	C [%]	50	33.99	5.03	18.81	32.11	37.37	41.36
		N [%]	50	1.66	0.20	1.04	1.53	1.79	2.11
	Ah	C [%]	60	6.43	2.14	3.16	4.86	7.81	13.88
		N [%]	60	0.34	0.14	0.17	0.25	0.41	1.08

The Hamamatsu and Veris spectra both showed the steady ascent through the whole visual range. In the NIR-range, the important reflectance dips around 1400 as well as around 1900 could be detected in both measured spectra using the Veris and Neospectra devices. They are also known as strong water absorption features. The preprocessing accentuated these trend for both devices. In the Neospectra data, the feature around 2200 could be seen as well as it ranges until 2500 nm.

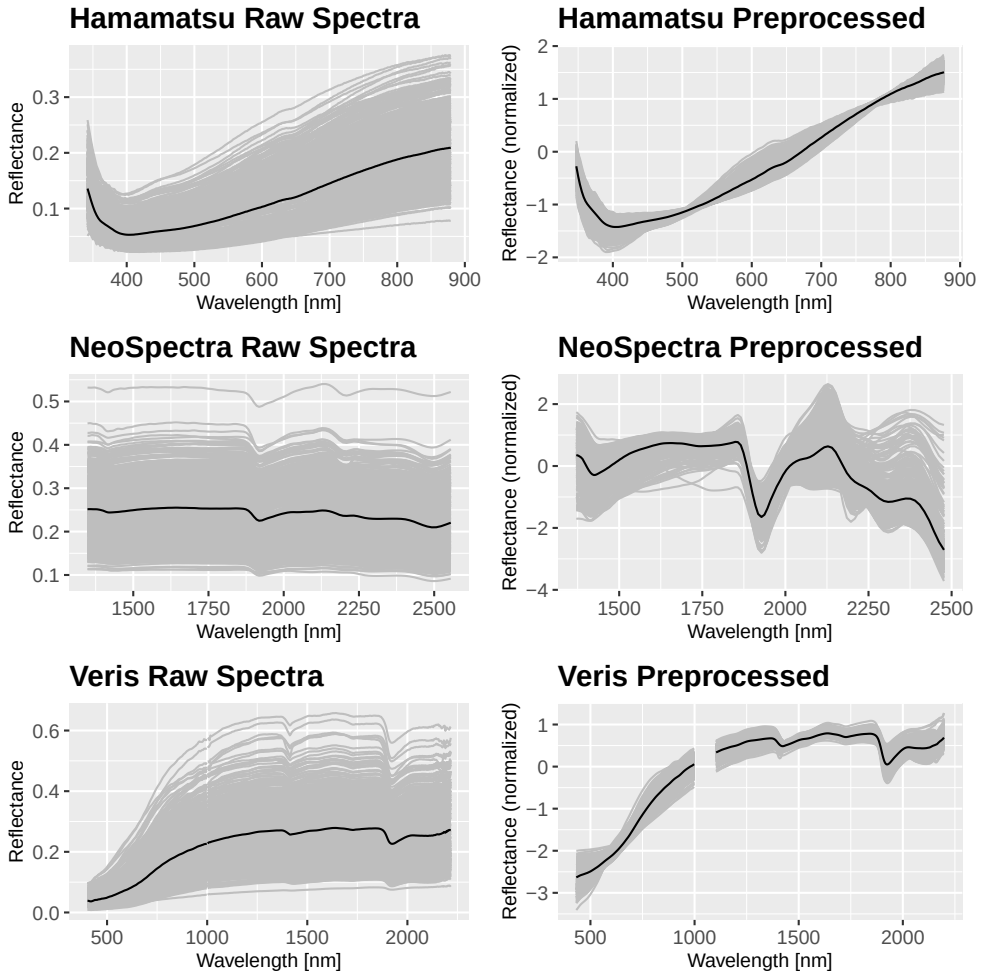


Figure 2: Raw (left) and preprocessed (S-G Filter and SNV, right) spectra of samples from both data sets using the selected devices, the black line represents the mean of all measurements

Predicting Total Carbon Content

To evaluate the application of the selected spectrometers for total C prediction of forest topsoil samples, we calibrated models for Oh and Ah horizon using PLSR and Cubist for every spectral data set, once for the BZE data from whole Saxony (regional scale), and once for the forest site Zellwald (local scale). An additional model was calibrated using samples from Oh and Ah horizons combined for the regional scale.

The validation results of the separate models for the Oh and Ah horizons for the regional BZE data set are shown in Table 3. Using the spectral data in the visual range derived by the Hamamatsu device to predict carbon, the results were: RMSE = 8.98%, R^2 = 0.01 and RPIQ = 1.48 (Oh) and 2.36%, 0.29 and 1.67 (Ah) for the PLSR approach. Using Cubist, RMSE, R^2 and RPIQ were 7.03%, 0.40

Table 3: Model validation results for total carbon and nitrogen values from Oh (left) and Ah (right) horizon separately using PLSR and Cubist and spectral data from different devices for the regional BZE data set.

			Oh Horizon			Ah Horizon		
Parameter	**Algorithm**	**Sensor**	**RMSE %**	R^2	**RPIQ**	**RMSE %**	R^2	**RPIQ**
C	PLSR	Hamamatsu	8.98	0.01	1.48	2.36	0.29	1.67
		Neospectra	6.87	0.43	1.94	1.97	0.48	2
		Hamamatsu + Neospectra	5.87	0.57	2.27	2.01	0.49	1.97
		Veris	6.79	0.47	1.96	1.93	0.55	2.05
	Cubist	Hamamatsu	7.03	0.40	1.90	2.13	0.36	1.86
		Neospectra	6.70	0.43	1.99	1.69	0.61	2.34
		Hamamatsu + Neospectra	5.60	0.61	2.38	1.75	0.55	2.25
		Veris	5.98	0.58	2.23	1.59	0.62	2.48
N	PLSR	Hamamatsu	0.38	0.18	1.75	0.13	0.17	1.55
		Neospectra	0.36	0.31	1.84	0.09	0.55	2.15
		Hamamatsu + Neospectra	0.29	0.51	2.28	0.10	0.52	2.05
		Veris	0.30	0.48	2.21	0.13	0.66	1.48
	Cubist	Hamamatsu	0.36	0.23	1.83	0.14	0.04	1.37
		Neospectra	0.26	0.61	2.56	0.09	0.54	2.15
		Hamamatsu + Neospectra	0.27	0.57	2.42	0.11	0.33	1.74
		Veris	0.25	0.66	2.64	0.06	0.78	3.08

and 2.90 (Oh) and 2.13%, 0.36 and 2.86 (Ah), respectively. When calibrating the models with NIR range data from Neospectra, results for PLSR regression were: RMSE = 6.87%, R^2 = 0.43, RPIQ = 1.94 (Oh) and RMSE = 1.97%, R^2 = 0.48 and RPIQ = 2.00 (Ah). The Cubist regression resulted in lower RMSE values of 6.70% and R^2 and RPIQ of 0.43 and 1.99 for Oh horizons. For the Ah horizon data, model performance was more accurate as well (RMSE = 1.69% and R^2 = 0.61, RPIQ = 2.34). The combination of Hamamatsu and Neospectra data using both visual and NIR range for regression resulted in RMSE, R^2 and RPIQ values of: 5.87%, 0.57 and 2.27 (PLSR, Oh), 2.01%, 0.49 and 1.97 (PLSR, Ah), 5.60%, 0.61 and 2.38 (Cubist, Ah) and 1.75%, 0.55 and 2.25 (Cubist, Ah).

Modeling results on basis of the full-range Veris spectrometer with PLSR achieved: RMSE = 6.79%, R^2 = 0.47, RPIQ = 1.96 (Oh) and RMSE = 1.93%, R^2 = 0.55 and RPIQ = 2.05 (Ah). The Cubist estimations results were calculated as: RMSE = 5.98%, R^2 = 0.58 and RPIQ = 2.23 (Oh) and RMSE = 1.59%,

$R^2 = 0.62$ and RPIQ = 2.48 (Ah), respectively. Therefore, the most accurate predictions of C content were reported using the full-range approaches. The usage of MEMS-spectrometer in combination led to similar predictive performance (Oh: 105%, Ah:89% of the full range models R^2 values) while the visual range model showed the least precise results (Oh: 69%, Ah: 58% of the full range models R^2 values). Estimated and observed values of the independent validation sets of the Cubist regression models based on data from all spectrometers and both Oh and Ah horizon are displayed in Figure 3 on the left side. It can be seen that deviations of the predictions from the observed values were not evenly distributed for the models based on the visual range. The other approaches show a better orientation along the x = y line. For the Oh horizon, high values seem to be overestimated while low values tend to be underestimated. The residual plots (see Figure 6 in the appendix 6) underline this observation.
For the regional BZE data, we also calibrated models using a combined approach of both Oh and Ah horizons samples. The results of this approach can be seen in Table 4. Using the visual range to predict C, the results were: RMSE = 6.64%, R2 = 0.75 and RPIQ = 3.47 (PLSR) and RMSE = 6.36%, $R^2 = 0.76$ and RPIQ= 3.63 (Cubist). Using the only the NIR range for model calibration, RMSE, R2 and RPIQ were 6.67%, 0.74 and 3.46 for PLSR and 5.01%, 0.85 and 4.60 for Cubist regression, respectively.

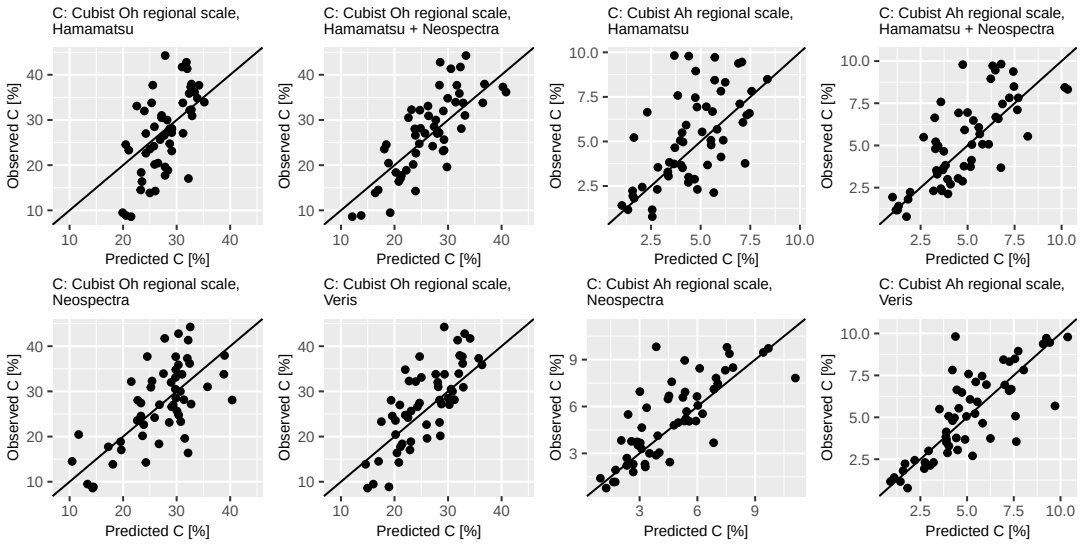


Figure 3: Predicted vs. observed C content values for validation of cubist regression models for Oh and Ah horizon based on spectral data obtained with the selected devices

When calibrating the models with data from both visual and NIR ranges combined, results for PLSR were: RMSE = 6.98%, $R^2 = 0.73$, RPIQ = 3.30 (PLSR) and

Table 4: Model validation results for total carbon and nitrogen using combined horizons (Oh and Ah) for calibration, PLSR and Cubist and spectral data from different devices for the regional BZE data set.

Parameter		**C**			**N**		
Algorithm	**Sensor**	**RMSE %**	R^2	**RPIQ**	**RMSE %**	R^2	**RPIQ**
PLSR	Hamamatsu	6.64	0.75	3.47	0.33	0.72	3.26
	Neospectra	6.67	0.74	3.46	0.35	0.67	3.08
	Hamamatsu + Neospectra	6.98	0.73	3.30	0.34	0.71	3.17
	Veris	5.41	0.83	4.26	0.29	0.79	3.80
Cubist	Hamamatsu	6.36	0.76	3.63	0.33	0.72	3.34
	Neospectra	5.01	0.85	4.60	0.24	0.85	4.51
	Hamamatsu + Neospec	5.13	0.84	4.49	0.24	0.85	4.57
	Veris	4.29	0.89	5.38	0.21	0.88	5.24

RMSE = 5.13%, R^2 = 0.84 and RPIQ = 4.49 (Cubist). Using the full range spectral data of the Veris device to predict carbon, the results were: RMSE = 5.41%, R^2 = 0.83 and RPIQ = 4.26 (PLSR) and 4.29%, 0.89 and 5.38 for the Cubist regression approach.

In this case, the most accurate predictions of C content were reported using the full-range device. The approaches using NIR range alone and MEMS-spectrometer in combination led to similar predictive performance. The model based on the visual range again showed less precise results. Calculated predicted and observed values of the independent validation sets from the BZE data of the Cubist regression models based on data from all spectrometers are displayed in Figure 4. It can be seen that deviations of the predictions from the observed values were generally higher for the samples from Oh-horizons, which were distinguishable from the Ah samples.

Table 5: Model validation results for total carbon (left) and nitrogen (right) values from Ah horizon using PLSR and Cubist and spectral data from different devices for the local Zellwald data set.

Parameter		**C**			**N**		
Algorithm	**Sensor**	**RMSE %**	R^2	**RPIQ**	**RMSE %**	R^2	**RPIQ**
PLSR	Hamamatsu	0.99	0.62	2.66	0.10	0.24	1.46
	Neospectra	1.44	0.44	1.83	0.07	0.67	2.15
	Hamamatsu + Neospectra	1.58	0.66	1.66	0.09	0.58	1.54
	Veris	0.74	0.89	3.55	0.06	0.87	2.19
Cubist	Hamamatsu	1.08	0.56	2.42	0.08	0.45	1.67
	Neospectra	1.50	0.35	1.75	0.11	0.15	1.23
	Hamamatsu + Neospectra	0.62	0.86	4.22	0.06	0.71	2.41
	Veris	0.90	0.86	2.92	0.04	0.84	3.37

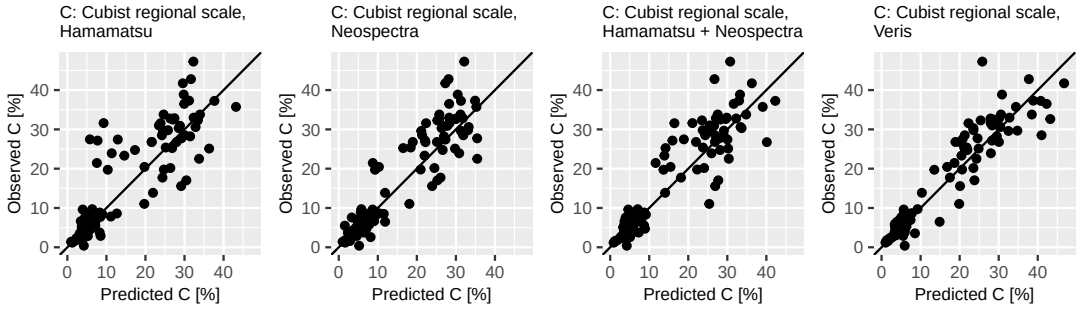


Figure 4: Predicted vs. observed C content for validation of cubist regression models using both Oh and Ah horizon for regional scale (BZE Saxony) based on spectral data obtained with the selected devices

For the visual range, it is further notable that, in contrary to the other approaches, the deviations of predicted values were less oriented along the x = y line. Models including data from the NIR area were more precise in this aspect.

The results of the model validation procedure for the Ah horizon of the local Zellwald data set can be seen in Table 5 on the left side.

Using the spectral data in the visual range to predict carbon, the model results were: RMSE = 0.99%, R^2 = 0.62 and RPIQ = 2.66 for PLSR and 1.08, 0.56 and 2.42 for the Cubist approach. Using NIR spectral data for the models, RMSE, R^2 and RPIQ were 1.44%, 0.44 and 1.83 (PLSR) and 1.50%, 0.35 and 1.75 (Cubist). When calibrating the models with data from combined visual and NIR range, results for PLSR regression were: RMSE = 1.58%, R^2 = 0.66, RPIQ = 1.66. For Cubist, model results were RMSE = 0.62%, R^2 = 0.86 and RPIQ = 4.22.

The full-range Veris approach resulted in lower RMSE values of 0.74%, and higher R^2 and RPIQ of 0.89 and 3.55 for PLSR. For the Cubist model, performance was calculate as RMSE = 0.90%, and R^2 = 0.86, RPIQ = 2.92.
Calculated predicted and observed values of the independent validation sets of the Cubist regression models based on data from all spectrometers are displayed in Figure 5. It shows that that the models including data from both visual and NIR range were more accurate, as the points cluster tight around the x = y line. It was not possible to calibrate meaningful models based on the Oh horizon only (data not shown).

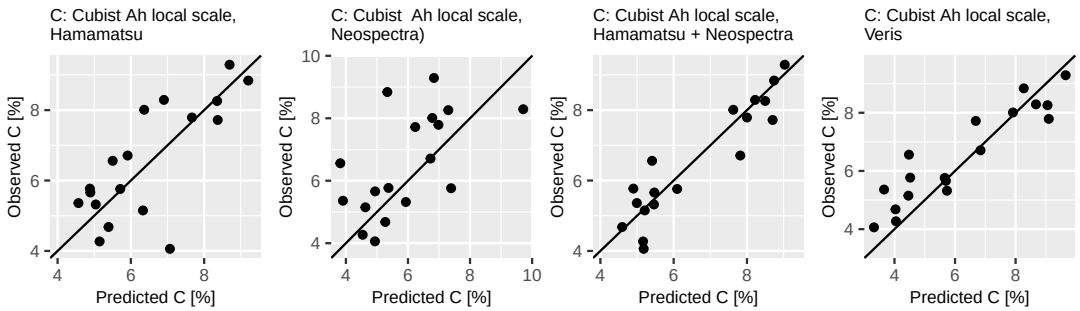


Figure 5: Predicted vs. observed Ah horizon C content values for validation of cubist regression models for local scale (Zellwald) based on spectral data obtained with the selected devices

Predicting Total Nitrogen Content

In a second step, the performance of the different devices for total nitrogen content prediction was assessed for Oh and Ah horizon for both data sets of the study using PLSR and Cubist.

The results of the separate models of N prediction for the Oh and Ah horizons of the regional BZE data set are shown in the lower part of Table 3. Regressions for Oh horizon based on spectral data in the visual range were more precise using Cubist, with values of RMSE = 0.36%, $R^2 = 0.23$ and RPIQ = 1.86. For models based on the Ah samples, performance was less precise.

For NIR range, Cubist model results were more precise with RMSE = 0.26%, $R^2 = 0.61$ and RPIQ = 2.56 for the organic Oh horizon. For the Ah horizon models, we achieved very similiar results for both approaches. Regarding the models for combined data set covering visual and NIR range, Oh results were: RMSE = 0.29%, $R^2 = 0.51$, RPIQ = 2.28 (PLSR) and RMSE = 0.27%, $R^2 = 0.57$, RPIQ = 2.42 when using the Cubist regression approach. PLSR outperformed Cubist when predicting total N content of the Ah soil samples Additionally, we used a full-range device for model calibration. The models based on Oh samples with PLSR resulted in RMSE = 0.30%, $R^2 = 0.48$, RPIQ = 2.42. The Cubist models were more precise with RMSE = 0.25%, $R^2 = 0.66$, RPIQ = 2.64. Using Ah samples the Cubist model again resulted in higher accuracy with RMSE = 0.06%, $R^2 = 0.78$ and RPIQ = 3.08. In total, the full range device resulted in best prediction performance for total N estimation. Predicted and observed total N content values for models based on data from both horizons and all used spectrometers for the regional BZE data are shown in Figure 7. Largest deviance in the predictions can clearly be seen for the models based on the visual range. Results for the other approaches were more precise, as they were distributed closer

and more along to the x = y line. Further, lower values tended to be overestimated, while higher ones were underestimated. This observation was stronger for the models of the Oh horizon.

In addition, we also calibrated models using a combined approach of both Oh and Ah horizons samples for the regional BZE data. The results of the calculations can be seen in Table 4. In this case, the models calibrated based on the visual range to predict N content achieved similar accuracy for both algorithms. Using the NIR range only, model accuracy increased. RMSE, R^2 and RPIQ were 0.35%, 0.67 and 3.08 for PLSR and 0.24%, 0.85 and 4.51 for Cubist regression, respectively. The results of the combined devices procedure resulted in similar results. PLSR achieved RMSE = 0.34%, R^2 = 0.71 and RPIQ = 3.17. The usage of Cubist regression resulted in RMSE = 0.24%, R^2 = 0.85 and RPIQ = 4.57. Models calibrated using data derived from the full-range device yielded best accuracy. The PLSR model resulted in RMSE = 0.29%, R^2 = 0.79 and RPIQ = 3.80, the Cubist approach in RMSE = 0.21%, R^2 = 0.88 and RPIQ = 5.24. The predicted and observed values of the Cubist model combing both horizons of the regional BZE data can be seen in Figure 8. The largest inaccuracies in the predictions could be observed for the models based on the visual range. The other approaches were more accurate, indicated by tighter point clouds and a better orientation along the x = y line.

We observed an equivalent prediction power of the combined MEMS-spectrometer approach compared to the Veris device.

The results of the independent validation procedure for the Ah horizon of local Zellwald data, separated by algorithm and sensor, can as well be seen in Table 5. The error measures for N content are on the right side. Regression based on spectral data in the visual range was more precise using Cubist and resulted in values of RMSE = 0.08%, R^2 = 0.45 and RPIQ = 1.67. Regarding the NIR range, model performance increased and was more accurate using PLSR, with RMSE = 0.07%, R^2 = 0.67 and RPIQ = 2.15 for PLSR. Using Cubist, models were less precise. Using the combination of visual and NIR data, the local model for Zellwald resulted in in RMSE values of 0.09% (PLSR) and 0.06% (Cubist), R^2 values ranged from 0.58 (PLSR) to 0.71 (Cubist). RPIQ was calculated as 1.54 for PLSR and 2.41 for Cubist. For the full range device data, prediction accuracy was the most precise. PLSR results were: RMSE = 0.06%, R^2 = 0.87, RPIQ = 2.19. For the Cubist regression, RMSE was 0.04%, $R2$ was 0.84 and RPIQ = 3.37. Predicted and observed total Ah horizon N content values for models based on local Zellwald data from all used spectrometers are shown in Figure 9.

Smallest deviance in the predictions can clearly be seen for the models based on the combined and full rage approaches. As for the C predictions, no suitable models could be calibrated for the Oh horizon of the local Zellwald data.

Discussion

Feasibility of MEMS-Spectrometer for Forest Soil C and N Content Estimation

This study aimed to investigate the feasibility of using MEMS-spectrometer for forest humus and topsoil total C and N content prediction. We used spectral data measured with MEMS-devices in the visual and NIR range, and a combination of both in addition. Models were calibrated separately for Oh and Ah horizon. Using the regional BZE data, we also modelled C and N content in an approach using both horizons. As Cubist regression showed higher prediction power, the discussion about feasibility and the comparison to conventional devices is based on these results. Models calibrated for Oh samples with the regional BZE data set showed comparable results. Again, the combination of the MEMS devices yielded moderate accuracy for both total C and N content prediction (Cubist: RPIQ $\geq$ 2.38, R^2 $\geq$ 0.57). The solely usage of the visual range was least precise and it was not possible to establish meaningful models. In the Ah horizon however, the NIR range device had better predictions, reaching the threshold for moderate correlations (Cubist: RPIQ $\geq$ 2.15, $R^2 \geq$ 0.54). The combination of both devices performed slightly less precise, the Hamamatsu alone was again insufficient (RPIQ ¡ 1.89). In addition, we calibrated models for the regional BZE data using data from both Oh and Ah horizon. In this case, the Neospectra and the combined MEMS devices yielded very similar and good model results (Cubist: RPIQ $\geq$ 4.49, $R^2 \geq$ 0.84). The predictions based on the visual range showed less accuracy. Even though the model reached the proposed threshold of RPIQ = 2.7, visual assessment revealed high uncertainties within the investigated horizons for both properties. In the Ah horizon of the local Zellwald data, Cubist models using data both MEMS-devices resulted in moderate prediction accuracy for both properties (RPIQ $\geq$ 2.41, R^2 $\geq$ 0.71). Results for the solely usage of the visual range were moderate only for C content. The estimations based on NIR range only were less precise. Therefore, especially a combination of MEMS devices seemed to be suitable for forest soil C and N content estimation. The solely usage of the visual range however was not sufficient. Regarding the Oh horizon, no meaningful model could be calibrated.

One reason for this could be the small sample size.
The similar results of C and N content predictions lead to the question, if soil N content is measured directly, or through auto-correlation with C content. In contrast, other studies presented results indicating that N content is measured independently from C content due to successful prediction of total N and C:N ratios (e.g., [52]).
Further, the results achieved using MEMS devices were to be compared to regression models built on spectral data obtained with a conventional full-range spectrometer. These results were therefore used as benchmark to see if the MEMS devices could reach the predictive performance of the full range device. In most cases the Veris full-range data yielded the best results, with highest R^2 and RPIQ values and lowest RMSE. However, depending on horizon and scale, it was possible to achieve results that could compete with the models based on the full-range device. Regarding the modelling of Oh samples of the regional BZE data, the Cubist model of combined MEMS approach even outperformed the Veris device for C content (Combined: $R^2 = 0.61$, RPIQ = 2.38, Veris: $R^2 = 0.58$, RPIQ = 2.23) and therefore achieved 105% of the conventional device. When used alone, the visual range approach had 69% and the NIR range approach 74% of the full range R^2 value. For N content, the models based on the full range data yielded better results, but the combined MEMS approach could still compete (Combined: $R^2 = 0.57$, RPIQ = 2.42, Veris: $R^2 = 0.66$, RPIQ = 2.64). In this case, 86% of the full range performance were reached. The models based on NIR spectra solely were more precise ($R^2 = 0.61$, RPIQ = 2.56, equals 92%). For Ah horizon, Cubist models based on the NIR range only were the most competitive for C and N content (Neospectra: $R^2 \geq 0.54$, RPIQ $\geq$ 2.15, Veris: $R^2 \geq 0.62$, RPIQ $\geq$ 2.48). This equals 98% of the R^2 values of the Veris device for C content and 69% for N content. The combined approach reached 89% for C and 56% for N content. In general, the NIR range and combined MEMS data devices as well as the full range approach resulted in model performance classified as moderate. Further, we modelled C and N content using samples from both horizons of the regional BZE data set. Similar to the results discussed above, in this approach the Cubist models based on NIR range and the combined MEMS data were able to compete with the full range device for both investigated properties (combined: $R^2 \geq 0.85$, RPIQ $\geq$ 4.49, Veris: $R^2 \geq 0.88$, RPIQ $\geq$ 5.24). Therefore, more than 95% of the Veris R^2 values were reached using MEMS devices, and the calibrated models can be classified as good. However, it is important to mention that the increase of the data range resulting from the usage of both Oh and Ah horizons

also led to increased values for the selected error measures. For the Ah horizon of the local approach in the Zellwald forest, the data from combined MEMS devices resulted in comparable accuracy when using Cubist for C (Combined: $R^2 = 0.86$, RPIQ = 4.22, Veris: $R^2 = 0.86$, RPIQ = 2.92) and N content (Combined: $R^2 = 0.71$, RPIQ = 2.41, Veris: $R^2 = 0.84$, RPIQ = 3.37). The MEMS as well as the conventional approach yielded moderate to good model predictions. In direct comparison of the R^2 values of the Cubist models, the combined MEMS approach reached 100% of the full range performance for C content and 85% for the N content.

Our results indicated that the MEMS spectrometers can generally be used to substitute common full-range devices. For the investigated data sets and properties, especially the combination of visual and NIR range data measured with MEMS devices showed predictive performance comparable with the full range device. In some cases, estimations even outperformed the conventional approach.

The two data sets used in this study allowed to investigate the impact of the scale on the model prediction accuracy of the Ah horizon. The results showed that the C content predictions calculated for the local Zellwald forest based on the combined MEMS and the full range devices data were more accurate than the ones based on the BZE data set for both algorithms. Exception is the NIR range model, which performed better on the regional data. The difference in accuracy is bigger for the MEMS-devices than for the full-range spectrometer. Similar observations could be made for the N content estimations. Again, the local results for the combined and full range data models were more precise for both properties. In this case, only the NIR range Cubist results represented an exception. One reason for the differences in the results could be the greater variability in the BZE data set due to the bigger geographical range. Further, data acquisition took place over several years and was therefore carried out by different persons. In addition, there was a longer time span between chemical and spectral measurements. In contrast, the data collection for the Zellwald area was conducted within a short amount of time (approximately one month), all samples were taken by the same samplers and chemical as well as spectral measurements were taken directly in the weeks after the sampling was finished.

Comparison to Other Studies

Few studies investigated the usage of MEMS-devices for soil properties prediction so far. Their applications were using only soil samples originating from agricultural areas. In Australia, e.g., Sharififar et al. [27] evaluated the prediction power of

different low-cost NIR spectrometer for organic as well as total carbon. Using the Neospectra device, they reported R^2 values of 0.78 (Cubist) and 0.73 (PLSR) for SOC. For total C content, their prediction metrics descended with $R^2 = 0.7$ for Cubist and $R^2 = 0.55$ when using PLSR. The models were therefore more precise than our results separated by horizon and less precise than our combined models. Another study from Australia investigated the Neospectra for total C content amongst other properties as well [26]. Soil material from 0 to 100 cm depth and a Cubist regression model were used. They achieved $R^2 = 0.74$, which is about the same accuracy we calculated using PLSR and combined horizons. However, our estimations based on separate horizons were less precise on local and regional scale. The discrepancies regarding prediction accuracy could lie in the substantial differences in the study setup. All studies investigated agricultural soils, where no humus layer is present. Further, different depth ranges were investigated and the study areas were covering much bigger scales than our study. In a study with focus on precision fertilization in Indonesia [28] reported $R^2 = 0.57$ for SOC and $R^2 = 0.52$ for total N content, which is within the same range as our regional Ah results. In this case, samples from 0 to 25 cm depth were used.

There were examples of studies using the visible range as well. Ref. [53] estimated SOC using spectral data corresponding to red, green and blue light at field scale, reporting $R^2 = 0.78$ using the random forest algorithm. This accuracy equals our regional results based on combined horizons. However, our results based on the visual range were less precise for separated horizons.

Ref. [54] investigated predictions using artificial spectral data, concluding that the range covering 350–975 nm increased inaccuracy when compared to approaches based on, or including NIR range. Ref. [14] found no prediction accuracy difference using vis and NIR range separately to estimate SOC ($R^2 = 0.6$ in both cases). This study was conducted on a local approach with sample material from 0 to 20 cm depth originating from an agricultural field in Australia. In our local approach, we reached similar results using the visual range for Ah horizon. However, we found different accuracies between visual and NIR range in the combined horizons approach.

For the differences in prediction accuracy between the local and the regional data set, opposed findings were reported. Ref. [55] investigated the scalability of soil total carbon prediction models using data from different fields individually and in a combined approach. They found the pooled data set and therefore the bigger scale to be more accurate than the single fields. On the other side, Ref. [56] found small scales model calibrations to be more accurate than large libraries when

investigating SOC at field scale. Similar observations were made by [20], who reported decreasing prediction accuracy with extension of the geographic range. In our case, the smaller scale also yielded better results. Possible reasons for this observations were suggested, e.g., by [42], who states that model accuracy decreases when containing samples from diverse geographic origins and that the usage of large diverse spectral libraries is therefore more difficult. Ref. [57] reported correlations between the model errors and the standard deviations of the predicted soil properties. It seems to us that the underlying correlations are still not sufficiently unterstood, and that more research including up- and downscaling of models calibrated for forest soils should be done.

Relevance for Forest Soil Monitoring

Based on the good prediction accuracy we achieved under laboratory conditions, we suggest that future in situ measurements are feasible with the investigated MEMS devices due to their small size and weight. This way, obtained data could be used solely or to supplement remote sensing approaches that lack applicability due to the vegetation cover. Further investigations are especially recommended for local forest stands and sites. On agricultural areas, first application of in situ measurements were already conducted [58]. Regarding in situ measurements, it is important to keep the possibility of wet conditions in mind. The influence of water content on spectral data was as well already subject of investigations in agricultural fields [59]. These effects should also be investigated for forest humus and topsoil in order to get reliable in-situ measurements. Another possibility that could be probed is to test a short drying of the soil surface directly before measuring. This way, the impact of soil moisture could possibly be reduced. Another factor that could influence in-situ measurements is the unsieved soil material.
The predictions could, e.g., be used to monitor long term processes. Over the last decades, steadily increasing carbon stocks were reported in forest soils, e.g., in western Europe where an increase of 65% is estimated between 1990 and 2050 [60]. Similar observations were made for China [61]. Such effects could be monitored more easily and with higher spatial resolution by data collection using MEMS devices, as needed efforts can be remarkably reduced.

Conclusions

In summary, this study demonstrates that low-cost MEMS spectrometers can be successfully used to predict forest humus total C and N content. Models based on

spectral data obtained with MEMS are can compete models built with data from full range spectrometer when combining visual (340–850 nm) and NIR (1350–2550 nm) range data. We achieved moderate prediction accuracy for local Ah horizons and regional Oh and Ah horizon samples with data from MEMS and full-range devices. Our results showed that the the performance decreased when using only the visual range, and that it is difficult to establish sufficient models to predict forest total C and N content in this case. Results for Ah horizons were more precise for the local Zellwald area when compared to models based on data from whole Saxony. We conclude that the investigated devices could be suitable for spectral in situ measurements of forest soils due to their small size and weight. The actual application of low-cost MEMS spectrometers in in situ measurements at forest soils should be investigated. Their usage could reduce expenditure of time and costs and of spectral data acquisition and could therefore contribute to build larger spectral libraries of forest soil that can be used for forest soil C and N content monitoring purposes.

Author contributions

Conceptualization, F.T., R.P. and U.W.; Methodology, F.T.; software, F.T.; validation, F.T., R.P. and U.W.; formal analysis, F.T.; investigation, F.T. and C.B.; resources, R.P. and U.W.; data curation, F.T. and C.B.; writing—original draft preparation, F.T.; writing—review and editing, U.W., R.P. and C.B.; validation, F.T., R.P., U.W., C.B.; visualization, F.T.; supervision, U.W. and R.P.; project administration, U.W. and R.P.; funding acquisition, U.W. and R.P. All authors have read and agreed to the published version of the manuscript.

Funding The study is part of the joint research project DIGI-Humus: "Verbundvorhaben: Erfassung und Regionalisierung von Humuseigenschaften mittels VIS-NIR und Digitaler Bodenkartierung" and was funded by the Federal Ministry of Food and Agriculure (project no. 22014417 and 22001316).

Data availability The regional data sets from this study are available through the PANGAEA open access repository under https://doi.org/10.1594/PANGAEA.921689 (Thomas et. al., 2020).

Acknowledgments

We want to thank the chemical laboratory of Public Enterprise Sachsenforst for analyzing the soil samples used in this study, and Marco Pohle and Solveig Landmark for their support conducting the spectral measurements. We thank the Federal Ministry of Food and Agriculture (BMEL) and the Fachagentur Nachwachsende Rohstoffe (FNR) for permanent support of the project DIGI-Humus (Recording and regionalization of humus properties using VIS-NIR and Digital Soil Mapping). This study received funding for F.T. (#22014417) and C.B. (#22001316) within the project DIGI-Humus. We further want to thank the European Environment Agency for providing the Copernicus Land Monitoring Service with funding by the European Union.

Conflicts of interest

The authors declare no conflict of interest. The funders had no role in the design of the study; in the collection, analyses, or interpretation of data; in the writing of the manuscript, or in the decision to publish the results.

Abbreviations

The following abbreviations are used in this manuscript:

NIR	near-infrared range of the electromagnetic spectrum
vis	visual range of the electromagnetic spectrum
MEMS	microelectro mechanical system
BZE	National Forest Soil Inventory
SOC	Soil organic carbon
clhs	Conditioned Latin hypercube sampling
SG	Savitzky - Golay Filter
SNV	Standard Normal Variate
PLSR	Partial Least Square Regression
RPD	Ratio of Performance to Deviation

Supplementary Data

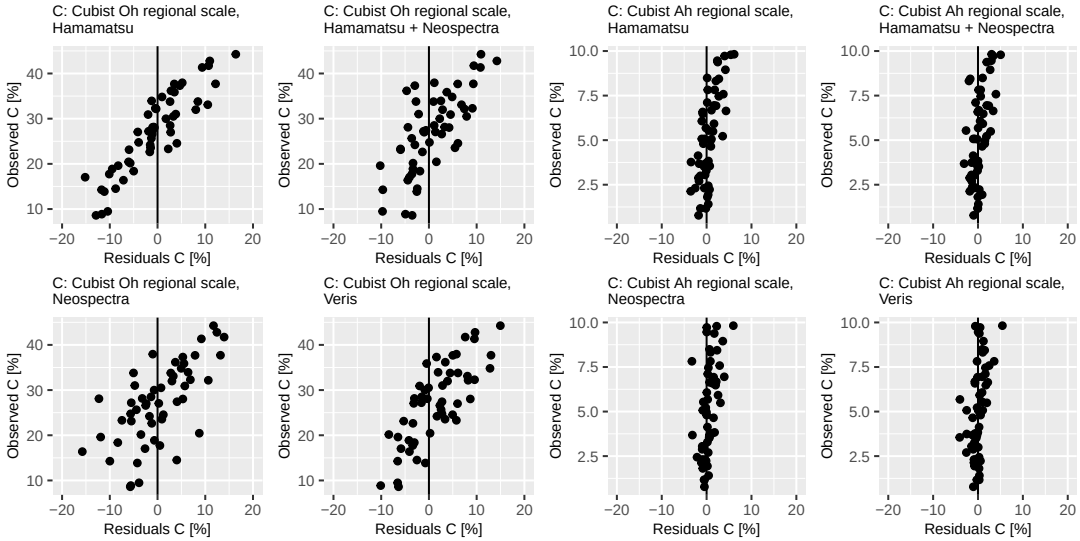


Figure 6: Residuals of C content prediction for validation of separate cubist regression models for Oh and Ah horizon based on spectral data obtained with the selected devices.

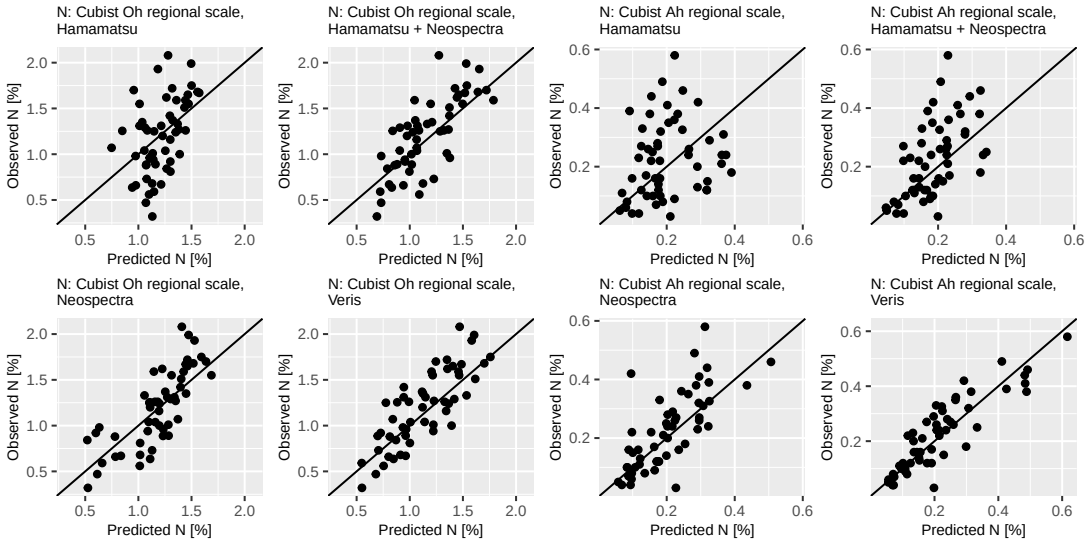


Figure 7: Predicted vs. observed N content values for validation of cubist regression models for Oh and Ah horizon based on spectral data obtained with the selected devices.

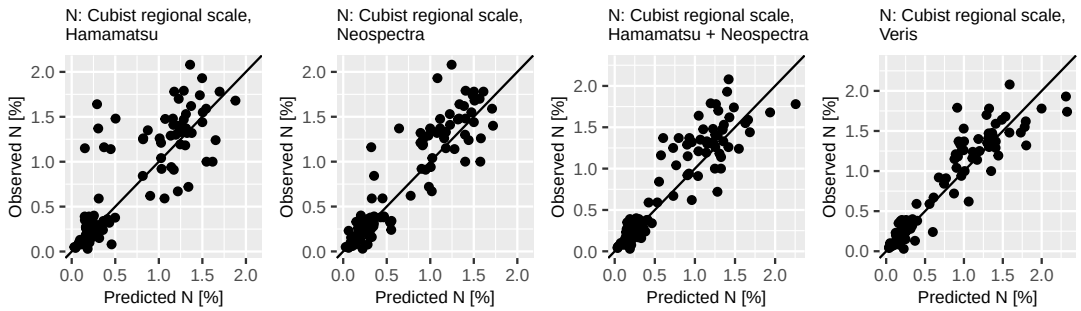


Figure 8: Predicted vs. observed N content for validation of cubist regression models using both Oh and Ah horizon for regional scale (BZE Saxony) based on spectral data obtained with the selected devices.

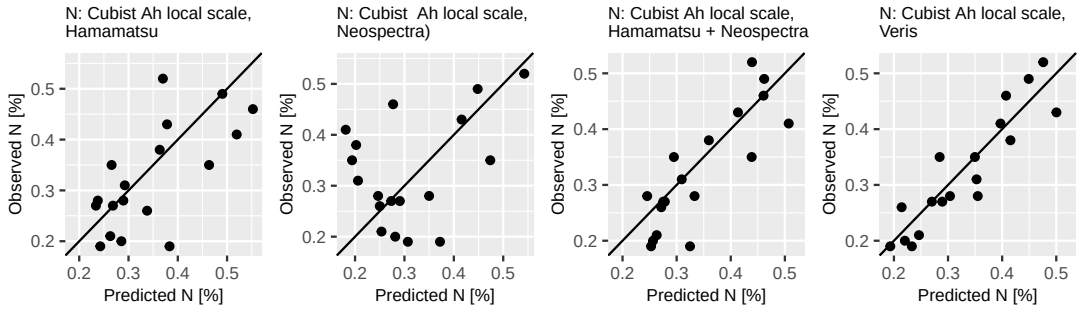


Figure 9: Predicted vs. observed Ah horizon N content for validation of cubist regression models for local scale (Zellwald) based on spectral data obtained with the selected devices.

References

[1] D. Barriopedro et al. “The hot summer of 2010: redrawing the temperature record map of Europe”. In: *Science* 332.6026 (2011), pp. 220–224.

[2] D. Barriopedro et al. “The exceptional Iberian heatwave of summer 2018”. In: *Bulletin of the American Meteorological Society* 101.1 (2020), S29–S34.

[3] A. Bastos et al. “Direct and seasonal legacy effects of the 2018 heat wave and drought on European ecosystem productivity”. In: *Science advances* 6.24 (2020), eaba2724.

[4] B. Schuldt et al. “A first assessment of the impact of the extreme 2018 summer drought on Central European forests”. In: *Basic and Applied Ecology* 45 (2020), pp. 86–103.

[5] C. Senf et al. “Canopy mortality has doubled in Europe’s temperate forests over the last three decades”. In: *Nature communications* 9.1 (2018), pp. 1–8.

[6] C. Peng et al. “A drought-induced pervasive increase in tree mortality across Canada’s boreal forests”. In: *Nature climate change* 1.9 (2011), pp. 467–471.

[7] P. J. Van Mantgem et al. “Widespread increase of tree mortality rates in the western United States”. In: *Science* 323.5913 (2009), pp. 521–524.

[8] C. D. Allen et al. “A global overview of drought and heat-induced tree mortality reveals emerging climate change risks for forests”. In: *Forest ecology and management* 259.4 (2010), pp. 660–684.

[9] A. Gessler, M. Schaub, and N. G. McDowell. “The role of nutrients in drought-induced tree mortality and recovery”. In: *New Phytologist* 214.2 (2017), pp. 513–520.

[10] A. Olness and D. Archer. “Effect of organic carbon on available water in soil”. In: *Soil Science* 170.2 (2005), pp. 90–101.

[11] E. Grüneberg et al. “Das Kohlenstoffspeicher-vermögen von Waldböden”. In: *AFZ Wald* 72 (2017), pp. 23–25.

[12] R. V. Rossel et al. “Proximal soil sensing: an effective approach for soil measurements in space and time”. In: *Advances in agronomy*. Vol. 113. Elsevier: Amsterdam, The Netherlands, 2011, pp. 243–291.

[13] T. Terhoeven-Urselmans et al. “Near-infrared spectroscopy can predict the composition of organic matter in soil and litter”. In: *Journal of Plant Nutrition and Soil Science* 169.2 (2006), pp. 168–174.

[14] R. V. Rossel et al. “Visible, near infrared, mid infrared or combined diffuse reflectance spectroscopy for simultaneous assessment of various soil properties”. In: *Geoderma* 131.1-2 (2006), pp. 59–75.

[15] B. Kuang and A. Mouazen. “Calibration of visible and near infrared spectroscopy for soil analysis at the field scale on three European farms”. In: *European Journal of Soil Science* 62.4 (2011), pp. 629–636.

[16] J. Reeves, G. McCarty, and J. Meisinger. “Near infrared reflectance spectroscopy for the analysis of agricultural soils”. In: *Journal of Near Infrared Spectroscopy* 7.3 (1999), pp. 179–193.

[17] R. V. Rossel and R. Webster. “Predicting soil properties from the Australian soil visible–near infrared spectroscopic database”. In: *European Journal of Soil Science* 63.6 (2012), pp. 848–860.

[18] A. Stevens et al. “Prediction of soil organic carbon at the European scale by visible and near infrared reflectance spectroscopy”. In: *PloS one* 8.6 (2013), e66409.

[19] F. Castaldi et al. “Estimation of soil organic carbon in arable soil in Belgium and Luxembourg with the LUCAS topsoil database”. In: *European Journal of Soil Science* 69.4 (2018), pp. 592–603.

[20] K. Sudduth and J. Hummel. “Geographic operating range evaluation of a NIR soil sensor”. In: *Transactions of the ASAE* 39.5 (1996), pp. 1599–1604.

[21] J. Wetterlind and B. Stenberg. “Near-infrared spectroscopy for within-field soil characterization: small local calibrations compared with national libraries spiked with local samples”. In: *European Journal of Soil Science* 61.6 (2010), pp. 823–843.

[22] M. Chodak et al. “Near infrared spectroscopy for determination of total and exchangeable cations in geologically heterogeneous forest soils”. In: *Journal of Near Infrared Spectroscopy* 12.5 (2004), pp. 315–324.

[23] B. Ludwig et al. “Near infrared spectroscopy of forest soils to determine chemical and biological properties related to soil sustainability”. In: *Forest Ecology and Management* 171.1-2 (2002), pp. 121–132.

[24] D. Xu et al. “Assessment of important soil properties related to Chinese Soil Taxonomy based on vis–NIR reflectance spectroscopy”. In: *Computers and electronics in agriculture* 144 (2018), pp. 1–8.

[25] S. Wang et al. "Predicting Soil Organic Carbon and Soil Nitrogen Stocks in Topsoil of Forest Ecosystems in Northeastern China Using Remote Sensing Data". In: *Remote Sensing* 12.7 (2020), p. 1115.

[26] Y. Tang, E. Jones, and B. Minasny. "Evaluating low-cost portable near infrared sensors for rapid analysis of soils from South Eastern Australia". In: *Geoderma Regional* 20 (2020), e00240.

[27] A. Sharififar et al. "Evaluating a low-cost portable NIR spectrometer for the prediction of soil organic and total carbon using different calibration models". In: *Soil Use and Management* 35.4 (2019), pp. 607–616.

[28] W. Ng et al. "Developing a soil spectral library using a low-cost NIR spectrometer for precision fertilization in Indonesia". In: *Geoderma Regional* 22 (2020), e00319.

[29] N. Wellbrock et al. *Entwicklung einer Methodik zur stichprobengestützten Erfassung und Regionalisierung von Zustandseigenschaften der Waldstandorte*. Thünen Report 36. Braunschweig, Germany: Johann Heinrich von Thünen-Institut, 2015.

[30] N. Wellbrock et al. "Concept and Methodology of the National Forest Soil Inventory". In: *Status and Dynamics of Forests in Germany*. Springer: Cham, Switzerland, 2019, pp. 1–28.

[31] © European Union. *Copernicus Land Monitoring Service 2018, European Environment Agency (EEA)*. Online. acessed on 04.02.2021.

[32] N. Wellbrock. *Arbeitsanleitung für die zweite bundesweite Bodenzustandserhebung im Wald:(BZE II);Arbeitsanleitung für die Außenaufnahmen*. Bundesministerium für Ernährung, Landwirtschaft und Verbraucherschutz, 2006.

[33] Gutachterausschuss Forstliche Analytik. *Handbuch Forstliche Analytik. Eine Loseblatt-Sammlung der Analysemethoden im Forstbereich*. 2014.

[34] DIN. "DIN 10694: Bestimmung des organischen Kohlenstoffgehaltes und des Gesamtkohlenstoffgehaltes nach trockener Verbrennung (Elementaranalyse)". In: *Deutsche Normen (ed. Fachnormenausschuß Wasserwesen, FNW, im DIN Deutsches Institut für Normung e.V.)* (1994).

[35] A. Mac Arthur, C. J. MacLellan, and T. Malthus. "The fields of view and directional response functions of two field spectroradiometers". In: *IEEE transactions on geoscience and remote sensing* 50.10 (2012), pp. 3892–3907.

[36] R Core Team. *R: A Language and Environment for Statistical Computing*. R Foundation for Statistical Computing. Vienna, Austria, 2018. URL: https://www.R-project.org/.

[37] Å. Rinnan, F. Van Den Berg, and S. B. Engelsen. "Review of the most common pre-processing techniques for near-infrared spectra". In: *TrAC Trends in Analytical Chemistry* 28.10 (2009), pp. 1201–1222.

[38] A. Savitzky and M. J. Golay. "Smoothing and differentiation of data by simplified least squares procedures." In: *Analytical chemistry* 36.8 (1964), pp. 1627–1639.

[39] A. Stevens and L. Ramirez-Lopez. *An introduction to the prospectr package*. R package version 0.1.3. R Core Team: Vienna, Austria, 2013.

[40] R. Barnes, M. S. Dhanoa, and S. J. Lister. "Standard normal variate transformation and de-trending of near-infrared diffuse reflectance spectra". In: *Applied spectroscopy* 43.5 (1989), pp. 772–777.

[41] Avian Technologies. *Fluorilon Gray Scale Standards & Targets*. Online. accessed on 13.06.2019. 2019. URL: https://aviantechnologies.com/product/gray-scale-standards/.

[42] L. Ramirez-Lopez et al. "The spectrum-based learner: A new local approach for modeling soil vis–NIR spectra of complex datasets". In: *Geoderma* 195 (2013), pp. 268–279.

[43] S. Wold, H. Martens, and H. Wold. "The multivariate calibration problem in chemistry solved by the PLS method". In: *Matrix pencils*. Springer: Cham, Siwtzerland, 1983, pp. 286–293.

[44] T. Hastie, R. Tibshirani, and J. Friedman. *The elements of statistical learning: data mining, inference, and prediction*. Springer Science & Business Media: Chams, Switzerland, 2009.

[45] J. R. Quinlan et al. "Learning with continuous classes". In: *5th Australian joint conference on artificial intelligence*. Vol. 92. World Scientific, Canberra, ACT, Autralia. 1992, pp. 343–348.

[46] A. Morellos et al. "Machine learning based prediction of soil total nitrogen, organic carbon and moisture content by using VIS-NIR spectroscopy". In: *Biosystems Engineering* 152 (2016), pp. 104–116.

[47] J. Im et al. "Hyperspectral remote sensing analysis of short rotation woody crops grown with controlled nutrient and irrigation treatments". In: *Geocarto International* 24.4 (2009), pp. 293–312.

[48] P. T. Sorenson et al. "Monitoring organic carbon, total nitrogen, and pH for reclaimed soils using field reflectance spectroscopy". In: *Canadian Journal of Soil Science* 97.2 (2017), pp. 241–248.

[49] V. Bellon-Maurel et al. "Critical review of chemometric indicators commonly used for assessing the quality of the prediction of soil attributes by NIR spectroscopy". In: *TrAC Trends in Analytical Chemistry* 29.9 (2010), pp. 1073–1081.

[50] C.-W. Chang et al. "Near-infrared reflectance spectroscopy–principal components regression analyses of soil properties". In: *Soil Science Society of America Journal* 65.2 (2001), pp. 480–490.

[51] M. Kuhn. *caret: Classification and Regression Training*. R package version 6.0-81. R Core Team: Vienna, Austria, 2018. URL: `https://CRAN.R-project.org/package=caret`.

[52] C.-W. Chang and D. A. Laird. "Near-infrared reflectance spectroscopic analysis of soil C and N". In: *Soil Science* 167.2 (2002), pp. 110–116.

[53] A. Gholizadeh et al. "Spectroscopic measurements and imaging of soil colour for field scale estimation of soil organic carbon". In: *Geoderma* 357 (2020), p. 113972.

[54] K. Lee et al. "Wavelength identification and diffuse reflectance estimation for surface and profile soil properties". In: *Transactions of the ASABE* 52.3 (2009), pp. 683–695.

[55] S. Grunwald, Y. Congrong, and X. Xiong. "Transferability and scalability of soil total carbon prediction models in Florida, USA". In: *Pedosphere* 28.6 (2018), pp. 856–872.

[56] M. Seidel et al. "Strategies for the efficient estimation of soil organic carbon at the field scale with vis-NIR spectroscopy: Spectral libraries and spiking vs. local calibrations". In: *Geoderma* 354 (2019), p. 113856.

[57] B. Stenberg et al. "Visible and near infrared spectroscopy in soil science". In: *Advances in agronomy*. Vol. 107. Elsevier: Amsterdam, The Netherlands, 2010, pp. 163–215.

[58] M. Knadel et al. "Soil organic carbon and particle sizes mapping using vis–NIR, EC and temperature mobile sensor platform". In: *Computers and Electronics in Agriculture* 114 (2015), pp. 134–144.

[59] M. Knadel et al. “The effects of moisture conditions—from wet to hyper dry—on visible near-infrared spectra of Danish reference soils”. In: *Soil Science Society of America Journal* 78.2 (2014), pp. 422–433.

[60] J. Liski, D. Perruchoud, and T. Karjalainen. “Increasing carbon stocks in the forest soils of western Europe”. In: *Forest Ecology and Management* 169.1-2 (2002), pp. 159–175.

[61] Y. Yang et al. “Increased topsoil carbon stock across China’s forests”. In: *Global Change Biology* 20.8 (2014), pp. 2687–2696.

Manuscript 3

Integrated framework for the assessment and spatial prediction of humus properties of forest soils

Submitted to Journal of Plant Nutrition and Soil Science

Felix Thomas[1*], Carina Becker[2, 5], Rainer Petzold[3], Karsten Schmidt[4], Thomas Scholten[2], Ulrike Werban[1]

[1] Department Monitoring & Exploration Technologies, Helmholtz Centre for Environmental Research—UFZ, Permoser Straße 15, 04318 Leipzig, Germany
[2] Soil Science and Geomorphology, Institute of Geography University of Tübingen, Rümelinstraße 19-23, 72070 Tübingen, Germany
[3] Public Enterprise Sachsenforst, Unit Site Survey, Soil Monitoring and Laboratory, Bonnewitzer Straße 34, 01796 Pirna, Germany
[4] Swiss Competence Center for Soils (KOBO), Data Science, BFH-HAFL CH-3052 Zollikofen, Switzerland
[5] Center for Information Services and High Performance Computing (ZIH) TU Dresden, 01062 Dresden

* Corresponding author
E-mail: felix.thomas@ufz.de

Abstract

Background

Nitrogen input and sulfur depositions have impacted the nutrient balance of European forest soils. Data about nutrient availability in the humus layer is vital for sustainable forest management. Currently used schemes based on indicator plants have shortcomings, and field campaigns and laboratory analysis are expensive. Digital Soil Mapping (DSM) and proximal soil sensing techniques can offer the necessary information.

Aims

We present an integrated framework as measuring system using DSM to provide spatial information about properties of the humus layer of forest soils. For effort reduction, we applied vis-NIR spectroscopy to determine the humus properties.

Methods

The framework uses soil forming factors (soil form class, climate, satellite data for vegetation, relief and parent material). Conditioned Latin Hypercube sampling determines the locations of the sampling points. We tested the framework in a case study, investigating C/N ratio, pH value, cation exchange capacity and base saturation.

Results

We were able to create high resolution maps of humus properties of forest soils. Models for spatial prediction achieved R^2 ¿ 0.9. For our test site, the framework revealed depleted humus conditions, which should be addressed by forest management. Vis-NIR predictions of humus properties achieved R2 values up to 0.69. The maps based on the vis-NIR predictions resulted in similar patterns of value distribution.

Conclusion

The framework is applicable and the produced maps allow the assessment of humus conditions for forest management. Vis-NIR spectroscopy can reduce the effort. The framework is suitable to provide spatial information about humus properties at forest stand scale.

Introduction

European forests are recently exposed to fast changing environmental conditions. The main drivers for this development are generally increasing temperatures [1, 2], and therefore a drastically higher occurrence of severe drought events [3, 4, 5]. This trend also impacts forest soils, which play an important role regarding water balance and nutrient supply in forest ecosystems.

Forest soil conditions in Central Europe are influenced by human land use and forest management as well as by the aftermath of acid rain and historic sulfur depositions, as acidification processes can go on despite substantial reductions in atmospheric acidic deposition [6, 7]. Persistently high nitrogen depositions from fuel combustion and agricultural fertilizer use affect the nutrient balance of forests soils in Europe [8, 9]. For sustainable forest management, all these changes have to be monitored for well-informed decision-making. On forest soils, the organic layer and the uppermost mineral soil horizon are most sensitive regarding chemical and morphological properties and therefore subject to periodic assessment. In Germany, the forest soil conditions including humus layer are periodically recorded by National Forest Soil Inventory (NFSI). However, its sampling grid is coarse (8 x 8 km, $>$ 10 years), and not sufficient to provide information needed for management decisions on forest stand scale.

The established forest site mapping scheme in East Germany defines and classifies humus forms by chemical properties of the organic layers and the uppermost mineral soil layer. Currently, the scheme consists of indicator plants used to map humus properties according to the mapping field guide for the Northeastern Lowland of Germany [10]. However, element input, climate and environmental change as well as forest management measures, forest conversions, thinning strategies and liming influence the local conditions and perpetually overprint vegetation as well as the morphological humus forms. The validity of conditions assessed solely based on analysis of the occurring vegetation and identification and description of the morphological humus form can therefore be deficient. Hence, there is a need to adapt and supplement the current schemes in order to avoid decreasing forest ecosystem services.

To face this, there is a need for sufficient amount of up to date data regarding the condition of forest soils. Repeated large field sampling campaigns and laboratory analysis of collected soil samples could provide the desired data basis, but are expensive due to the needed time, workforce and equipment. This raises the question how the data can be provided with acceptable effort. One approach offering a solution for the described set of problems is digital soil mapping (DSM).

It is already established and widely used on agricultural areas, but forest soils were not yet comparably investigated. DSM could be used to provide the desired and needed information for forested areas as well, at sufficient spatial scale [11, 12].
A variety of available input data related to soil forming factors can be the basis for an DSM approach. Therefore, generally available data like satellite imagery and climate data can be used in combination with information already available in forest management, e.g. about soil forms, parent materials and substrates.
Further, methods of proximal soil sensing (PSS) like vis-NIR spectroscopy can be applied to provide further basis information at reasonable cost [13]. Vis-NIR spectroscopy is already known as indirect, fast, non-destructive and cost-saving method for estimating a variety of physical and chemical soil properties [14, 15, 16, 17, 18, 19]. It allows that more measurements can be made compared to conventional laboratory methods. The determination of soil properties with vis-NIR spectroscopy is always based on a calibration model, which is created using a regression method to detect the correlation between spectra and soil properties [20]. Thus, it also can be useful for DSM purposes [21]. Numerous studies deal with the determination of organic matter and total nitrogen, but also the derivation of pH value, cation exchange capacity (CEC) and base saturation (BS) has been successfully performed with vis-NIR [16, 22, 23, 24]. There are also studies demonstrating that the method can be successfully applied on forest sites for the analysis of topsoil and the humus layer [25, 26, 27, 28].
An entire integrated approach as measuring system using available input data as well as DSM and PSS techniques with the aim of providing spatial information about soil properties is sought after. Especially forest soils are so far rather less investigated regarding DSM and PSS approaches. It could provide the information needed for assessing humus conditions in forest soils with reasonable effort and resulting in maps that can be used to support forest management. The workflow should work as procedure for forest stands and be suitable for future repetitions. This would also enable the possibility to detect changes over time in the investigated properties.
We present an integrated framework capable of spatially mapping soil properties that are important for assessing humus conditions. The goal of the framework is to provide maps of forest soils at sufficient scale to support silvicultural decisions and represent soil variation within forest stands. This could increase the data availability regarding the selected properties at forest stand scale, as there is currently no information available. The maps provide an additional decision tool

to deal with current problems. Decades of cultivation of coniferous trees species outside of their natural distribution resulted in highly vulnerable stands and severe challenges regarding drought occurrences and bark beetle calamities. In addition, coniferous trees generally affect the humus layer as their needles gradually lead to acidification of the soil.
Our framework uses basis information originating from various sources, covering vegetation, relief, geology, soil types and climate data. This data is used to select representing sampling points within the study area. After the collection, the samples are measured by conventional laboratory methods to determine the humus properties. For further reduction of the effort, the samples can be measured using vis-NIR spectroscopy and the recorded spectra are used for modelling of the soil properties. The measured or the predicted values from the spectral modeling can then build the basis to produce maps of the study area containing continuous property values.
In this study, we (I) present, test and evaluate this framework, aiming to close the data gap by providing information about humus properties at forest stand scale, on a study site in Saxony, Germany, (II) evaluate the usage of vis-NIR spectroscopy within the approach to substitute chemical measurements and (III) use the gained information to discuss recommendations for action regarding the forest management of the test site.

Material and Methods

In this section, we describe the developed workflow as well as the used input data, the pre-processing steps, the sampling design and sample preparation, the spatial prediction as well as the modelling steps using the vis-NIR spectra. A schematic representation of the complete workflow can be seen in figure 1. It shows the used input data, the approach of the sampling design, the methods of the chemical and spectral soil analysis, and the modelling step that predicts the humus properties based on vis-NIR data as well as the spatial model to produce the results in form of maps of C/N, pH, CEC and BS for practical applications.

Input data and predictors

The predictors for the integrated approach were selected in accordance to the SCORPAN model representing the soil-forming factors [29, 30]. Table 1 provides an overview of the selected factors and their corresponding predictors.

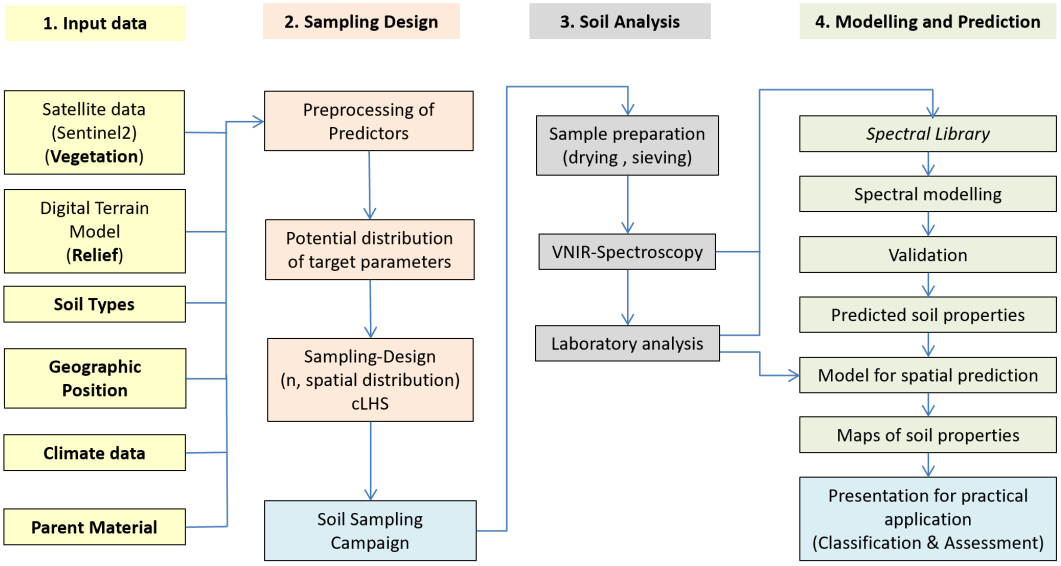


Figure 1: Workflow of the integrated approach to map forest humus properties

For the soil factor (S), the local soil forms (aggregated to 23 classes) of the corresponding forest site map with a resolution of 1:10,000 were used as predictor. The factor climate (C) was represented by temperature, potential evaporation, grass reference evaporation, precipitation and climatic water balance, all at 30-year average from 1985 to 2014.

As vegetation predictors for the factor organisms (O), we used Normalized Difference Vegetation Index (NDVI) values derived from the high-resolution satellite imagery of the Sentinel-2 mission. NDVI corresponds to the reflectance of vegetation and was used as basis to provide detailed information regarding the current vegetation.

The NDVI was calculated as follows in equation 12:

$$NDVI = \frac{(NIR - RED)}{NIR + RED} \tag{12}$$

For calculation of the NDVI values, we used best-available-pixel composite of satellite imagery from eight different time ranges, collected in the year prior to the sampling and in the year of the sampling campaign (2018 and 2019). The data was pre-processed using the open source software FORCE [35, 36].

A detailed image of the relief (R) was extracted from the Digital Elevation Model (DEM) with a resolution of 4 meters. The desired specific relief parameters were computed using R and SAGA-GIS. Information about the substrate (P) was derived from the forest site map at scale 1:10,000. The factors N (geographic

Table 1: Selected soil forming factors and corresponding predictors for spatial prediction of humus properties, modified after [30]

Factor	**Data used as predictor**
Soil	soil form classes (aggregated to 23 classes)
Climate	temperature (T), evapotranspiration (ETP), precipitation (P), climatic water balance (CWB), grass reference evaporation (GRE)
Organisms (vegetation)	NDVI based on Sentinel-2 data
Relief	height above sea level, slope
	aspect as exposure in northness and eastness [31]
	cross-sectional, longitudinal and mean curvature [32]
	SAGA wetness index [33, 34]
Parent material	geological information from forest soil map (1:10.000)

position) and time (A) were neglected as predictors in our case, since we only investigate a study area and want to map the properties as a snap-shot.
All predictor raster data sets were scaled to 4x4 m resolution to allow a detailed prediction of humus properties.

Selection of sampling points

To ensure a statistically well-founded selection of the sampling points within the area, we applied conditioned Latin Hypercube sampling (cLHS) based on our predictor data [37]. It ensures that the property space of the multivariate distribution of the predictors is described as best as possible [38].
In addition, we calculated the Gowers Similarity Index to be more flexible during the field sampling campaign and to be able to select statistically correct alternative sampling points.
During sample collection in the forest, sampling points calculated by means of cLHS are not always suitable for collecting soil material (e.g. due to disturbances like skid trails, drag marks, lying deadwood or ground disturbance caused by wild boars). If sampling is not possible, an alternative sampling point can be selected via the Gowers Similarity Index (G) [39], representing similarity of the surrounding pixels within a certain area around each cLHS point.
In total, we selected 60 points within the study area using the R Package "clhs" [40].

Collection of soil sample material

Soil sampling was performed following german-wide standards for forest soil sampling campaigns, suggesting to take mixed samples [41]. We established four sub-points per sampling point within a radius of five meters, directed to the four main cardinal directions. At every sub-point, we then took two samples next to each other. The sample material from Oh horizon was collected using a core cutter. The Oh horizon was separated from the mineral soil by visual assessment of the probed soil. The soil material from 0-5 cm depth was extracted using a Pürckhauer device. Then, all eight collected samples per horizon were mixed, resulting in one Oh and one 0-5 cm depth sample per sampling point. A schematic representation of the sampling design is shown in figure 2.

Chemical Analysis

The chemical analysis of the soil samples was carried out in the laboratory of Sachsenforst Public Enterprise. It was done according to the the German standard procedure for forest soil samples [42]. For the chemical analysis, the sample material was dried at 40°C and milled. To quantify total carbon and nitrogen content the dry combustion method with elementary analysis was applied [43]. For analysis of the pH value, we used KCl suspension on basis of the norm [44], following the standard procedure for forest soils in Germany [41]. For Oh samples, cation exchange capacity and base saturation were determined in barium chloride. For the samples from 0-5 cm ammonium chloride solution was used.

Spectral analysis

The spectral analysis of the soil samples was conducted in the laboratory at the Centre for Environmental Research in Leipzig. For the spectral data acquisition, dried and sieved (2 mm mesh) soil material was used. Beforehand, we developed a laboratory protocol based on literature research and test measurements to ensure a solid data acquisition. We measured two petri dishes per soil sample, with five repetitions and rotations between the measurements to balance the results within the area [45]. Thus, we collected ten spectra per soil sample. Data collection was done using a Spectrophotometer by Veris Technologies Inc. (Salina, KS, USA) with a wavelength range of 350 - 2220 nm, and two sensors with a spectral resolution of 6 nm at range 350–1000 nm and 5 nm at range 1100–2220 nm. Calibration of the spectrometer was done using four Fluorillon grey standards as external references [46]. Spectral pre-processing can be used to reduce noise in

the measured spectra [47]. We smoothed our data by means of Savitzky-Golay filter [48] and normalized it using standard normal variate [49]. All pre-processing steps were carried out by means of the R package "prospectr" [50].

Spectral modelling

In order to reduce the amount of field work and needed sampling points, we integrated the possibility of using vis-NIR spectroscopy to determine the humus property values to our approach.
To build the spectral models an predict the selected soil properties, we used partial least squares regression (PLSR). It was initially presented to solve multivariate calibration problems [51] and is a well known algorithm for predictive modelling of soil properties using spectral data, as there are many collinear predictors [52, 16]. PLSR was already successfully used to predict numerous properties of forest soils in previous studies, e.g. by Ludwig et al. [53], Thomas et al. [25], and Conforti et al. [52].
To calibrate the prediction models, ensure robust tuning and to validate the results, we performed a nested cross validation. It provides a more stable assessment of the model performance than a single test set and is commonly used to evaluate machine learning models [54, 55, 56, 57, 58, 59, 60]. It uses an outer and an inner cross validation. The outer K-fold cross-validation was used to estimate realistic prediction error measures. The inner K-fold cross-validation was used for robust optimization of the hyperparameter. In both cases, we used 10 splits ($K = 10$). During this procedure, a predefined set of values is tested and the values that produce the smallest model error is selected. In case of PLSR, the number of components (*ncomp*) used for the regression has to be optimized. We used RMSE as error metric for the decision.
The RMSE is calculated as shown in equation 13.

$$RMSE = \sqrt{\frac{1}{n}\sum_{i=1}^{n}(y_i - x_i)^2} \tag{13}$$

where x_i are the measured and y_i the predicted values.
In addition, the model performance was assessed using the model efficiency coefficient developed by [61]. It is shown in equation 14.

$$R^2 = 1 - \frac{\sum(x_i - y_i)^2}{\sum(y_i - \bar{x})^2} \tag{14}$$

The best model was then validated with the test set of the outer cross validation. To assess the model performance for the whole data set, we calculated the mean of the error measures of the ten outer folds. The calibration and validation procedure was carried out for all investigated soil parameters by means of the R package "caret" [62]. We log-transformed all property values except BS prior to the modelling procedure. The values were back-transformed before evaluating the prediction accuracy.

Spatial modelling and prediction

We used Random Forest (RF) to calibrate the models for spatial prediction of the soil properties [63]. RF models predict with high accuracy and are suitable for small sample sizes and a high number of predictors [64]. Therefore, RF models are commonly used for digital soil mapping purposes [65, 66].
For our approach, we extracted the predictor values from the corresponding raster data sets at each sampling point. This procedure results in a data set with all predictors and collected soil chemical parameters for each sampling point. These data set was used to train the models. Separate RF models were calibrated per horizon for each selected soil property. The RF models were trained using Leave-one-out-cross-validation (LOOCV). This procedure is a special case of k-fold cross validation in which all data points but one observation are used to calibrate the model and the remaining one is used for testing. The optimization of the hyperparameter *mtry* was done by means of a grid search. During the optimization, a predefined set of values was tested and the values that produce the smallest model error was selected. As for the spectral models, $RMSE$ was used for the decision. The performance of the model calibration was assessed using $RMSE$ (see formula 13) and R^2 (see formula 14) as error measures. The created models were then used to predict the selected properties for the whole study area in order to receive spatial information about humus conditions. The results rely on the correlation between predictors and the humus properties. The influence of the single predictors was assessed using the feature importance derived by the R package "caret" [62].

Study Area of test experiment

We tested our framework at the forest site Zellwald, located in the hilly less region of Saxony. It covers an area of 2336 ha. The mean annual temperature is 9.5 C°, with a mean annual precipitation of approximately 750 mm. Parent

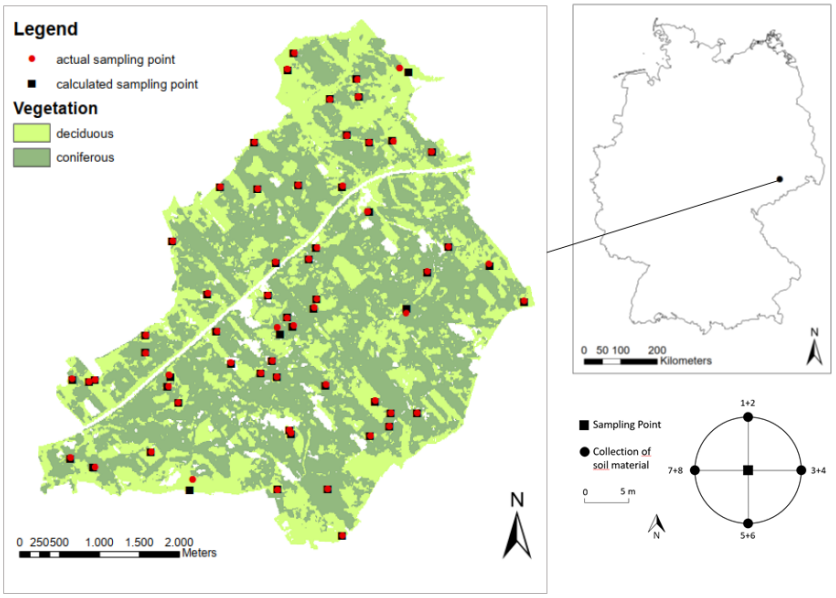


Figure 2: Location of the study area "Zellwald" in Saxony, Germany, with distribution of the sampling points within the area and an illustration of the sample taking design

material consists of loess loam top layers of variable thicknesses and metamorphic rocks like shale, quartzite slate, clay slate, diabase, greywacke in the geological subsurface. The predominant soil types are luvisols and stagnic luvisols (loess-gleysols and cambic gleysols). Currently, the vegetation is dominated by coniferous stands mainly consisting of Norway Spruce (*Picea abies*) and Scots Pine (*Pinus sylvestris*), with smaller deciduous areas formed by oak (*Quercus spp.*), birch (*Betula pendula*) and some portions of other broadleaf species. In the last years, the Norway Spruce is affected by large bark beetle calamity and loses its share in the forest composition.

Results

In this chapter we report on the application of the developed workflow on the test site "Zellwald", as well as presenting the results we achieved for the study area.

Collecting of soil samples

The data collection was carried out according to the proposed sampling design. The location of sample points within the study area were calculated by the cLHS

procedure, then located during the field campaign and probed according to the described sampling procedure. The Gowers similarity index enhanced field work by providing information about possible alternative sampling locations nearby. In four cases, the actual sampling point had to be shifted considerably in order to conduct the sampling (see figure 2), as local disturbances or other circumstances prevented us from sampling at the initially suggested point. We collected only 50 Oh samples, as there was no developed Oh horizon present at ten sampling points. The samples from 0-5 cm depth were collected as intended at all 60 sampling locations.

Chemical analysis

The results of the chemical analysis of the soil samples collected in the study can be seen in figure 3.

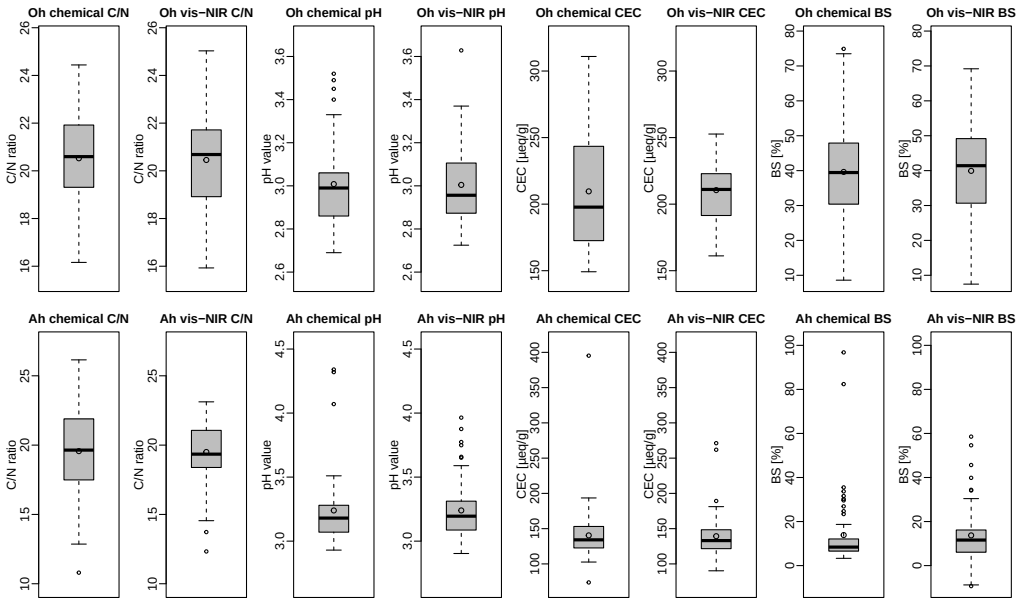


Figure 3: Box-Whisker-Plots of the chemical analysis and the vis-NIR predictions, the line represents the median and the point marks the mean

In Oh samples, chemically determined C/N values ranged from 16.2 to 24.4, with a mean of 20.5. The pH values were found to be in a range between 2.7 and 3.5. Therefore, the whole study area is dominated by very acidic conditions. Values for CEC were measured between 149.2 and 310.9 µeq/g, with a mean of 209.6 µeq/g, BS was measured ranging from 9 to 75 %, with a mean of 39.6 %. In 0-5 cm depth, the C/N values had a wider range of 10.8 to 26.2, and lower mean of 19.6. The pH values again showed acidic conditions within the study area with a

Table 2: Model error measures for predictions of soil properties using vis-NIR spectroscopy

Horizon	Error measure	C/N	pH	CEC [µeq/g]	BS [%]
Oh	RMSE	1.58	0.11	46.60	10.69
	R^2	0.63	0.64	0.17	0.69
0 - 5 cm	RMSE	2.89	0.15	26.69	9.93
	R^2	0.43	0.65	0.40	0.62

mean value of 3.2 and a wider data range of the collected samples, ranging from 2.9 to 4.3. CEC in mineral topsoil was measured between 73.6 and 395.3 µeq/g, the mean value was 140.5 µeq/g, BS lay between 3.3 and 96.8 %, with a mean value of 13.9 %.

Spectral analysis and modelling

The spectral data acquisition protocol, was found to be easy to use and a robust procedure. The spectral data built the basis for predicting soil properties based on vis-NIR spectra using PLSR. Box-Whisker-Plots of the predicted soil properties derived from vis-NIR spectroscopy are shown in table 3. The values are the independent results of the outer cross validation procedure. In the Oh models, mean values of the predictions were close to the chemically determined values. Standard deviation and data range were close for C/N, pH and BS. However, the CEC range was not properly predicted and showed higher deviations.
Similar observations could be made for samples from 0-5 cm depth. For all properties, mean values were close to the chemically measured values. Data ranges for CEC and BS showed deviations when compared to chemical results.
Performance measures of the PLSR models to estimate soil properties using vis-NIR data are given in table 2. The table shows the mean values of the error measures derived from the outer folds of the nested cross validation procedure. For the Oh horizon, the models achieved RMSE = 1.58 and $R^2 = 0.63$ for C/N ratio. Similar results were reported for pH value with RMSE = 0.11 and $R^2 = 0.64$. The RMSE for CEC was calculated to be 46.6 while the model for BS reached a value of 10.69. In 0-5 cm depth, model performance for C/N was lower with RMSE = 2.89 and $R^2 = 0.43$. Predictions for pH value were similar to the results for Oh horizon with RMSE = 0.15 and $R^2 = 0.65$. Regarding CEC, RMSE was 26.69 and R^2 was 0.4. The predictions for BS were of similar accuracy as for Oh samples, with RMSE = 9.93 and $R^2 = 0.62$.

Spatial prediction

As last step of the integrated approach, spatial RF models were calibrated. This was done on basis of the predictor data and chemically determined values as well as on data predicted by the vis-NIR models and then used to predict humus properties. This way, we were able to produce maps of humus properties for the whole study area. In both cases, RF models were calibrated using the selected predictors according to the SCORPAN model. Oh horizon and 0-5 cm depth were modeled separately. Error measures values from the model calibration using the chemical and vis-NIR spectroscopy measured soil properties can be seen in table 3. Due to the low performance of vis-NIR prediction for CEC in Oh horizons, we did not proceed with the spatial prediction in this case.

Table 3: Error measures of RF model calibration for selected humus properties

Data source	Property	Oh		0-5 cm	
		RMSE	R^2	RMSE	R^2
Chemical	C/N	0.61	0.93	1.27	0.94
	pH	0.07	0.92	0.12	0.91
	CEC [µeq/g]	19.11	0.94	18.45	0.96
	BS [%]	7.2	0.93	7.5	0.94
Vis-NIR	C/N	0.82	0.94	1.44	0.9
	pH	0.07	0.95	0.08	0.94
	CEC [µeq/g]	-	-	13.85	0.95
	BS [%]	6.3	0.94	5.06	0.95

Calibrated models for C/N ratio resulted in R^2 values between 0.9 and 0.94, with RMSE values ranging from 0.61 to 1.44. Regarding pH values, the models reported R^2 values between 0.91 and 0.95, corresponding RMSE were 0.07 - 0.12. For CEC, the error measures were similar, with R^2 ranging from 0.94 to 0.96 and RMSE between 13.85 and 19.11, with lower values for the model based on vis-NIR data. Spatial model calibration for BS resulted in R^2 values of 0.93 and 0.95, while RMSE lay between 5.06 and 7.5. All model calibrations for the selected properties achieved R^2-values higher than 0.9.

The results of the spatial prediction for C/N ratio and pH value is shown in figure 4, including the input points with their corresponding values. The most important predictor parameters can be seen in table 4.

The prediction results for C/N ratio show similar values and patterns for both chemical and vis-NIR based models. The vis-NIR results have generally higher minima and lower maxima, indicating less distinct extreme values. Predicted

values were higher for Oh horizon than for 0-5 cm depth for both chemical and vis-NIR based results. For Oh horizon, the six most important predictors were NDVI and eastness. In 0-5 cm depth, climate parameters were important as well. The observable patterns in the values match with the spatial distribution of coniferous trees, resulting in higher, and deciduous tree species resulting in lower C/N ratios. Predictions based on vis-NIR were smoother and lay closer together, but still showed the spatial distinctions.

Table 4: Most important predictors of Random Forest model calibration for selected humus properties, number in parenthesis indicate the amount of normalized difference vegetation index (NDVI) values recorded at multiple dates, T = temperature, ETP = evapotranspiration, P = precipitation, CWB = climatic water balance, GRE = grass reference evaporation, wetness = SAGA wetness index, geod = geological information

Data source	Property	Oh predictors	0-5 cm predictors
Chemical	C/N	NDVI (5), eastness	NDVI (4), CWB, GRE
	pH	NDVI (4), eastness, slope	CWB, P, NDVI (3), ETP
	CEC	P, ETP, GRE, T, CWB, NDVI	NDVI (2), eastness, GRE, P, NDVI
	BS	ETP, T, P, GRE, CWB, elevation	P, CWB, elevation, T, GRE, ETP
Vis-NIR	C/N	NDVI (4), eastness, T	NDVI, P, GRE, CWB, T, NDVI
	pH	NDVI (3), elevation, ETP	NDVI (2), northness, wetness, geod, CWB
	CEC	-	CWB, P, NDVI, wetness, ETP, GRE
	BS	ETP, KRK, GRE, P, T, northness	NDVI (2), wetness, cross-sectional and mean curvature, northness

The results of the pH values within the study area show similar patterns. The deciduous areas show higher values, and the lower estimates spatially match with the areas timbered with spruce and pine trees. In the Oh horizon, the vis-NIR results show less distinctive values over the area with smoother patterns. Important predictors were NDVI as well as relief parameters. However, in 0-5 cm depth vis-NIR data does not result in a smoother result. For the chemical data, NDVI and climate data were important predictors while for vis-NIR, relief data showed high influence as well. Very acidic soil conditions were predicted for the study area in both investigated horizons. The results of the spatial prediction

for CEC and BS is shown in figure 5, again including the input points with their corresponding values.

Regarding CEC in the Oh horizon, the predictions based on chemical data shows lower values in the north and south of the study area. These resembles with variations in climate derived input variables, which are also the most important predictors. In 0-5 cm depth, the calculated results show little differences within the study area. Here, next to climate parameters, NDVI and relief data were important predictors. There is no remarkable difference in predicted values between the chemical and the vis-NIR based models. The spatial patterns are less distinct when compared to the other properties, and the estimated data range is generally narrow.

For BS in Oh horizon, both model approaches resulted in similar prediction patterns. The chemical values showed more defined structures with vegetation influence in the northern part of the study area, while the vis-NIR models structure resembled more with climate and elevation. Climate data were most important for model calibration. In both cases, large parts of the area have estimated BS values between 20 and 40. The observations for 0-5 cm show little variation in the predicted values. In the vis-NIR based map, deciduous areas show higher BS values. This trend is less visible in the map using chemically measured input values. Model calibration using chemical data relied mostly on climate data and relief. For the vis-NIR models, NDVI and relief showed high feature importance.

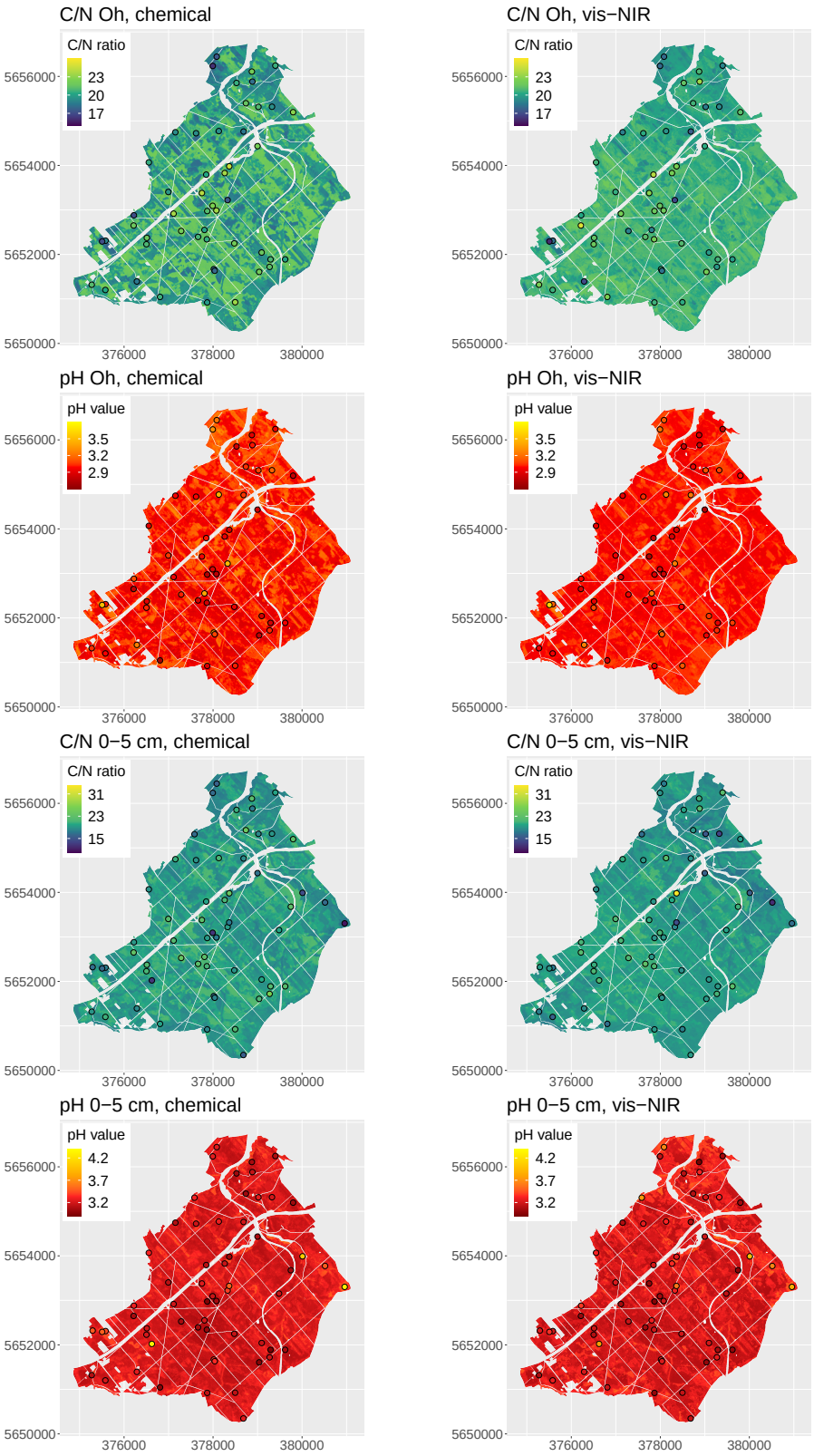


Figure 4: Results of the spatial prediction in the case study area for C/N ratio and pH value with corresponding input values at the measuring points

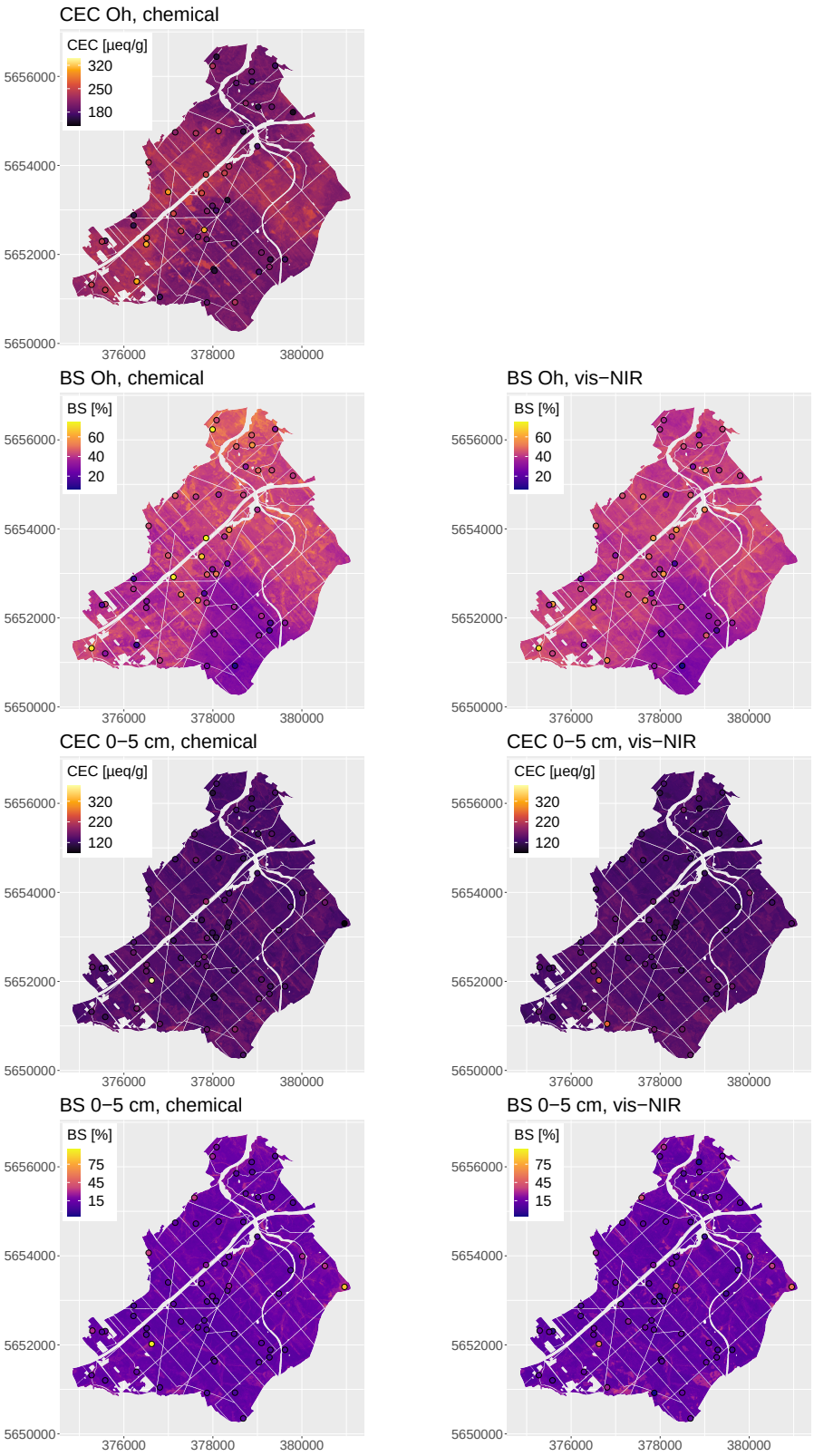


Figure 5: Results of the spatial prediction in the case study area for CEC and BS with corresponding input values at the measuring points

Discussion

Assessment of complete procedure and model performance

This study presented an integrated framework for spatial prediction of humus properties on forest soils. The application of the workflow was tested on a study site in Saxony. The implementation as case study has shown that the developed framework is feasible and can be applied to obtain spatial information on humus conditions on forest sites. The whole approach was carried out step by step, and every step was assessed separately, from collecting input data, defining sample points, collecting sample material, the determination of the properties by chemical analysis as well as the modelling and spatial prediction with in the study area. In addition, the possibility of using vis-NIR spectroscopy within the framework was investigated in an exemplary manner. The framework can be used to close the current data gap by providing spatial information about humus properties at forest stand scale.

If used within the framework, vis-NIR spectroscopy has the potential to reduce the required amount of chemical analysis. In this case, it is not necessary to use all data for model calibration. Instead, a small percentage can be used for calibration, and the rest of the samples properties can then be estimated. If the procedure is repeated, it is also possible to make use of the previously built spectral database. The performance of the spectral modelling step using PLSR was satisfying model for C/N, pH value and BS. The prediction resulted in RMSE values that are reasonable in context of data range and study area. Higher uncertainties were found for CEC in Oh horizon, where R^2 values were low and deviations to the chemically measured values were higher. We expected a stronger correlation to the vis-NIR spectra, as already reported in other studies investigating soils from agricultural areas and forests in different countries [25, 67, 68]

The spatial models showed differences in the results of the investigated humus properties, affecting the potential usage of the obtained information. For C/N ratio and pH value, the estimations were promising using both chemical and vis-NIR prediction values. One reason for this could be the strong correlation of these properties to the vegetation. The value patterns in the spatial prediction of C/N and pH mostly match the occurrence of deciduous and coniferous stands within the study area. These properties are more influenced by the litter of the vegetation, and can therefore be predicted better on basis of the NDVI information provided by the used satellite data. The correlation of CEC with the vegetation is apparently weaker and therefore has less influence to the spatial distribution

of the predicted values. The model using chemical data shows the influence of the climate data. BS prediction in Oh horizons were influenced by climate data, which were the most important predictors. However, results in 0-5 cm depth were difficult to assess, with values being very similar for the whole area. Further, the most important predictors were different for models based on chemical and vis-NIR data. As for CEC, this could be caused by uncertainties originating from the spectral modelling. Despite these differences in performance, the successful application is a huge improvement regarding data availability.
If requested, the usage of vis-NIR can help to reduce costs by decreasing the amount of samples that have to be analysed chemically. A certain part of the collected samples can be sufficient to establish the regression model. The humus properties of the rest of the samples can then be predicted with the trained model. This approach could provide sufficiently accurate estimates for practical assessment of humus condition in forests. More accurate results can however be achieved by using chemically determined values directly.

Comparison to other studies

There are few other studies to broach the issue of spatial prediction of humus properties in forest soils and the limited spatial data availability of forested areas. Empirical mapping approaches with focus on forest inventory and planning were developed in Russia in the 20th century [69]. More recently, digital soil mapping approaches were used for spatial prediction of soil properties. For example, Zirlewagen et al. [70] used soil, topography and vegetation to zone forest health conditions in Saxony, Germany. Heitkamp et al. [71] mapped soil properties with focus on soil nutrient regimes by integrating soil chemistry with fuzzy-logic in Hesse and Aertsen et al. [72] compared location-based, attribute-based and hybrid spatial prediction techniques for mapping forest site productivity in Flanders, Belgium. Using model approaches similar to our study, Hanes et al. [73] predicted organic layer thickness in Alberta, Canada. Organic layer thickness is not part of our introduced approach, but the prediction of further humus layer properties might be simply integrated in our framework and would also complete the original methodological site mapping approach of [10]. However, these studies all followed different purposes and objectives, and results are not directly comparable to our approach.

Potential use for forest management and recommendations based on findings

Generally, the presented framework provides information regarding humus properties at forest stand level, where the current mapping schemes do not provide any information. For comparison of the data availability, e.g. the current NFSI mapping only contains two sample points within the whole study area. The availability of spatial information of soil properties can enhance forest management decision making in a more profound way.

We achieved useful spatial results especially for the properties C/N, pH value and BS. By nature, the C/N ratio of organic layers of natural forests is mainly influenced by tree species and soil type [74]. However, significant nitrogen input into forest ecosystems of central Europe is attributed to deposition from external sources [75]. This N supply increases the risk of nutrient imbalances, nitrate leaching, gaseous losses of N2O and further soil acidification.

The pH value in the humus layer and the upper mineral soil layer allows for conclusions about acidification, hence the leaching of base cations (i.e. K, Mg, Ca) [76]. Furthermore, low pH values affect fine roots, ectomycorrhiza [77] and germination and emergence of seeds of certain tree species [78]. The appearance of earthworms as an indicator for bioturbation and biomass is as well dependant from predominant pH value. Our study confirms degraded humus conditions in the study area that should be taken care of by future forest management strategies.

The findings produced by the presented framework for the study area raise the question which measures could help to restore the natural soil quality and overcome the acidified conditions. Beside the problematic humus conditions, also degraded soil physical properties have been reported for comparable loess dominated forest soils in the hilly loess region of Saxony [79, 80].

Therefore, recommendations could include soil preparation for improvement of rooting conditions for planted or seeded deep and intensive rooting tree species e.g. by mixing of organic layer and uppermost mineral soil via strip milling machinery and initial liming.

However, certification standards of the Forest Stewardship Council Germany [81] prohibit driving away from permanent logging lanes and interventions in the mineral soil. In practice, it complicates the ecological restoration of degraded, compacted forest soils.

Further, intensive forms of usage like whole tree harvesting should be reduced in order to reduce nutrient removal from the forest stands. On the long term, unwanted high C/N and low pH values can e.g. be addressed and mitigated by

tree species selection. As C/N ratios below 25 increase the risk of nitrate leaching after clear-felling, continuous-cover forestry and selective felling systems should be preferred [82].

Assessment and outlook

When assessing the developed framework, some points have to be kept mind. Our framework is ready to use when determining the humus properties using standard lab methods. As this requires much time and effort, we also investigated vis-NIR spectroscopy as possibility to derive the humus properties. As usual, we assessed the accuracy of the models using common error measures. However, the impact of the uncertainty resulting from the prediction of humus property values based on vis-NIR spectra due to error propagation is currently not quantified and could be object of further research. Moreover, the increasing availability of regional and national spectral libraries offers potential to include these additional data sources. However there is no state-of-the-art approach how to merge different libraries and further research is needed before implementation. Current developments in DSM are evolving fast and all applied statistical approaches undergo continuous developments. However, the algorithms in our modular framework can be easily replaced and therefore held up to date with respect to future trends in the field. We were only able to test our approach on a local study area. The approach is ready to be tested on larger areas covering a bigger variety of vegetation and soil types. Further, the sensor development regarding handheld vis-NIR devices could enhance and facilitate the acquisition of spectral data. Especially developments regarding small handheld devices are of interest, as they could make in-situ measurements possible. This would simplify the data acquisition even further, as the samples would not have to be transported to a laboratory. The prediction based on chemical values are not affected by uncertainties resulting from the vis-NIR predictions. Improvements of sensors integrated in satellites could improve data quality and therefore model performance of the spatial prediction, especially for C/N and pH, where NDVI values were most important for model calibration.

Conclusions

This study presented an integrated framework for spatial prediction of humus properties on forest soils. The framework was tested on a study site in Saxony, and its feasibility and results have been assessed. In addition, the derived results

were exemplary used to derive and discuss recommendations for the future forest management of the test site.

We conclude that the main advantage lies in the possibility of providing spatially available humus properties at forest stand scale, as the current mapping schemes do not include this information. Model calibration using random forest for spatial prediction achieved $R^2 > 0.9$ for all investigated humus properties (pH, C/N, BS, CEC). It therefore has the potential to close the existing data gap to support decision making in forest management.

We further investigated the possibility of using of vis-NIR spectroscopy to determine humus properties within the framework in order to reduce the needed amount of laboratory analysis. It is possible to substitute parts of the chemical analysis by integrating vis-NIR spectroscopy predictions. Especially C/N, pH and BS could be predicted with an explained variance of 0.43-0.69 by proximal soil sensing. As disadvantage of this cost reduction, the achieved results are likely to be less precise and spatial variation of the properties is often smoothed. Further developments as sensor improvements could help to further decrease effort as well as increase its precision.

Finally, we used the information derived by our framework for the test study area to discuss and exemplary show a possible course of action for future forest management. The application of our method revealed degraded humus conditions in the test area. Based on these results, we were able to formulate measures and recommendations to mitigate the current situation and therefore also present the practical value of the introduced framework.

References

[1] D. Barriopedro et al. “The exceptional Iberian heatwave of summer 2018”. In: *Bulletin of the American Meteorological Society* 101.1 (2020), S29–S34.

[2] P. Shukla et al. “IPCC, 2019: Climate Change and Land: an IPCC special report on climate change, desertification, land degradation, sustainable land management, food security, and greenhouse gas fluxes in terrestrial ecosystems”. In: Intergovernmental Panel on Climate Change (IPCC), 2019.

[3] D. Rind et al. “Potential evapotranspiration and the likelihood of future drought”. In: *Journal of Geophysical Research: Atmospheres* 95.D7 (1990), pp. 9983–10004.

[4] M. G. Grillakis. “Increase in severe and extreme soil moisture droughts for Europe under climate change”. In: *Science of The Total Environment* 660 (2019), pp. 1245–1255.

[5] C. I. Millar and N. L. Stephenson. “Temperate forest health in an era of emerging megadisturbance”. In: *Science* 349.6250 (2015), pp. 823–826.

[6] R. A. Warby, C. E. Johnson, and C. T. Driscoll. “Continuing acidification of organic soils across the northeastern USA: 1984–2001”. In: *Soil Science Society of America Journal* 73.1 (2009), pp. 274–284.

[7] R. F. Hüttl and W. Schaaf. “Nutrient supply of forest soils in relation to management and site history”. In: *Plant and Soil* 168 (1995), pp. 31–41.

[8] P. Gundersen et al. “Impact of nitrogen deposition on nitrogen cycling in forests: a synthesis of NITREX data”. In: *Forest Ecology and management* 101.1-3 (1998), pp. 37–55.

[9] W. De Vries et al. “Impacts of acid deposition, ozone exposure and weather conditions on forest ecosystems in Europe: an overview”. In: *Plant and Soil* 380.1 (2014), pp. 1–45.

[10] Schulze and Kopp. “Anleitung für die forstliche Standortserkundung im nordostdeutschen Tiefland”. In: *Standortserkundungsanleitung 95* (2013).

[11] B. Minasny and A. B. McBratney. “Digital soil mapping: A brief history and some lessons”. In: *Geoderma* 264 (2016), pp. 301–311.

[12] E. C. Brevik et al. “Soil mapping, classification, and pedologic modeling: History and future directions”. In: *Geoderma* 264 (2016), pp. 256–274.

[13] R. V. Rossel et al. "Proximal soil sensing: an effective approach for soil measurements in space and time". In: *Advances in agronomy*. Vol. 113. Elsevier: Amsterdam, The Netherlands, 2011, pp. 243–291.

[14] E. Ben-Dor and A. Banin. "Near-infrared analysis as a rapid method to simultaneously evaluate several soil properties". In: *Soil Science Society of America Journal* 59.2 (1995), pp. 364–372.

[15] C.-W. Chang et al. "Near-infrared reflectance spectroscopy–principal components regression analyses of soil properties". In: *Soil Science Society of America Journal* 65.2 (2001), pp. 480–490.

[16] R. V. Rossel et al. "Visible, near infrared, mid infrared or combined diffuse reflectance spectroscopy for simultaneous assessment of various soil properties". In: *Geoderma* 131.1-2 (2006), pp. 59–75.

[17] J. B. Reeves III. "Near-versus mid-infrared diffuse reflectance spectroscopy for soil analysis emphasizing carbon and laboratory versus on-site analysis: where are we and what needs to be done?" In: *Geoderma* 158.1-2 (2010), pp. 3–14.

[18] B. Stenberg et al. "Visible and near infrared spectroscopy in soil science". In: *Advances in agronomy*. Vol. 107. Elsevier: Amsterdam, The Netherlands, 2010, pp. 163–215.

[19] A. Gubler. "Quantitative Estimations of Soil Properties by Visible and Near Infrared Spectroscopy: Applications for Laboratory and Field Measurements". PhD thesis. University of Bern, Bern, Switzerland, 2011.

[20] R. V. Rossel and T. Behrens. "Using data mining to model and interpret soil diffuse reflectance spectra". In: *Geoderma* 158.1-2 (2010), pp. 46–54.

[21] R. V. Rossel and A. McBratney. "Diffuse reflectance spectroscopy as a tool for digital soil mapping". In: *Digital soil mapping with limited data*. Springer, 2008, pp. 165–172.

[22] C. Gomez, R. A. V. Rossel, and A. B. McBratney. "Soil organic carbon prediction by hyperspectral remote sensing and field vis-NIR spectroscopy: An Australian case study". In: *Geoderma* 146.3-4 (2008), pp. 403–411.

[23] V. Genot et al. "Near infrared reflectance spectroscopy for estimating soil characteristics valuable in the diagnosis of soil fertility". In: *Journal of Near Infrared Spectroscopy* 19.2 (2011), pp. 117–138.

[24] F. S. Terra, J. A. Demattê, and R. A. V. Rossel. "Spectral libraries for quantitative analyses of tropical Brazilian soils: Comparing vis–NIR and mid-IR reflectance data". In: *Geoderma* 255 (2015), pp. 81–93.

[25] F. Thomas et al. "Estimating Forest Soil Properties for Humus Assessment—Is Vis-NIR the Way to Go?" In: *Remote Sensing* 14.6 (2022), p. 1368.

[26] F. Thomas et al. "Application of Low-Cost MEMS Spectrometers for Forest Topsoil Properties Prediction". In: *Sensors* 21.11 (2021), p. 3927.

[27] A. Gholizadeh et al. "National-scale spectroscopic assessment of soil organic carbon in forests of the Czech Republic". In: *Geoderma* 385 (2021), p. 114832.

[28] D. Xu et al. "Assessment of important soil properties related to Chinese Soil Taxonomy based on vis–NIR reflectance spectroscopy". In: *Computers and electronics in agriculture* 144 (2018), pp. 1–8.

[29] H. Jenny. "Factors of soil formation: a system of quantitative pedology New York". In: *Macgraw Hill* (1941).

[30] A. B. McBratney, M. M. Santos, and B. Minasny. "On digital soil mapping". In: *Geoderma* 117.1-2 (2003), pp. 3–52.

[31] D. W. Roberts. "Ordination on the basis of fuzzy set theory". In: *Vegetatio* 66.3 (1986), pp. 123–131.

[32] L. W. Zevenbergen and C. R. Thorne. "Quantitative analysis of land surface topography". In: *Earth surface processes and landforms* 12.1 (1987), pp. 47–56.

[33] J. Böhner et al. "Soil regionalisation by means of terrain analysis and process parameterisation". In: *Soil classification* 7 (2001), p. 213.

[34] J. Böhner and T. Selige. "Spatial prediction of soil attributes using terrain analysis and climate regionalisation". In: *Gottinger Geographische Abhandlungen* 115 (2006), pp. 13–28.

[35] D. Frantz. "FORCE v. 2.0—Technical User Guide". In: *ResearchGate: Berlin, Germany* (2018).

[36] D. Frantz. "FORCE—Landsat+ Sentinel-2 analysis ready data and beyond". In: *Remote Sensing* 11.9 (2019), p. 1124.

[37] B. Minasny and A. B. McBratney. "A conditioned Latin hypercube method for sampling in the presence of ancillary information". In: *Computers & geosciences* 32.9 (2006), pp. 1378–1388.

[38] K. Schmidt et al. “A comparison of calibration sampling schemes at the field scale”. In: *Geoderma* 232 (2014), pp. 243–256.

[39] C. Brungard and J. Johanson. “The gate’s locked! I can’t get to the exact sampling spot... can I sample nearby”. In: *Pedometron: Newsletter of the Pedometrics Commission of the IUSS. Pedometron (37): Newsletter of the Pedometrics Commission of the IUSS* (2015).

[40] P. Roudier. *clhs: a R package for conditioned Latin hypercube sampling.* 2011.

[41] J. Höhle et al. *Bodenzustandserhebung im Wald-Dokumentation und Harmonisierung der Methoden.* Tech. rep. Johann Heinrich von Thünen-Institut: Braunschweig, Germany, 2018.

[42] Gutachterausschuss Forstliche Analytik. *Handbuch Forstliche Analytik. Eine Loseblatt-Sammlung der Analysemethoden im Forstbereich.* 2014.

[43] DIN. “DIN 10694: Bestimmung des organischen Kohlenstoffgehaltes und des Gesamtkohlenstoffgehaltes nach trockener Verbrennung (Elementaranalyse)”. In: *Deutsche Normen (ed. Fachnormenausschuß Wasserwesen, FNW, im DIN Deutsches Institut für Normung e.V.)* (1994).

[44] DIN ISO 10390: 2005. *Bodenbeschaffenheit—Bestimmung des pH-Wertes.* 2005.

[45] A. Mac Arthur, C. J. MacLellan, and T. Malthus. “The fields of view and directional response functions of two field spectroradiometers”. In: *IEEE transactions on geoscience and remote sensing* 50.10 (2012), pp. 3892–3907.

[46] Avian Technologies. *Fluorilon Gray Scale Standards & Targets.* Online. accessed on 13.06.2019. 2019. URL: `https://aviantechnologies.com/product/gray-scale-standards/`.

[47] Å. Rinnan, F. Van Den Berg, and S. B. Engelsen. “Review of the most common pre-processing techniques for near-infrared spectra”. In: *TrAC Trends in Analytical Chemistry* 28.10 (2009), pp. 1201–1222.

[48] A. Savitzky and M. J. Golay. “Smoothing and differentiation of data by simplified least squares procedures.” In: *Analytical chemistry* 36.8 (1964), pp. 1627–1639.

[49] R. Barnes, M. S. Dhanoa, and S. J. Lister. “Standard normal variate transformation and de-trending of near-infrared diffuse reflectance spectra”. In: *Applied spectroscopy* 43.5 (1989), pp. 772–777.

[50] A. Stevens and L. Ramirez-Lopez. *An introduction to the prospectr package*. R package version 0.1.3. R Core Team: Vienna, Austria, 2013.

[51] S. Wold, H. Martens, and H. Wold. "The multivariate calibration problem in chemistry solved by the PLS method". In: *Matrix pencils*. Springer: Cham, Siwtzerland, 1983, pp. 286–293.

[52] M. Conforti, G. Matteucci, and G. Buttafuoco. "Using laboratory Vis-NIR spectroscopy for monitoring some forest soil properties". In: *Journal of soils and sediments* 18.3 (2018), pp. 1009–1019.

[53] B. Ludwig et al. "Near infrared spectroscopy of forest soils to determine chemical and biological properties related to soil sustainability". In: *Forest Ecology and Management* 171.1-2 (2002), pp. 121–132.

[54] W. T. Norman. "Double-split cross-validation: An extension of Mosier's design, two undesirable alternatives, and some enigmatic results." In: *Journal of Applied Psychology* 49.5 (1965), p. 348.

[55] S. Varma and R. Simon. "Bias in error estimation when using cross-validation for model selection". In: *BMC bioinformatics* 7.1 (2006), pp. 1–8.

[56] A. Statnikov and C. Aliferis. "Are random forests better than support vector machines for microarray-based cancer classification?" In: *AMIA annual symposium proceedings*. Vol. 2007. American Medical Informatics Association. 2007, p. 686.

[57] G. Cawley and N. Talbot. "On over-fitting in model selection and subsequent selection bias in performance evaluation". In: *The Journal of Machine Learning Research* 11 (2010), pp. 2079–2107.

[58] M. Gütlein et al. "A large-scale empirical evaluation of cross-validation and external test set validation in (Q) SAR". In: *Molecular Informatics* 32.5-6 (2013), pp. 516–528.

[59] D. Krstajic et al. "Cross-validation pitfalls when selecting and assessing regression and classification models". In: *Journal of cheminformatics* 6.1 (2014), pp. 1–15.

[60] D. Baumann and K. Baumann. "Reliable estimation of prediction errors for QSAR models under model uncertainty using double cross-validation". In: *Journal of cheminformatics* 6.1 (2014), pp. 1–19.

[61] J. E. Nash and J. V. Sutcliffe. "River flow forecasting through conceptual models part I—A discussion of principles". In: *Journal of hydrology* 10.3 (1970), pp. 282–290.

[62] M. Kuhn. *caret: Classification and Regression Training*. R package version 6.0-81. R Core Team: Vienna, Austria, 2018. URL: `https://CRAN.R-project.org/package=caret`.

[63] L. Breiman. "Random forests". In: *Machine learning* 45.1 (2001), pp. 5–32.

[64] E. Scornet, G. Biau, J. Vert, et al. "Consistency of random forests". In: *The Annals of Statistics* 43.4 (2015), pp. 1716–1741.

[65] R. Grimm et al. "Soil organic carbon concentrations and stocks on Barro Colorado Island—Digital soil mapping using Random Forests analysis". In: *Geoderma* 146.1-2 (2008), pp. 102–113.

[66] T. Behrens et al. "Hyper-scale digital soil mapping and soil formation analysis". In: *Geoderma* 213 (2014), pp. 578–588.

[67] H. U. Rehman et al. "Comparison of cation exchange capacity estimated from Vis–NIR spectral reflectance data and a pedotransfer function". In: *Vadose Zone Journal* 18.1 (2019), pp. 1–8.

[68] Y. Ulusoy et al. "Prediction of soil cation exchange capacity using visible and near infrared spectroscopy". In: *Biosystems Engineering* 152 (2016), pp. 79–93.

[69] O. Chertov and M. Nadporozhskaya. "Development and application of humus form concept for soil classification, mapping and dynamic modelling in Russia". In: *Applied Soil Ecology* 123 (May 2017).

[70] D. Zirlewagen, G. Raben, and M. Weise. "Zoning of forest health conditions based on a set of soil, topographic and vegetation parameters". In: *Forest Ecology and Management* 248 (Aug. 2007), pp. 43–55.

[71] F. Heitkamp et al. "Inference of forest soil nutrient regimes by integrating soil chemistry with fuzzy-logic: Regionwide application for stakeholders of Hesse, Germany". In: *Geoderma Regional* 23 (Oct. 2020), e00340.

[72] W. Aertsen et al. "Comparison of location-based, attribute-based and hybrid regionalization techniques for mapping forest site productivity". In: *Forestry* 84 (June 2012), pp. 539–550.

[73] C. Hanes et al. "Mapping organic layer thickness and fuel load of the boreal forest in Alberta, Canada". In: *Geoderma* 417 (July 2022), p. 115827.

[74] N. Cools et al. "Tree species is the major factor explaining C: N ratios in European forest soils". In: *Forest Ecology and Management* 311 (2014), pp. 3–16.

[75] S. Fleck et al. “Nitrogen Status and Dynamics in German Forest Soils”. In: Springer International Publishing, Sept. 2019, pp. 123–166. ISBN: 978-3-030-15732-6. DOI: 10.1007/978-3-030-15734-0_5.

[76] H. Meesenburg et al. “Soil Acidification in German Forest Soils”. In: *Status and Dynamics of Forests in Germany : Results of the National Forest Monitoring*. Cham: Springer International Publishing, 2019, pp. 93–121. ISBN: 978-3-030-15734-0. DOI: 10.1007/978-3-030-15734-0_4. URL: https://doi.org/10.1007/978-3-030-15734-0_4.

[77] P. Cudlin et al. “Fine roots and ectomycorrhizas as indicators of environmental change”. In: *Plant Biosystems - An International Journal Dealing with all Aspects of Plant Biology* 141.3 (2007), pp. 406–425. DOI: 10.1080/11263500701626028.

[78] M. Axer et al. “Modelling natural regeneration of Oak in Saxony, Germany: identifying factors influencing the occurrence and density of regeneration”. In: *Identification of seed and establishment limitation of beech and oak natural regeneration at the forest enterprise level using large-scale inventory data* (2022), p. 184.

[79] G. Krauss et al. “Standortsgemäße Durchführung der Abkehr von der Fichtenwirtschaft im nordwestsächsischen Niederland”. In: *Tharandter Forstl. Jahrbuch* 90 (1939), pp. 481–715.

[80] S. Julich et al. “Hydraulic properties of forest soils with stagnic conditions”. In: *Forests* 12.8 (2021), p. 1113.

[81] Forest Stewardship Council Germany. *Deutscher FSC-Standard 3.0*. 2018.

[82] P. Högberg et al. “Large differences in plant nitrogen supply in German and Swedish forests – Implications for management”. In: *Forest Ecology and Management* 482 (2021), p. 118899. ISSN: 0378-1127. DOI: https://doi.org/10.1016/j.foreco.2020.118899. URL: https://www.sciencedirect.com/science/article/pii/S0378112720316686.